Hydrogen combustion in marine two-stroke engines using LPDI

T.S.A. de Haas

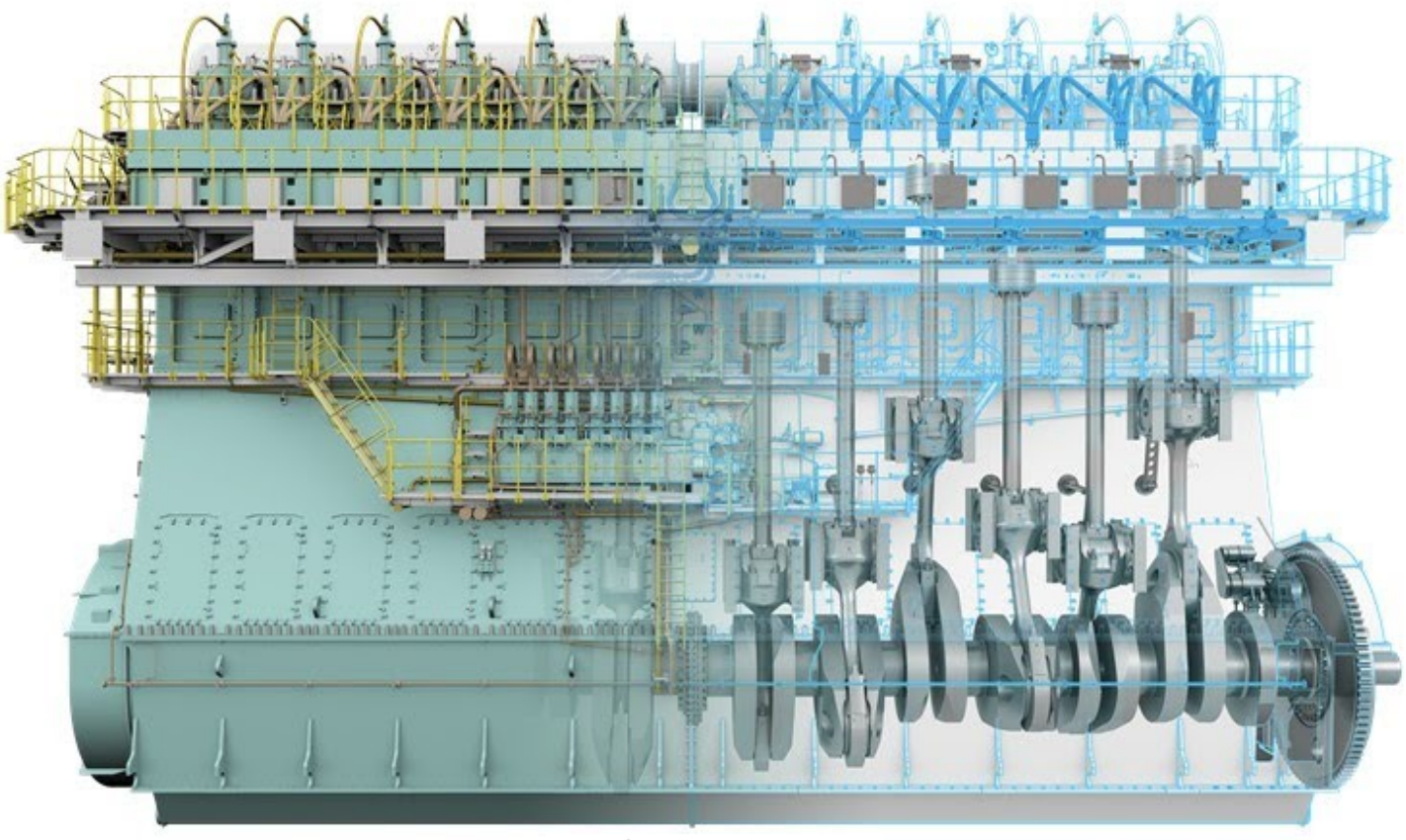

TU Delft

Thesis for the degree of MSc in Marine Technology in the specialization of Marine Engineering

Hydrogen combustion in marine two-stroke engines using LPDI

by

T.S.A. de Haas

This thesis (MT.24/25.034.M) is classified as confidential in accordance with the general conditions for projects performed by the TUDelft.

29 April 2025

Thesis exam committee

Chair:	Dr. ir. P. de Vos	TU Delft, supervisor
Staff member:	Ir. M. C. van Benten	TU Delft
Staff member:	Dr. ir. L. van Biert	TU Delft

Author details
Studynumber: 4378709

Cover: WinGD X92DF-2.0 [1]

An electronic version of this thesis is available at http://repository.tudelft.nl/.

TU Delft

Preface

This thesis marks the completion of my Master's programme in Marine Technology at Delft University of Technology. It presents the results of my graduation project, which focused on modelling the feasibility and implications of hydrogen combustion in large two-stroke marine engines using low-pressure direct injection.

The subject reflects the increasing urgency within the maritime industry to explore alternative fuels and reduce greenhouse gas emissions. Working on this topic has allowed me to deepen my understanding of thermodynamic modelling, combustion processes, and the engineering challenges involved in adapting conventional engine technologies to future fuel strategies.

I would like to express my sincere gratitude to my graduation supervisor, Peter de Vos, for his guidance, constructive feedback, and clear direction throughout this project. I also thank the members of my graduation committee, Marcel van Benten and Lindert van Biert, for their valuable contributions and support during the assessment of my work.

Lastly, I am thankful to my friends and family for their ongoing encouragement. In particular, I wish to thank my partner, Diede Wijnbergen, for her patience, understanding, and support during the many long days and evenings of this process.

T.S.A. de Haas
Delft, April 2025

During the preparation of this work, the author used ChatGPT in order to generate LaTeX code quickly, retrieve literature efficiently, and assist with translation. After using this tool/service, the author reviewed and edited the content as needed and takes full responsibility for the content of the publication.

Abstract

The maritime industry faces increasing pressure to reduce its environmental impact, particularly through the reduction of greenhouse gas emissions. This thesis investigates the feasibility and technical implications of operating large, low-speed, two-stroke marine engines on hydrogen using low-pressure direct injection. The study addresses the lack of specialized combustion models for hydrogen in large marine engines by developing a tailored in-cylinder thermodynamic combustion model.

A comprehensive literature review highlights hydrogen's unique combustion characteristics, such as high flame speeds, low ignition energy, and wide flammability range, along with associated challenges like pre-ignition, knocking, and NOx emissions. Existing combustion strategies and injection technologies, particularly those adapted from natural gas-fueled engines, are evaluated for their applicability to hydrogen combustion.

The developed combustion model integrates a Seiliger cycle representation enhanced by temperature-dependent thermodynamic properties. It systematically assesses the effects of hydrogen combustion on key engine parameters, including pressure rise rate, peak cylinder pressures, and temperatures, under various operational scenarios. The results highlight the importance of combustion phasing and air-excess ratios in managing hydrogen combustion characteristics, indicating that careful optimisation of injection timing and combustion strategy is crucial to ensure safe and efficient engine operation. Although the model reveals risks associated with aggressive combustion scenarios, such as exceeding mechanical design limits due to high peak pressures, it provides a structured framework for identifying realistic operating conditions for hydrogen LPDI combustion.

This research thus offers critical insights into the technical feasibility and practical limitations of hydrogen combustion in large two-stroke marine engines, contributing valuable guidance for future development and experimental validation efforts.

Contents

List of Figures

List of Tables

Nomenclature

Abbreviations

Abbreviation	Definition
0D	Zero-dimensional
BDC	Bottom Dead Center
bmep	brake mean effective pressure
bsfc	brake specific fuel consumption
CFD	Computational Fluid Dynamics
CI	Compression Ignition
CO	Carbon Monoxide
CO_2	Carbon Dioxide
DI	Direct Injection
EC	Exhaust Closing
EO	Exhaust Opening
H_2	Hydrogen
H2DDI	Hydrogen-Diesel Dual Direct-Injection
HES	Hydrogen Energy Share
HPDI	High-Pressure Direct Injection
IC	Inlet Closing
IO	Inlet Opening
LNG	Liquefied Natural Gas
LPDI	Low-Pressure Direct Injection
MVEM	Mean Value Engine Models
MVFP	Mean Value First Principle
N_2	Nitrogen
NG	Natural Gas
NOx	Nitrogen Oxides
O_2	Oxygen
PFI	Port Fuel Injection
RON	Research Octane Number
SI	Spark Ignition
TDC	Top Dead Center
TJI	turbulent jet ignition
UHC	Unburned Hydrocarbons

Symbols

Symbol	Definition	Unit
A	NIST polynomial coefficient	[-]
a	Iso-volumetric pressure ratio Seiliger process	[-]
a	Wiebe parameter	[-]
B	NIST polynomial coefficient	[-]
b	Isobaric volume ratio in Seiliger process	[-]
C	NIST polynomial coefficient	[-]
c	Isothermal volume ratio in Seiliger process	[-]
c_p	Specific heat at constant pressure	[kJ/kgK or J/molK]
c_v	Specific heat at constant volume	[kJ/kgK or J/molK]
D	Cylinder bore	[m]
D	NIST polynomial coefficient	[-]
E	NIST polynomial coefficient	[-]
L	Connecting rod length	[m]
m	Mass	[kg]
m	Wiebe parameter	[-]
n	Polytropic exponent	[-]
p	Pressure	[Pa]
q	Heat per unit of mass	[kJ/kg]
R	Crank radius	[m]
R	Gas constant	[kJ/kgK or J/molK]
r_c	Compression ratio	[-]
r_{exp}	Expansion ratio	[-]
T	Temperature	[K]
t	Temperature divided by 1000	[K]
V	Volume	[m^3]
w	Work per unit of mass	[kJ/kg]
x	Mass fraction	[-]
γ	Ratio of specific heats	[-]
$\Delta\theta$	Total combustion duration	[degree]
ε	Geometric compression ratio	[-]
η	Efficiency	[-]
θ	Crank angle	[degree]
λ	Air excess ratio	[-]
σ	Stoichiometric air/fuel ratio	[-]
ϕ	Equivalence ratio	[-]
ϕ	Crank angle	[degree]

Subscripts

Symbol	Definition
0	Start of combustion
1	Seiliger point 1
2	Seiliger point 2
3	Seiliger point 3
4	Seiliger point 4
5	Seiliger point 5
6	Seiliger point 6
12	Seiliger stage 1-2
23	Seiliger stage 2-3
34	Seiliger stage 3-4
45	Seiliger stage 4-5
56	Seiliger stage 5-6
S	Stroke
TDC	Top Dead Center
a	air
b	burned
c	compression
exp	expansion
f	fuel
i	Indicated
max	Maximum
min	Minimum
mix	mix of air and fuel
td	Thermodynamic
th	theoretical
u	Universal

Introduction

1

Introduction

Considering climate change and the significant role that the shipping industry plays in global greenhouse gas emissions, there is a pressing need for fuels that are less harmful to the environment [2–4]. The maritime sector, responsible for approximately 3% of global carbon dioxide (CO_2) emissions, is under increasing scrutiny to adopt more sustainable practices [5–7]. One of the promising options explored is hydrogen, due to its potential to be produced sustainably and zero CO_2 emissions during combustion [8–10].

The large, low-speed, two-stroke diesel engine is the standard engine type used in the shipping industry. These engines are favoured for their high efficiency and durability. Given their prevalence, it is particularly interesting to investigate whether these engines can be adapted to run on hydrogen, and what modifications are necessary to make this technically feasible. The successful conversion of these engines to hydrogen could represent a significant step forward in reducing the maritime sector's carbon footprint.

In contrast to the limited research, development and application of hydrogen in large maritime engines, there has already been considerable progress with smaller spark-ignited hydrogen combustion engines [11, 12]. Additionally, research is ongoing into converting smaller compression-ignited diesel engines to run on hydrogen [13, 14]. These studies provide valuable insights and pave the way for further exploration into modifying larger engines.

There are several methods to introduce hydrogen into the combustion chamber of an engine. Among these, low-pressure direct injection (LPDI) is emerging as a promising strategy in particular. Research indicates that LPDI can mitigate some of the undesirable combustion characteristics often associated with hydrogen, such as pre-ignition, knocking, and backfiring. Moreover, LPDI offers additional advantages in terms of safety and cost. The lower injection pressures reduce the risk of hydrogen leaks and the complexity of the injection system, making it a more practical and economical choice for large engines [14–18].

Based on the considerations outlined above, this report aims to explore the feasibility and implications of using hydrogen as a fuel for large, two-stroke marine engines, with a specific focus on LPDI as the hydrogen introduction method. To support this exploration, a comprehensive literature study is conducted to identify the key combustion characteristics of hydrogen, the specific challenges associated with applying it in large engines, and the modelling approaches that can represent this process effectively.

The outcome of the literature study forms the foundation for the second part of the report, in which a thermodynamic model is developed to simulate the combustion of hydrogen in a large two-stroke engine. This model is used to investigate engine performance, identify potential limitations, and evaluate critical parameters under various combustion scenarios. In doing so, the study aims to provide a deeper understanding of how hydrogen could be integrated into maritime propulsion systems, and which modelling techniques are best suited to support further development in this area.

2

Scope

2.1. Problem definition

Various models exist for simulating the behaviour and properties of combustion engines, but most are primarily focused on traditional diesel engines [19]. These models typically do not account for the unique properties of hydrogen combustion, such as its higher flame speed and lower ignition energy [20]. As a result, there is a need for advanced modelling techniques specifically tailored to hydrogen as a fuel. These models must capture the essence of hydrogen's combustion behaviour, including the effects of different injection strategies and the resulting impact on engine performance. Developing a robust model for hydrogen combustion in large two-stroke diesel engines is essential for understanding the feasibility and optimising the conversion process. Such models can help identify the optimal injection parameters and predict the engine's performance under various operating conditions.

Furthermore, using these models to evaluate whether techniques applied in smaller hydrogen engines could also be effective in larger, slow-speed two-stroke engines would be interesting. Techniques such as using a high air-excess ratio, incorporating spark plugs, or adding a prime fuel have shown promise in smaller engines. Additionally, the operation of a two-stroke engine, as opposed to the more extensively researched four-stroke engines, may present additional challenges. Research by Qu et al. [21] highlights that hydrogen slipping due to the overlap of exhaust valve openings and LPDI can occur. Addressing these unique challenges in two-stroke engines through modelling and simulation is crucial for developing effective hydrogen combustion strategies and ensuring the successful implementation of hydrogen as a fuel in the maritime sector.

2.2. Objective

The primary objective of the literature review part of this project is to assess the possibilities, challenges, and key parameters involved in running a large two-stroke engine on hydrogen, using an LPDI system. Following that, an in-cylinder combustion model specifically tailored to hydrogen combustion in large two-stroke engines will be developed. This model will be used to make predictions on the combustion behaviour and characteristics and potential issues such as pre-ignition, knocking, and hydrogen slipping. By developing and verifying this model, the project seeks to provide a robust tool for simulating and optimising hydrogen combustion, thereby contributing to the broader goal of reducing the maritime sector's carbon footprint and advancing the use of sustainable fuels in shipping.

2.3. Research questions

To provide direction and structure to this study, the following research question has been formulated:

How can an in-cylinder combustion model be used to evaluate the feasibility and technical implications of hydrogen operation with LPDI in large two-stroke marine engines?

To further elaborate on the research direction, the following sub-questions are established:

- What key parameters are found to be of influence on the reliable combustion of hydrogen in existing hydrogen internal combustion engines?
- How are the main characteristics of combustion in large two-stroke diesel engines generally modelled to determine the feasibility of reliable running?
- How does an in-cylinder combustion model need to be adapted to represent hydrogen combustion in a large two-stroke engine?
- Which type of combustion model is most suitable for predicting the feasibility of reliable hydrogen operation in large two-stroke marine engines?
- What is the effect of different combustion scenarios and model assumptions on key engine performance outcomes when simulating hydrogen operation?

2.4. Scope

This project focuses on modelling the in-cylinder combustion processes of hydrogen in large two-stroke engines. It will utilise existing models to gain insight into modelling techniques used for in-cylinder combustion processes. However, the focus will not extend to developing a complete engine model for hydrogen-powered engines. The research will specifically concentrate on creating an closed-cylinder combustion model tailored to hydrogen, while excluding the broader scope of constructing a fully integrated hydrogen engine model. The emphasis remains on understanding the feasibility of hydrogen combustion within large two-stroke engines, assuming the use of LPDI for hydrogen delivery. While detailed investigations into the specifications of the injection system are relevant, they fall outside the scope of this research.

As a baseline for modelling and a comparison point for the results, the design of the WinGD X92DF-2.0 engine will be used. This is currently the largest two-stroke dual-fuel engine in production, using low-pressure LNG (Liquefied Natural Gas) as the primary fuel. This engine has also been used as a reference in a research project aimed at designing LPDI injectors for this type of two-stroke engines [22].

2.5. Outline

This thesis is structured in three main parts: an introductory section, a literature review, and the research section. The structure is as follows:

- **Chapters 1–2: Introduction and Scope**
  These chapters introduce the background, objectives, and research questions that form the foundation of this study.
- **Chapters 3–6: Literature Review**
  This section provides an overview of relevant literature on large two-stroke marine engines, hydrogen combustion characteristics, and combustion modelling strategies. It concludes with a gap analysis and a project approach.
- **Chapters 7–13: Research**
  The core of the thesis, this section describes the setup, implementation, and results of a combustion model tailored to simulate hydrogen operation in a large two-stroke engine. It includes details on model parameters, refinements, and alternative modelling strategies such as the Wiebe function.
  - **Chapters 7–9: Modelling Approach and Refinement** — These chapters outline the baseline modelling strategy using the Seiliger process and discuss the implementation of temperature-dependent specific heat capacities.
  - **Chapters 10–11: Supplementary Physics and Alternative Models** — These provide additional context on combustion physics and explore an alternative modelling strategy using a simplified Wiebe function.
  - **Chapter 12: Results** — Presents model outcomes such as pressure and temperature profiles for different combustion scenarios.
  - **Chapter 13: Conclusions and Recommendations** — Answers the research questions and offers suggestions for further research and development.

Literature review

3

Large two-stroke low-speed marine engines

This chapter introduces the fundamental working principles and key technical characteristics of large two-stroke low-speed marine diesel engines. These engines are the dominant propulsion systems in commercial shipping due to their high efficiency, fuel flexibility, and durability. The chapter provides an overview of the two-stroke cycle, the process of compression ignition, and the challenges associated with scavenging. These insights are essential to understand the specific requirements and constraints when considering alternative fuels such as hydrogen for this engine type.

3.1. Two-stroke process

The two-stroke engine is widely used at both extremes of engine sizes, including small engines for portable devices and very large engines for marine and power generation applications [24, 25]. These large two-stroke diesel engines are particularly valued in the marine industry for their robustness, efficiency and cost-effectiveness, serving as prime movers that offer high power output and low fuel consumption, as illustrated in Figure 3.1.

The fundamental distinction between two-stroke and four-stroke engines is the number of crankshaft revolutions required to complete one power cycle. In four-stroke engines, the full cycle of compression, expansion, exhaust, and air intake spans two crankshaft revolutions. In contrast, the two-stroke engine completes this cycle in just one revolution, integrating the gas exchange process with the power stroke [23]. This principle is schematically illustrated in Figure 3.2.

Large two-stroke slow-turning marine engines (with bores between 0.2 to 1 meter) are well-suited for ship propulsion due to their ability to meet the power and speed requirements of direct-drive propeller systems [26]. These engines are typically turbocharged to achieve high brake mean effective pressures and optimize specific output. This contributes to their high fuel efficiency, with brake fuel conversion efficiencies reaching up to 55% in the largest engines in the best possible conditions.

Despite their efficiency, the two-stroke process has inherent limitations. Near BDC (Bottom Dead Center), when the gas exchange occurs, the piston movement provides minimal assistance, resulting in a relatively short duration for exhaust and intake. This can leave a considerable amount of hot residual gases in the cylinder, reducing the fresh air charge and limiting the amount of fuel that can be burned [23]. This compromises the potential power output and highlights the challenge of achieving optimal scavenging in two-stroke engines.

The next two sections evaluate the injection and ignition methodology typically utilized in these engines as well as the challenges with regards to scavenging.

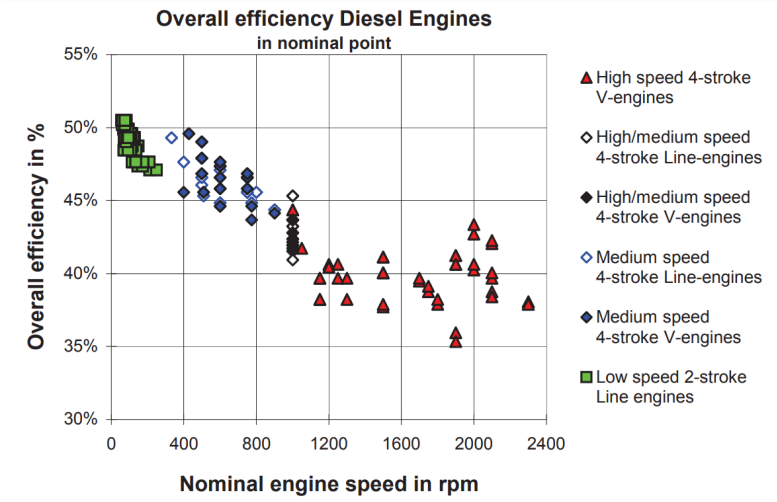

(a) Trend of engine efficiency versus engine speed

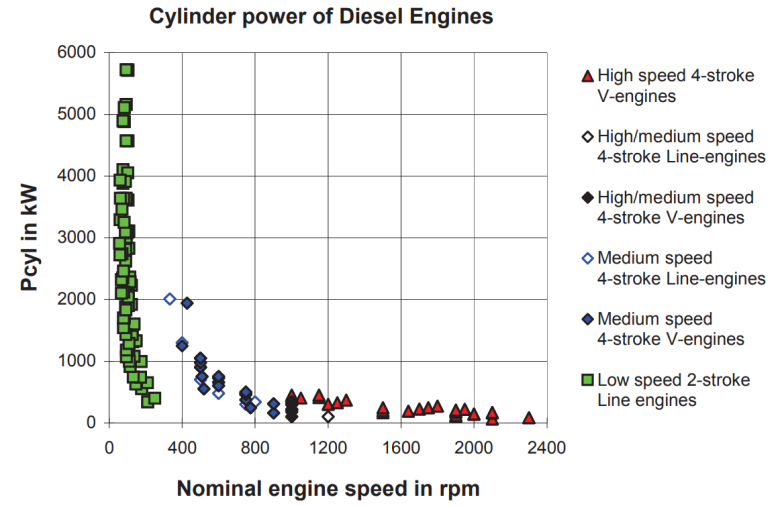

(b) Trend of cylinder power versus engine speed

Figure 3.1: Comparison of overall efficiency and cylinder power of various types of diesel engines [23]

3.2. Injection and ignition

Large marine two-stroke engines typically operate using diesel-type fuels and employ the compression ignition (CI) process. This ignition method is central to their operation, providing the high efficiency and reliability required for maritime propulsion. In this section, we will discuss the working principles of the compression ignition process in these engines, focusing on how the fuel is ignited and the intricacies of the fuel injection system that supports this process.

In conventional operation, diesel fuel is introduced into the combustion chamber using high-pressure direct injection (HPDI). In this method, the fuel is injected at extremely high pressures, often exceeding 1000 bar, near the end of the compression stroke [27]. The high pressure ensures rapid atomisation of the fuel into fine droplets, which promotes efficient mixing with the hot compressed air in the cylinder, which is schematically represented in Figure 3.3 [28]. This rapid mixing, combined with the high in-cylinder temperature resulting from compression, leads to immediate auto-ignition of the diesel, initiating combustion. The precise control over injection timing and pressure is crucial for achieving optimal performance and emissions characteristics in these engines. This method contrasts with spark ignition, where the air-fuel mixture is ignited by an electric spark and wherein combustion takes place via flame propagation through the mixture. Instead, in CI engines, individual fuel droplets ignite in a “sea” of air, enabling lean combustion [25].

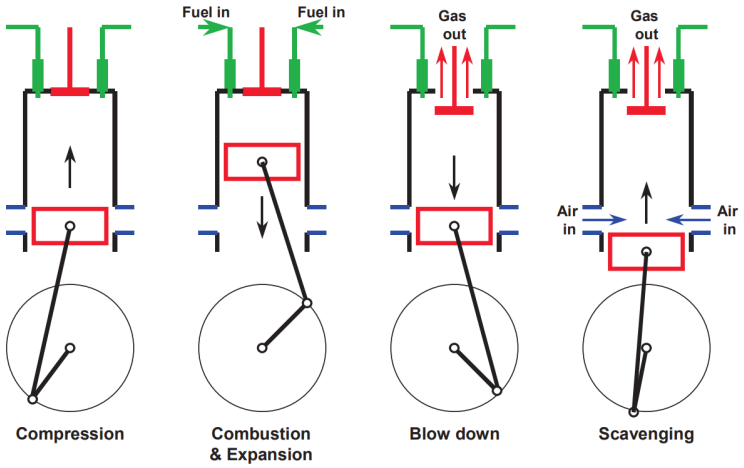

(a) two-stroke

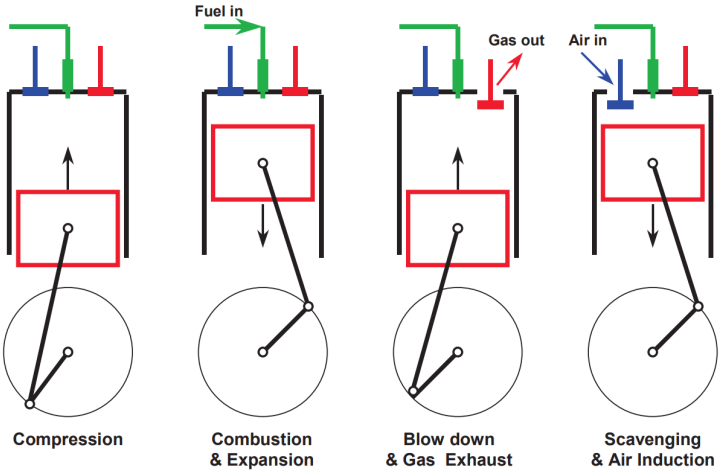

(b) four-stroke

Figure 3.2: Principle of operation of two-stroke and four-stroke diesel engines [23]

CI is the fundamental process underlying diesel engine operation and is central to the function of large marine engines. Unlike spark ignition (SI) engines, where a fuel-air mixture is ignited by a spark, CI engines rely on the auto-ignition of fuel injected into highly compressed air within the cylinder [23]. This ignition process results from the high temperature reached at the end of the compression stroke, which exceeds the auto-ignition temperature of the fuel used. This characteristic allows CI engines to combust fuel efficiently even under lean conditions, using air-fuel ratios that are much higher than the stoichiometric mixture [25].

In large two-stroke marine engines, this process begins with the intake of air into the cylinder. The fuel, often heavy residual fuel oil that is preheated, is injected directly into the cylinder just before combustion is supposed to start [26]. The injection timing is critical for controlling engine load and performance, as the amount of fuel injected per cycle determines the power output. Unlike SI engines, where both fuel and air are mixed prior to entering the combustion chamber, the CI process ensures that only air is compressed, allowing for greater control over the combustion conditions and reduced risk of pre-ignition.

The compression ratios in CI engines are significantly higher than those in SI engines. This higher compression results in elevated air temperatures that are essential for the auto-ignition of the injected fuel. The absence of a throttle in naturally aspirated CI engines means that airflow remains constant at a given engine speed, with load control being achieved solely by adjusting the amount of fuel injected [26].

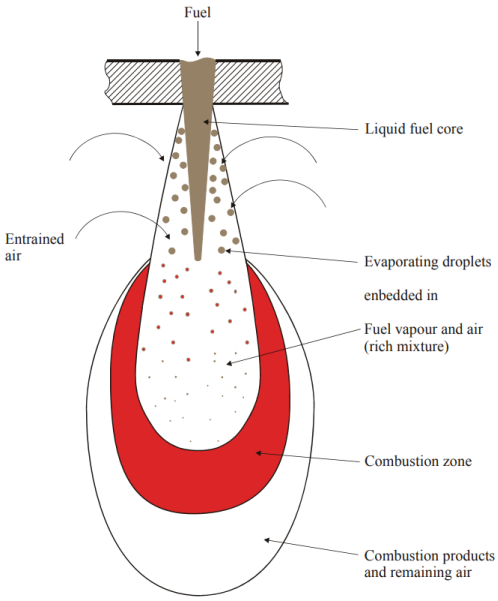

Figure 3.3: Fuel jet and flame [28]

This feature contributes to the fuel efficiency of CI engines, as they can operate at high compression ratios with excess air and leaner mixtures, promoting complete combustion and lower emissions.

The compression ignition process also lends itself well to the use of lower-quality fuels, which is particularly advantageous in large marine engines. The robust combustion process can handle the use of heavy residual fuels, which are more economical but require preheating due to their higher viscosity and lower volatility. Despite these challenges, large marine CI engines achieve high thermal efficiency and are capable of maintaining high performance over prolonged periods of operation, making them the standard in the shipping industry.

3.3. Scavenging

The air intake process in large two-stroke marine engines is an essential part of the gas exchange cycle, which aims to remove burned gases from the cylinder at the end of the power stroke and replace them with fresh air. This cycle, known as scavenging, ensures that the engine is prepared for the next combustion cycle [26]. Unlike in four-stroke engines, where the intake and exhaust processes are separate and distinct, two-stroke engines must complete this process during the short period when the piston passes through bottom dead center (BDC) [26].

In two-stroke engines, every downward stroke of the piston serves as a power stroke, which means that gas exchange must be conducted efficiently to maintain performance. This requires the burned gases to be expelled from the cylinder and fresh air to be introduced while the piston is near BDC. The gas exchange process is divided into two main periods: the exhaust blowdown period, which starts when the exhaust valve opens, and the scavenging period, when fresh air displaces the remaining exhaust gases [26]. These periods are marked in Figure 3.4a, where the cylinder pressure of a typical combustion cycle is plotted against the displaced volume.

Uniflow scavenging, the most common type used in modern large two-stroke diesel engines, involves air entering the cylinder through ports located low in the cylinder wall and exiting through an exhaust valve in the cylinder head [23], as illustrated in Figure 3.5. This setup optimizes the scavenging process by allowing air to move in a single, consistent direction, which improves the efficiency of gas displacement. The higher efficiency of uniflow scavenging compared to other methods helps reduce the presence of residual gases and enhances the overall combustion process.

To maintain the necessary air capacity for efficient operation, large two-stroke engines often rely on

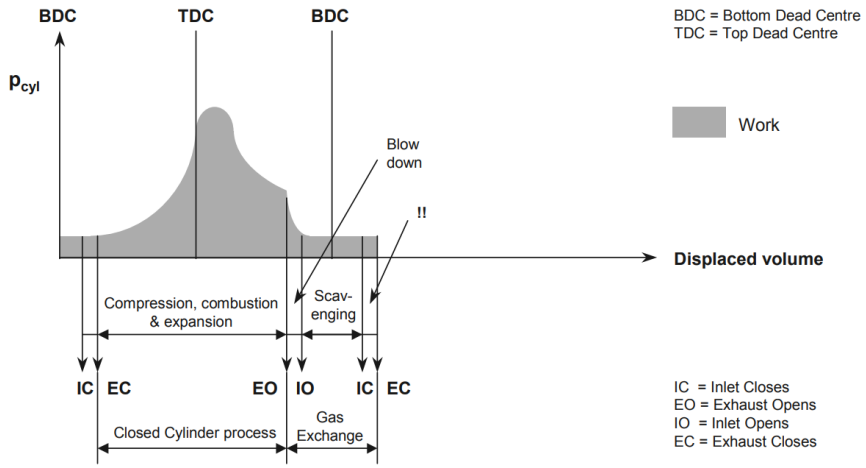

(a) two-stroke

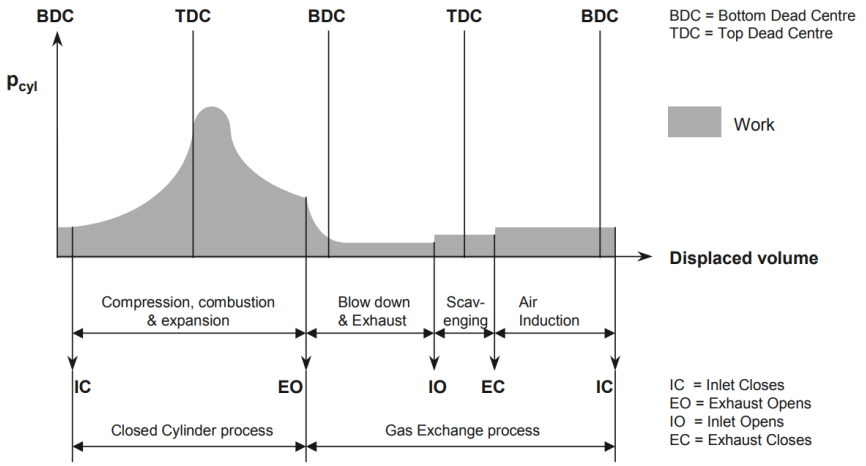

(b) four-stroke

Figure 3.4: Pressure in cylinder versus displaced volume [23]

turbochargers and intercoolers to boost air pressure, ensuring that sufficient air mass flow is achieved [26]. Despite these efforts, the short duration of the gas exchange period can limit the effectiveness of the scavenging process. This can leave residual exhaust gases in the cylinder, which could negatively impact the subsequent combustion cycle and overall engine performance.

Air slip

Scavenging in two-stroke engines comes with inherent challenges. One of the most significant issues is charging losses. Heywood [24] notes that, under normal conditions, approximately 20% of the fresh air charge can be lost through short-circuiting or slip, a process where the fresh charge passes straight through the cylinder and exits the exhaust without contributing to combustion. In engines where fuel is introduced during the scavenging process, such as Port Fuel Injection (PFI) or LPDI engines, an engine type which will be further explained in chapter 4, this process results in emissions of unburned fuel and thereby causes poor fuel economy in case the timing of the fuel injection is overlapping with the exhaust valve being open [29].

To mitigate air slip and minimize fuel losses during scavenging, various strategies can be employed. Serrano [30] discusses two primary solutions to address this issue. The first approach involves adjusting the timing of the exhaust valve closure. By closing the exhaust valve earlier, the time available for fuel to escape is reduced, thereby decreasing the amount of unburned fuel that slips through the

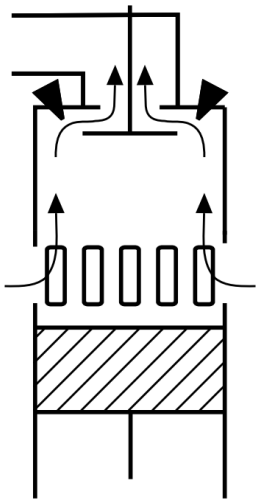

Figure 3.5: Scavenging in a two-stroke diesel engine [23]

exhaust. This method can be implemented with minimal modifications to the engine, as it only requires adjustments to the exhaust valve's opening cam.

The second proposed solution is to inject the fuel after the exhaust valve has closed. This strategy ensures that there is no opportunity for hydrogen to escape during the scavenging phase, as the exhaust pathway is already sealed. It should be noted, however, that this injection would take place during the beginning of the compression stroke. Therefore, careful consideration must be given to the required fuel pressure to ensure that sufficient fuel can be delivered into the cylinder, which is already under increasing pressure.

Jiao [22] investigated whether it would be possible to inject the required amount of hydrogen during the early part of the compression stroke for this specific type of engine. His findings suggest that this can indeed be achieved successfully, making this a promising option for hydrogen fuelling in large two-stroke marine engines.

3.4. Summary and outlook

The information presented in this chapter underscores the wealth of knowledge available on two-stroke marine diesel engines, which have been a mainstay in the maritime industry for decades due to their efficiency and reliability. The established use and extensive documentation of these engines provide a solid foundation for understanding their operation.

There is also relevant information available on LPDI two-stroke engines that run on alternative fuels, such as LNG [31–37]. These engines share similar concepts and design principles with what could potentially be used for hydrogen adaptation. The experience gained from these LNG-powered systems provides useful insights into how modifications might be made to accommodate hydrogen as a fuel in large two-stroke engines. However, despite these parallels, the literature specifically addressing the use of hydrogen in large marine two-stroke engines remains scarce.

To bridge this knowledge gap, the next chapter will explore the general combustion properties of hydrogen across various engine types. This analysis will provide a comprehensive understanding of hydrogen's combustion behaviour, highlighting its unique characteristics and the challenges it presents. The chapter will ultimately aim to identify which aspects of hydrogen combustion can be applied or adapted for use in large two-stroke marine engines.

4

Hydrogen as a fuel for Internal Combustion Engines

Hydrogen is increasingly being explored as a clean alternative to conventional fossil fuels in internal combustion engines. Its unique chemical and physical properties offer both opportunities and challenges for practical implementation. This chapter provides an overview of the hydrogen combustion process, including its emissions profile and the fundamental combustion characteristics of hydrogen.

Different engine types that have been tested or adapted for hydrogen use are discussed, with a particular focus on how hydrogen behaves in four-stroke and two-stroke engine configurations. The chapter also explores the most pressing combustion-related issues, such as backfiring, pre-ignition, and knocking, and examines the strategies developed to address these problems. Key topics include the effect of air-fuel equivalence ratios, suitable ignition methods, and fuel injection techniques, all of which play a critical role in achieving stable and efficient hydrogen combustion.

4.1. Combustion process

To understand the application of hydrogen in internal combustion engines, it is essential to first examine the fundamental combustion process. This section outlines the key physical and chemical properties of hydrogen that influence its combustion behaviour, such as flame speed, ignition energy, and diffusivity. Additionally, the emissions characteristics of hydrogen combustion are discussed, highlighting both the environmental benefits and the specific challenges related to pollutant formation.

Combustion characteristics

Hydrogen as a combustion fuel has various distinct combustion characteristics, which are represented with respect to other common combustion fuels in table 4.1. One of its most notable properties is the much higher laminar flame speed compared to conventional hydrocarbon fuels. The laminar flame speed of hydrogen in air is several times faster than that of hydrocarbon-air mixtures due to its higher diffusivity [26]. Specifically, Akal [11] highlights that under stoichiometric and atmospheric conditions, hydrogen's flame speed can reach 2.83 m/s, while gasoline achieves only 0.3 m/s. This rapid combustion can be advantageous for efficiency, but it also requires careful control to avoid combustion instabilities and overloading of engine limits such as maximum pressure rise rate [38]. Another crucial property is hydrogen's wide flammability range, spanning from 4% to 75% by volume in air [26]. This extensive range facilitates ultra-lean combustion, significantly impacting the emissions of a hydrogen as further explained in section 4.1.

Hydrogen's impact on engine performance is also significant. Heywood [26] notes that when mixed with air in stoichiometric proportions, hydrogen occupies approximately 30% of the fuel-air mixture's volume, compared to less than 2% for gasoline. This large volume fraction results in a reduction in power output per unit of displaced cylinder volume. Verhelst [39] echoes this, highlighting that hydrogen's large volume fraction directly influences the attainable engine power density. This reduction in volumetric

efficiency is especially noticeable in pre-mixed engines, where it can lead to lower torque and power [11].

Table 4.1: Hydrogen properties compared with gasoline, diesel, and methane [40]

Property	Hydrogen	Methane	Gasoline	Diesel
Carbon content (mass%)	0	75	84	86
Lower (net) heating value (MJ/kg)	119.9	45.8	43.9	42.5
Density (at 1 bar & 273 K; kg/m^3)	0.089	0.72	730–780	830
Volumetric energy content (at 1 bar & 273 K; MJ/m^3)	10.7	33.0	33 × 10^3	35 × 10^3
Auto-ignition temperature (K)	853	813	~623	~523
Minimum ignition energy in air (mJ)	0.02	0.29	0.24	0.24
Stoichiometry air/fuel mass ratio	34.4	17.2	14.7	14.5
Quenching distance (mm)	0.64	2.1	~2	-
Laminar flame speed in air (m/s)	1.85	0.38	0.37–0.43	0.37–0.43
Flammability limits in air (vol%)	4–76	5.3–15	1–7.6	0.6–5.5

Emissions

Hydrogen combustion offers significant advantages in reducing carbon emissions compared to traditional hydrocarbon fuels, but it presents unique challenges in controlling nitrogen oxides (NOx) emissions, particularly under certain combustion conditions. In this section, the emissions characteristics of hydrogen are examined, with a focus on its impact on carbon and nitrogen emissions.

Carbon

One of the most compelling reasons for exploring hydrogen as a fuel for internal combustion engines is its potential to eliminate carbon-based emissions. Since hydrogen does not contain carbon, its combustion results in no carbon monoxide (CO), CO_2, or unburned hydrocarbons (UHC). As represented in equation 4.1, the complete combustion of hydrogen with oxygen simply results in the formation of water [41].

$$2H_2 + O_2 \rightarrow 2H_2O \tag{4.1}$$

This absence of carbon-based pollutants is a significant advantage over traditional hydrocarbon fuels, which are major contributors to global greenhouse gas emissions and urban air pollution. The use of hydrogen, therefore, holds the promise of drastically reducing the carbon footprint of internal combustion engines, making it an attractive alternative for decarbonising heavy-duty transport and marine applications.

It should be noted, however, that even in a hydrogen-fuelled engine, trace amounts of carbon emissions may still occur due to the combustion of lubrication oil. During operation, small quantities of engine oil can enter the combustion chamber and partially burn, resulting in minor carbon-based emissions. While these emissions are expected to be negligibly small compared to those from conventional fuels, they do contribute a minimal amount of CO_2 to the exhaust and should be acknowledged in a complete emissions analysis.

However, it is important to acknowledge that hydrogen combustion only results in zero carbon emissions if the hydrogen itself is produced through sustainable means, such as electrolysis powered by renewable electricity. In many cases, hydrogen is still produced from natural gas through processes such as steam methane reforming, which release significant amounts of CO_2 during production [26]. Thus, while hydrogen is technically a non-carbon-emitting fuel at the point of use, the overall carbon footprint depends heavily on how the hydrogen is produced. Only when hydrogen is generated using renewable energy can it be considered a fully carbon-free fuel.

Nitrogen

While hydrogen fuel completely eliminates carbon emissions, its effect on NOx emissions, is more complex. NOx emissions are primarily influenced by combustion temperature, and the high combustion rate of hydrogen tends to increase temperatures and therefore NOx production [11]. This is particularly concerning for stoichiometric combustion, where the high adiabatic flame temperature of hydrogen can

result in significantly increased NOx levels [39]. In these conditions, some of the nitrogen (N_2) which is abundantly present in the air, reacts with oxygen (O_2) as represented in equitions 4.2 and 4.3 to form NO and NO_2 [41].

$$N_2 + O_2 \rightarrow 2NO \tag{4.2}$$

$$2NO + O_2 \rightarrow 2NO_2 \tag{4.3}$$

However, strategies exist to mitigate these NOx emissions. Onorati [42] highlights that ultra-lean combustion, where the air-fuel mixture is heavily diluted with air, can substantially reduce NOx formation. During lean combustion, the peak temperatures in the combustion chamber are much lower, slowing down the rate at which NOx is produced. Akal [11] supports this by noting that in lean mixtures, the temperature does not rise significantly at the end of combustion, thereby reducing NOx formation. Furthermore, White [38] explains that under ultra-lean operation, combustion temperatures are low enough to bring NOx formation rates near zero, effectively minimising engine-out emissions.

4.2. Engine types

The focus of this study is on the feasibility of hydrogen combustion in large two-stroke marine engines. However, since there are currently no practical implementations of hydrogen-fuelled two-stroke marine engines, it is essential to broaden our perspective by examining hydrogen combustion in other types of engines. Understanding the typical challenges and opportunities of hydrogen combustion in various engine configurations provides valuable insights and possible pathways for adapting two-stroke marine engines to hydrogen as a fuel.

This section is organized into three parts. First, we will review four-stroke SI engines and four-stroke CI engines, both of which have been successfully adapted to run on hydrogen in various applications. By analysing these engine types, we can identify the specific adaptations and technologies that enable hydrogen combustion, as well as any recurring issues such as pre-ignition and backfire. These insights can serve as a foundation for understanding how hydrogen behaves as a fuel under different combustion conditions.

Additionally, we will examine two-stroke marine engines that operate on alternative fuels (other than diesel), focusing on the unique characteristics and the adaptations required for non-diesel fuel types. This includes a review of engines running primarily on fuels like Natural Gas (NG), which might share some handling and combustion challenges with hydrogen. Through this examination, we aim to identify potential strategies and adaptations that could inspire the future development of hydrogen-fuelled two-stroke marine engines.

Four-stroke spark ignited engines

Four-stroke SI engines have gained significant attention as a feasible platform for hydrogen combustion, especially within the automotive and heavy-duty sectors. Since the early 21st century, hydrogen-fuelled SI engines have become a reality in the automotive market, with research institutions demonstrating that hydrogen engines can meet stringent EU and US regulatory standards. These engines have shown promising results in terms of performance, reliability, and emission control, establishing their viability in vehicle applications [12].

Despite these advancements, hydrogen combustion in four-stroke SI engines presents distinct challenges, primarily due to the unique properties of hydrogen as a fuel. Hydrogen's low ignition energy make it prone to abnormal combustion events [12]. These issues are particularly critical in applications with larger cylinder bores and higher mean effective pressures, characteristics that are common in marine engines. The interest in hydrogen combustion for heavy-duty and marine engines has grown significantly in recent years. Various studies have begun to explore the potential of hydrogen as a clean alternative fuel in larger applications, particularly for four-stroke SI engines that operate at mid-range speeds. This interest reflects the potential for hydrogen to meet strict emission standards while providing reliable performance in applications beyond the automotive sector [43–45].

In the marine sector, medium-speed four-stroke engines are currently in use for smaller vessels and auxiliary power generation. Companies like ABC Engines, for instance, produce four-stroke SI engines that operate at 1000 rpm with power outputs ranging from 500 kW to 2670 kW. These engines utilize PFI, a technique which will be further explored in the following sections [46].

Four-stroke compression ignited engines

The use of hydrogen as a fuel for four-stroke CI engines offers a promising path towards cleaner and more efficient combustion. However, due to hydrogen's high auto-ignition temperature, implementing hydrogen in CI engines is far from straightforward. Hydrogen's resistance to auto-ignition presents a significant challenge in traditional diesel engine configurations, as even compression ratios as high as 29:1 are insufficient to reliably ignite hydrogen without external assistance [13].

Given these limitations, hydrogen combustion in CI engines typically relies on a dual-fuel approach, where hydrogen is introduced alongside a secondary fuel with a lower auto-ignition temperature, such as diesel [47, 48]. This principle is further elaborated on in section 4.4. Dual-fuel strategies for hydrogen in CI engines are not without their own challenges. The high reactivity and fast flame speed of hydrogen can lead to issues such as pre-ignition and knocking if not carefully managed. Recent advances have focused on implementing hydrogen-diesel dual direct-injection (H2DDI) systems, where both hydrogen and diesel are injected directly into the cylinder at high pressure. This technique, tested on modified single-cylinder diesel engines, allows precise control over injection timing and fuel ratio, helping to mitigate the risk of abnormal combustion events [49].

While controlled auto-ignition of hydrogen in CI engines has been explored, it requires very specific conditions and has not yet proven practical for consistent and reliable operation in real-world applications [50, 51]. For practical purposes, dual-fuel configurations remain the most effective solution for hydrogen use in CI engines, especially in applications where diesel engines are traditionally favoured. Experimental setups using hydrogen-enriched intake air have demonstrated improved efficiency and emissions performance, particularly under carefully controlled injection timings and flow rates, highlighting the potential of this approach under optimized conditions [52].

In summary, while the direct use of hydrogen in CI engines is limited by its high auto-ignition threshold, dual-fuel configurations provide a feasible and promising pathway for hydrogen integration in compression-ignited engines.

Two-stroke marine engines on alternative fuels

In recent years, research has begun exploring the feasibility of using hydrogen as a fuel in large two-stroke marine engines. Although this research is still in its early stages, initial investigations focus on validating the core concept of hydrogen combustion in two-stroke marine engines [21, 30]. Current studies primarily build upon the design of two-stroke engines that operate on NG using LPDI. This design offers a foundation upon which to test hydrogen as a potential fuel, given that both NG and hydrogen share challenges related to storage, handling, and controlled combustion in high-power marine applications.

An important feature of NG two-stroke engines is the use of pilot fuel injection to initiate combustion. Similar to the dual-fuel approach seen in hydrogen four-stroke CI engines, a small amount of diesel is injected to trigger the combustion of the main fuel. In these engines, the quantity of pilot fuel needed is minimal, less than 1% of the total energy input at full engine load [35–37].

The success of LPDI and pilot fuel injection in NG engines provides a pathway to consider a similar approach for hydrogen-fuelled two-stroke marine engines. While hydrogen-fuelled two-stroke marine engines remain a conceptual prospect, the advancements in NG two-stroke engines provide valuable insights. By adapting the LPDI technique and pilot fuel injection approach, it may be feasible to develop a robust hydrogen combustion system for two-stroke marine applications.

4.3. Combustion problems

Hydrogen-fueled internal combustion engines face several combustion challenges that can impact performance and reliability. The most notable issues are backfiring, pre-ignition, and knocking, each of which arises from the specific combustion properties of hydrogen. These phenomena must be carefully managed to ensure the safe and efficient operation of hydrogen engines. The following sections provide an overview of these abnormal combustion events and their underlying causes.

Backfiring

Backfiring is triggered by uncontrolled combustion of the fresh hydrogen-air mixture, often initiated by hot spots left by waste gases in the combustion chamber. These hot spots can ignite the hydrogen prematurely, causing the flame to propagate backward into the intake manifold [11]. This issue is exacerbated by hydrogen's small flame quenching distance, the minimum distance at which a flame can be extinguished. Hydrogen flames can propagate through much smaller gaps compared to conventional hydrocarbon fuels, such as the gaps between the intake valve and valve seat, which increases the risk of backfiring [42].

Backfiring is primarily a problem in four-stroke engines, particularly those using port fuel injection. In these engines, the intake and compression strokes are separate, allowing hydrogen to be present in the intake manifold for a longer period before combustion occurs. During the intake stroke, the fuel-air mixture is drawn into the cylinder, and if any hot spots or residual gases are present, they can ignite the mixture prematurely, resulting in backfiring. Park [53] points out that in four-stroke engines using port fuel injection, the risk of backfire is heightened due to the presence of hydrogen in the intake manifold during the intake stroke, where heat sources can ignite the mixture.

However, this issue is much less prominent in two-stroke engines, especially those utilizing in-cylinder direct injection systems. In two-stroke engines, the intake and compression occur during the same stroke, and hydrogen would be injected directly into the cylinder during the compression stroke, avoiding the intake manifold altogether. This method fundamentally eliminates the risk of backfiring, as hydrogen does not exist in the intake manifold during the intake process [53]. In two-stroke engines, the direct injection of hydrogen into the cylinder means that the fuel can be introduced at the moment when the inlet ports are already closed, and not during the intake stroke where backfiring risks arise. This shorter time window for hydrogen exposure in the cylinder, combined with the absence of hydrogen in the intake manifold, significantly reduces the likelihood of backfiring in two-stroke configurations.

Pre-ignition

Pre-ignition is a significant issue in hydrogen-fueled internal combustion engines. Pre-ignition refers to the spontaneous combustion of the fuel-air mixture in the combustion chamber before the intended start of the combustion, often caused by residual heat or hot spots in the chamber. This early combustion disrupts the intended ignition timing and can lead to abnormal combustion events such as knocking.

Hydrogen's low ignition energy plays a critical role in its susceptibility to pre-ignition. Hydrogen's minimum ignition energy in air, particularly at stoichiometry, is an order of magnitude lower than that of hydrocarbon fuels [18]. This low threshold makes hydrogen more prone to being ignited by hot spots or residues in the combustion chamber, such as leftover exhaust gases or overheated engine components [38]. Consequently, even minor heat sources can initiate combustion during the compression stroke, well before the intended combustion moment.

The risk of pre-ignition increases with certain engine configurations and operational conditions. High compression ratios and increased mixture temperatures are known to exacerbate pre-ignition issues, as they raise the likelihood of hot spots forming in the combustion chamber. White [38] observed that the pre-ignition-limited equivalence ratio ϕ decreases as the compression ratio and mixture temperature increase, further constraining the operability of hydrogen engines near stoichiometric conditions. This phenomenon highlights why it is challenging to operate hydrogen internal combustion engines near stoichiometric conditions without encountering frequent pre-ignition events.

In-cylinder direct injection can also play a crucial role in minimizing pre-ignition. In-cylinder direct injection of hydrogen, particularly when injected late in the compression stroke, reduces the time the hydrogen-air mixture is present in the combustion chamber, limiting its exposure to potential hot spots. However, even with early direct injection, where hydrogen is introduced in the first half of the compression stroke, there is still a possibility of pre-ignition due to heat sources within the chamber. This risk, although reduced compared to port fuel injection systems, underscores the importance of carefully controlling injection timing and chamber conditions in hydrogen engines.

Knocking

Knocking occurs when the unburned air-fuel mixture in the cylinder spontaneously ignites ahead of the propagating flame front. As the flame front progresses through the air-fuel mixture, the pressure in the cylinder increases, compressing and heating the gas mixture to the point where it auto-ignites before the flame reaches it. This creates shockwaves that reverberate through the cylinder, causing the characteristic knocking sound. In hydrogen-fueled engines, the cause for the occurrence of knocking is a topic of debate, as the literature presents conflicting perspectives on the octane rating of hydrogen, which is directly linked to its resistance to knock.

Poursadegh [54] highlights this contradiction, noting that some studies report hydrogen's Research Octane Number (RON) to be as low as 60–64, while others suggest values above 130. Standard RON test methods, which were originally developed for liquid fuels, show lower values for hydrogen. However, these tests do not accurately reflect the real-world conditions in which hydrogen engines would operate. When more practical testing methods are used, hydrogen's RON appears to range between 93.7 and over 120, depending on the equivalence ratio.

One of the primary reasons why knocking is a concern in hydrogen engines is hydrogen's high flame speed. The fast flame propagation in hydrogen-fueled engines can compress the gas mixture more rapidly than in conventional hydrocarbon engines, increasing the likelihood of autoignition. Boretti [55] describes knocking as a "race against time" to burn the fuel-air mixture before it self-ignites due to rising pressure and temperature during the compression stroke.

Despite hydrogen's fast flame speed, its high autoignition temperature helps reduce the overall risk of knocking compared to hydrocarbon fuels. White [38] notes that hydrogen's higher autoignition temperature and fast flame propagation actually give the end gas less time to ignite before the flame front reaches it.

The distinction between knock and pre-ignition can be difficult to detect in hydrogen engines, as both phenomena produce similar audible knocking sounds. While knock can be controlled by retarding spark timing, pre-ignition cannot, making it crucial to differentiate between the two when designing hydrogen engines. [38]

To mitigate knocking, several strategies can be employed. As Akal [11] suggests, controlling the compression ratio and maintaining an appropriate air excess ratio (λ) are key factors in preventing knock. For hydrogen engines, lean-burn strategies are particularly effective. Bekdemir [56] found that operating with a λ value between 1.8 and 2.4 yields the best thermal efficiency while minimising the risk of knocking. This lean mixture reduces the reactivity of the hydrogen-air mixture, lowering the end-gas temperatures and reducing the likelihood of autoignition. Furthermore, introducing water or nitrogen into the combustion chamber can help to cool the mixture and prevent excessive pressure and temperature rise, further decreasing the risk of knocking [11].

Next to that, HPDI systems can eliminate the risk of knock by avoiding the premixing of hydrogen and air. Bekdemir [56] notes that in HPDI compression ignition systems, where hydrogen is injected directly into the combustion chamber just before ignition, the risk of knock is virtually absent. This is because the fuel does not spend enough time in the combustion chamber to autoignite prematurely, and the combustion process is more tightly controlled. However, this system often leads to higher NOx emissions, which must be addressed with additional after-treatment solutions.

4.4. Combustion strategies

In this section, various combustion strategies are explored that are used in practice to improve the performance of hydrogen-fueled engines and address the typical combustion problems discussed earlier. These strategies, which include adjustments to the air equivalence ratio, ignition systems, and injection methods, are critical to ensuring the safe and efficient operation of hydrogen engines. By understanding and optimizing these combustion techniques, it is possible to mitigate many of the unique challenges associated with hydrogen as a fuel.

Air equivalence ratio

In hydrogen-fueled internal combustion engines, the air equivalence ratio plays a critical role in determining engine performance, efficiency, and emissions. Hydrogen is well-suited to lean combustion, meaning it can operate efficiently with a significant excess of air. While this is not unique to hydrogen, since large marine diesel and dual-fuel engines also typically operate under lean-burn conditions with λ values often exceeding 2, it is particularly beneficial for hydrogen due to its high reactivity and susceptibility for pre-ignition and knocking. Operating under lean conditions helps mitigate these issues, improves thermal efficiency, and contributes to reduced NOx emissions when carefully managed. Thus, the air-fuel ratio becomes a key parameter in addressing the specific combustion challenges associated with hydrogen.

Running a hydrogen engine on a lean mixture can significantly improve thermal efficiency while simultaneously reducing harmful emissions, particularly NOx. Bekdemir [56] notes that lean operation increases the heat capacity ratio (γ), which enhances thermal efficiency. The hydrogen engines in his experimental setup typically achieve their best brake thermal efficiency and robust operation when λ values are between 1.8 and 2.4. This lean running strategy is facilitated by hydrogen's wide flammability range, which allows stable combustion across a broad spectrum of air-fuel mixtures [13]. Moreover, Stepien [40] explains that the lower flame temperatures associated with lean mixtures reduce heat transfer to the engine walls and improve fuel economy, further enhancing overall efficiency.

One of the key factors affecting hydrogen engines' lean operation is flame speed. According to Heywood [26], flame propagation in hydrogen-air mixtures is much faster than in hydrocarbon-air mixtures, especially near stoichiometric conditions. This rapid flame propagation can lead to pre-ignition and knocking under rich or stoichiometric conditions, as discussed earlier. To prevent these issues, hydrogen engines typically run far lean of stoichiometric, where the flame speed is lower and more manageable, reducing the risk of combustion problems such as pre-ignition and knocking. Boosting the engine under lean conditions helps compensate for the power loss that typically accompanies lean mixtures, maintaining acceptable brake mean effective pressure (bmep) levels.

In terms of emissions control, lean running plays a crucial role in minimizing NOx formation, which is particularly problematic in high-temperature combustion environments. Early research by De Boer [57] demonstrated that NOx concentrations in hydrogen engines are strongly influenced by the air-fuel ratio, with a rapid increase in NOx occurring for λ values below 1.6. By operating at λ values above this threshold, NOx formation is reduced because flame temperatures are lower in lean mixtures. Similarly, White [38] highlights that under ultra-lean operation, the combustion temperatures are sufficiently low to slow NOx formation rates, resulting in near-zero engine-out NOx emissions. This makes lean operation an attractive strategy for hydrogen engines in terms of both efficiency and emissions reduction.

However, lean running also introduces new challenges. One key issue is the increased susceptibility to autoignition at lean conditions. While lean mixtures generally reduce the risk of pre-ignition and knock, overly lean mixtures can extend the combustion duration and create the conditions for autoignition resulting in knocking [54]. This highlights the delicate balance required to optimize hydrogen engine performance under lean conditions while avoiding the combustion issues discussed in the previous section.

Finally, Akal [11] points out that knocking can still occur under lean conditions if the compression ratio or mixture richness is not adequately controlled. For this reason, strategies such as introducing water or nitrogen into the mixture can help cool the combustion process and prevent the excessive pressure and temperature rise that leads to knocking. These measures, combined with lean running, can significantly mitigate the risk of abnormal combustion events in hydrogen engines.

Ignition

Ignition plays a critical role in determining the performance and efficiency of hydrogen engines, and the method of ignition varies depending on the engine type. Two main engine types can be distinguished, which are SI engines and CI engines. In SI engines, the fuel-air mixture is ignited by a spark plug, which initiates a flame front that propagates through the mixture. In contrast, CI engines, such as diesel engines, rely on autoignition, where the fuel ignites spontaneously due to high pressure and temperature conditions within the cylinder.

CI engines have become the standard in heavy-duty applications and the maritime sector due to their efficiency and durability under high loads, making them natural candidates as a design starting point for marine hydrogen (H_2) engine design. However, converting these engine designs to hydrogen combustion poses significant challenges, primarily because hydrogen is not inherently suitable for autoignition in CI engines. Hydrogen's high auto-ignition temperature, approximately 584 °C, presents a major obstacle for direct combustion in CI engines. This temperature is significantly higher than that of gasoline or natural gas, meaning hydrogen will not spontaneously ignite under typical compression conditions in a diesel engine. To overcome this limitation, an internal ignition source is required to trigger combustion, such as a spark or the use of a supplementary fuel with a lower auto-ignition temperature [11, 13]. Furthermore, the high pressure DI method commonly used in CI engines is not directly applicable to hydrogen as a fuel, which will be elaborated on in the next section.

The subsections that follow will explore three ignition strategies that are either commonly used or show potential for application in hydrogen-fuelled engines: spark plugs, prime fuel, and pre-chamber ignition.

Spark plugs

In SI engines, the combustion process is initiated by a spark plug, which ignites the premixed fuel-air mixture. This ignition system is fundamental to SI engines, as the spark discharge triggers the flame front, which then propagates through the cylinder, consuming the mixture and ultimately extinguishing at the combustion chamber walls [26]. For hydrogen-fueled SI engines, the role of the spark plug is particularly crucial due to the high reactivity of hydrogen and the need for precise control of the ignition timing [58].

Premixed combustion is characteristic of SI engines, where the air and fuel are mixed before entering the combustion chamber. Pu [59] notes that this homogeneous mixture, once ignited by the spark plug, forms a propagating flame front that travels through the combustion chamber. The presence of turbulence can enhance the speed of this flame propagation, leading to shorter combustion duration at higher loads, which is often desirable in SI engines. However, with hydrogen's high flame speed, careful management of the spark timing and air-fuel ratio is critical to avoid abnormal combustion events such as pre-ignition or knocking.

One of the key challenges in hydrogen engines, particularly for large two-stroke marine hydrogen engines, is that traditional spark ignition systems may not provide enough energy to reliably ignite ultra-lean hydrogen-air mixtures [60]. Qu [21] highlights that in these large engines, ordinary spark plugs are often insufficient to penetrate and ignite the lean mixture uniformly throughout the large cylinder bore. This can lead to unstable flame propagation, which compromises engine efficiency and stability. To address this, additional ignition strategies, such as pilot diesel injection, are sometimes employed to assist in the ignition process, providing more reliable combustion under ultra-lean conditions.

In summary, spark plugs play a central role in the ignition process for SI engines, including hydrogen-fueled configurations. While they work effectively in smaller engines or under stoichiometric conditions, larger hydrogen engines with leaner mixtures might require enhanced ignition strategies to ensure stable combustion and efficient operation.

Prime fuel

In CI engines, the combustion process relies on the autoignition of fuel under high pressure and temperature conditions. Traditionally, fuel is directly injected just before combustion is required. This leads to spontaneous ignition due to the high temperatures reached during compression [26]. However, when hydrogen is used as the primary fuel in CI engines, its high autoignition temperature presents a significant challenge. Hydrogen alone cannot autoignite reliably under the conditions typical of CI operation, requiring alternative strategies to trigger combustion [61].

One of the most practical solutions for overcoming this challenge is the use of a prime fuel to initiate the combustion process [62]. As Dimitriou [13] explains, hydrogen's implementation in CI engines has proven more effective when combined with a supplementary fuel that has a lower autoignition temperature. Diesel fuel, which autoignites more readily under compression, is often used as this combustion trigger. The diesel is typically injected into the cylinder near top dead center (TDC), where it ignites and initiates the combustion of the premixed hydrogen-air mixture. This dual-fuel approach

allows the engine to harness hydrogen's efficiency and cleanliness while maintaining the reliability of the autoignition process.

The challenge of using hydrogen alone in CI engines has been well-documented. Homan et al. [63] attempted to operate a hydrogen-fueled CI engine without any supplementary fuel but found the operational range to be extremely limited. Even at an extreme compression ratio of 29:1, hydrogen's resistance to autoignition remained a critical barrier, making it clear that hydrogen, by itself, is not well-suited for conventional CI combustion processes. This highlights the necessity of incorporating a prime fuel in hydrogen-fueled CI engines to ensure stable and consistent combustion.

Pre-chamber ignition

Pre-chamber ignition is an advanced ignition strategy that shows great promise for enabling stable and efficient combustion of hydrogen under ultra-lean conditions. In this concept, a small auxiliary chamber, called the pre-chamber, is connected to the main combustion chamber via one or more narrow orifices. During operation, a small quantity of fuel is injected into the pre-chamber, which is then ignited by a spark plug. The resulting combustion in the pre-chamber generates high-temperature, high-pressure gases that are expelled through the orifices into the main chamber as a series of turbulent flame jets. These jets act as distributed ignition sources, effectively igniting the ultra-lean mixture in the main chamber at multiple points simultaneously, thus enhancing combustion stability and speed.

The advantage of this approach lies in its ability to initiate combustion reliably even at very high air excess ratios, which are typical in hydrogen-fuelled engines operating under lean conditions. Multiple studies have demonstrated that pre-chamber systems, particularly turbulent jet ignition (TJI), can extend the lean limit significantly while also reducing cycle-to-cycle variation, emissions, and combustion duration [64, 65]. These characteristics are especially valuable for hydrogen combustion, which is known for its susceptibility to pre-ignition and knock under stoichiometric or rich conditions, and for its tendency to become unstable under ultra-lean conditions.

While pre-chamber ignition systems are more commonly investigated for smaller spark-ignited engines, the underlying principles could be highly relevant to large, low-speed marine engines running on hydrogen. These engines generally operate at high loads and benefit from lean combustion to suppress NOx emissions. Implementing a pre-chamber system in such engines could enable stable ignition and combustion of hydrogen with minimal reliance on fossil-based pilot fuels.

Fuel injection

The unique properties of hydrogen as a fuel require careful consideration of the fuel injection method employed, as each method has distinct advantages and limitations in controlling combustion characteristics. Hydrogen's low ignition energy makes it particularly sensitive to timing and mixture conditions, necessitating precise fuel injection strategies to manage these challenges effectively.

Hydrogen fuel can be introduced into the engine using PFI, LPDI, or HPDI methods [53, 66]. PFI, where hydrogen is injected into the intake manifold, has been the preferred option for many hydrogen engine prototypes due to its simplicity and ease of adaptation from existing gasoline engines [42]. However, challenges related to backfire, pre-ignition, and volumetric efficiency have limited the widespread adoption of PFI in high-power applications [15, 17, 43].

Direct injection methods, which deliver hydrogen directly into the combustion chamber, have become increasingly favoured due to their potential to address the limitations associated with PFI. Direct injection systems allow for better control over fuel timing and mass flow, enabling higher power output, improved efficiency, and a reduction in abnormal combustion events [14, 43].

In the sections that follow, each of these fuel injection methods, PFI, HPDI, and LPDI, will be examined, highlighting their respective strengths and limitations in the context of hydrogen combustion.

Port Fuel Injection

PFI is a commonly used method for introducing hydrogen into the intake manifold of four-stroke internal combustion engines. In PFI systems, hydrogen is injected into the intake port upstream of the intake valve during the intake stroke, as visually represented in Figure 4.1. This system offers the advantage of uniform mixing of fuel and air prior to combustion, allowing a more straightforward conversion from

conventional gasoline engines to hydrogen-fuelled engines. Due to the relative simplicity of retrofitting gasoline engines with PFI systems for hydrogen use, this approach has been widely adopted in hydrogen engine prototypes, particularly in the automotive sector [16, 18, 42].

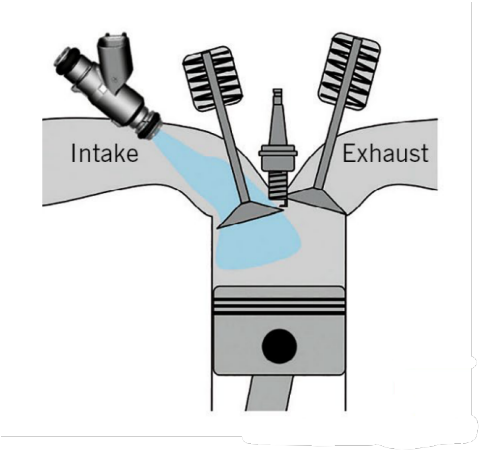

Figure 4.1: Schematic representation of PFI [15]

PFI, however, comes with notable limitations. Hydrogen's low minimum ignition energy and short quenching distance in combination with PFI, can further amplify issues such as pre-ignition, knock, and backfiring. Moreover, since hydrogen is introduced into the intake manifold alongside air, it displaces part of the fresh air charge, reducing volumetric efficiency and, consequently, power density. This is especially detrimental in applications where high power output is required, as it limits the engine's ability to perform at peak efficiency [18].

The use of PFI is typically limited to four-stroke engines that feature an intake manifold and an intake valve. Marine two-stroke engines, in contrast, do not employ traditional intake manifolds or intake valves; instead, they use intake ports for gas exchange, making PFI impractical for these engines. A notable exception exists in an engine design proposed by Serrano [30], who modelled a two-stroke engine designed to run on hydrogen-enriched air, where hydrogen is mixed with air in the engine plenum before entering the cylinder. However, the concept of hydrogen-enriched air poses significant risks for applications in marine two-stroke engines, due to the likelihood of abnormal combustion events occurring using this method. Given the scale of these engines and their operational demands, the consequences of such events could be catastrophic, making this approach less viable for marine applications. For this reason, PFI remains largely restricted to four-stroke hydrogen engines, where its limitations can be managed and the risks of abnormal combustion are comparatively lower.

High Pressure Direct Injection

HPDI represents a promising approach for hydrogen fuel injection in internal combustion engines, particularly due to its potential for higher efficiency and improved control over combustion characteristics. In an HPDI system, hydrogen is injected directly into the cylinder under high pressure, typically during the compression stroke, when the intake valves are already closed. A visual representation of this is given in Figure 4.2 This timing ensures that no ignitable mixture forms in the intake manifold, thus preventing backfire and minimizing the risk of pre-ignition by reducing the time hydrogen is exposed to hot spots within the cylinder [18, 67].

HPDI systems benefit from their ability to introduce hydrogen late in the compression stroke, which can enhance thermal efficiency and power output . By injecting hydrogen at higher pressures, HPDI enables precise control over the combustion process and avoids the volumetric efficiency losses seen in PFI, where hydrogen displaces air in the intake manifold [18]. Additionally, HPDI allows for a diffusive combustion process, similar to that in diesel engines, where the combustion initiation can be reliably controlled by a spark or glow plug without the risk of an ignitable mixture forming prematurely [14].

However, the implementation of HPDI systems comes with its own challenges. Achieving the necessary injection pressure for effective HPDI requires compressors to deliver hydrogen at high pressures, which

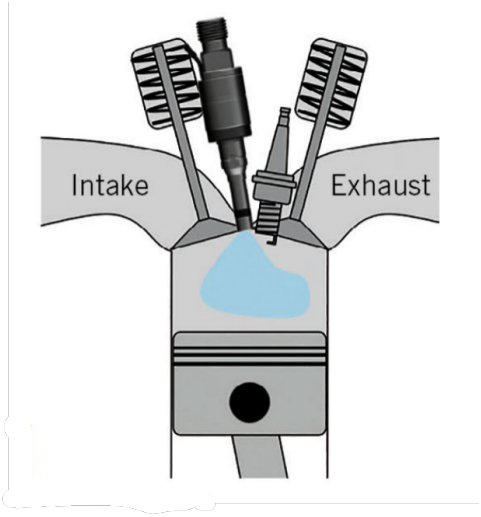

Figure 4.2: Schematic representation of HPDI [15]

may increase both the system's complexity and operational costs. Furthermore, the infrastructure needed to support high-pressure hydrogen injection, such as reinforced injectors and fuel lines, also adds to the initial cost and complexity of HPDI systems.

Despite these challenges, the potential gains in efficiency and the enhanced reliability of combustion make HPDI an attractive option for future hydrogen engine research, particularly in heavy-duty and marine applications where robust performance and reliability are essential. For example, MAN has developed a two-stroke dual-fuel engine that uses HPDI for NG, which could serve as a foundational design for adapting HPDI technology to hydrogen combustion [31, 32].

Low Pressure Direct Injection

LPDI has emerged as a promising solution for hydrogen combustion in large two-stroke engines, primarily due to its compatibility with the unique requirements and limitations of these engines. Unlike HPDI, which relies on very high injection pressures, LPDI operates at pressures typically below 50 bar, reducing system complexity and the associated infrastructure costs. While LPDI does present certain technical challenges, including the need for larger injector throat areas and specific timing adjustments, it does offers a viable approach to hydrogen injection in smaller four-stroke engines [14, 16]. This suggests that this method could be adapted effectively for larger marine applications, with specific adjustments tailored to the unique demands of two-stroke engines.

In LPDI systems for two-stroke engines, hydrogen injection would typically occur during the gas exchange phase or early in the compression stroke, as represented in Figure 4.3. This timing allows hydrogen to mix with the incoming air, forming a pre-mixture as the piston moves upward. Injection timing is critical in achieving an optimal balance between mixture homogeneity and efficiency. Early injection promotes a well-mixed pre-mixture but risks slip of unburned hydrogen through open exhaust valves, a particular challenge in two-stroke engines. Conversely, later injection can help prevent hydrogen loss but may lead to a less homogeneous mixture, affecting combustion stability and efficiency [21, 33].

Two-stroke LPDI technology has already been established for NG engines in the marine sector. The companies MAN and WinGD have succesfully implemented LPDI in two-stroke dual-fuel NG engines [35–37]. This existing infrastructure provides a foundation upon which hydrogen LPDI technology could be developed. Additionally, research is being conducted on the specific requirements for LPDI injectors in hydrogen-fuelled marine engines. Recent studies have focused on modifying injector design parameters to match the needs of large two-stroke engines, aiming to establish both the technical feasibility and the performance potential of LPDI for hydrogen applications [22].

In summary, LPDI presents a balanced approach that addresses the demands of two-stroke marine engines while managing the risks associated with hydrogen combustion. Given its compatibility with

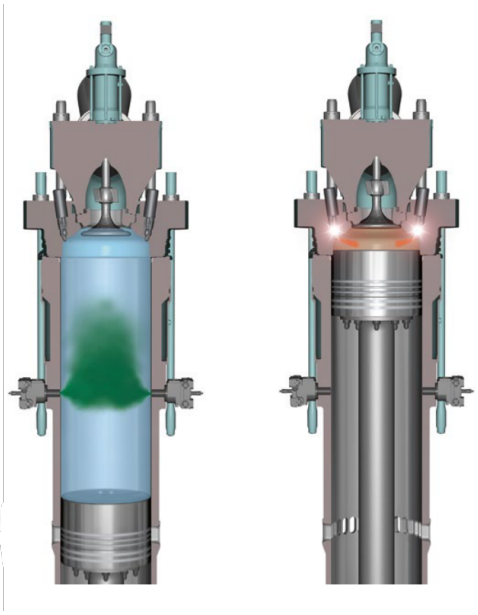

Figure 4.3: Schematic representation of LPDI and ignition by prime fuel injection in a marine two-stroke NG engine[68]

existing dual-fuel NG engine designs and its operational advantages, LPDI appears to be a highly promising solution for hydrogen-fuelled two-stroke engines. Consequently, this study adopts LPDI as the basis for evaluating hydrogen combustion in large two-stroke marine engines, positioning it as a realistic and effective injection strategy for future marine applications.

5

Engine combustion modelling

To assess the technical feasibility of hydrogen combustion in large two-stroke marine engines, a reliable and suitably detailed combustion model is essential. This chapter introduces several established modelling strategies for simulating in-cylinder processes, each with their own balance between complexity and computational demand. These include Mean Value Engine Models (MVEM), zero-dimensional (0D) models, and more advanced techniques.

Based on this overview, the modelling strategy selected for this project is introduced, including a rationale for the use of a Seiliger process to represent the combustion cycle. This forms the foundation for further refinement and analysis in subsequent chapters.

5.1. Engine modelling strategies

In engine simulation studies, various modelling techniques have been developed to balance accuracy, computational efficiency, and the ability to simulate complex internal processes. Each modelling approach has specific strengths and trade-offs, which makes them suitable for different applications in engine analysis. This section explores these modelling techniques and their applicability, followed by a discussion on selecting the most appropriate approach for this study's aim: evaluating the feasibility of hydrogen as a fuel for large, two-stroke marine engines.

Mean Value Engine Models

MVEM are widely employed for predicting the general performance characteristics of engines. MVEM approximate the processes occurring in the engine as a continuous flow across the entire operating cycle, focusing on averaged values rather than detailed crank-angle resolution [69]. By avoiding the per-cycle fluctuations in internal parameters, such as pressure and temperature, these models are computationally efficient, enabling quick evaluations of steady-state and transient behaviours [69, 70]. Due to their simplicity and reduced data requirements, MVEMs are frequently used in the design and analysis of engine control systems, where fast execution times are essential [71]. However, their reliance on averaged engine parameters limits their ability to provide detailed in-cylinder data, making them less suitable for simulations requiring precise insights into combustion characteristics.

Zero-dimensional models

0D models, in contrast, capture the internal state of the engine per crank angle, enabling the calculation of in-cylinder variables, such as pressure, temperature, and gas composition. These models rely on mass and energy conservation principles alongside gas state equations, solved in differential form [69]. Within 0D modelling, combustion can be represented through single-zone or multi-zone approaches, with single-zone models providing a practical balance between detail and computational effort [71]. The single-zone approach is particularly advantageous in applications that prioritize energy performance analysis without requiring detailed emissions modelling, as it offers reasonable accuracy with moderate computational requirements [19]. Multi-zone models, however, provide additional detail on exhaust gas

emissions and combustion characteristics, though at the cost of increased complexity and execution time.

The modular approach combining MVEM and 0D techniques represents an intermediate solution, merging the simplicity of MVEMs with the enhanced in-cylinder accuracy of 0D models. For example, in studies focusing on large marine engines, MVEMs are often extended through 0D modelling of the cylinder closed cycle, while the open cycle is left to the MVEM approximation [69, 70]. This hybrid approach benefits applications requiring accurate cylinder data without the computational burden of fully detailed models, as it enhances the MVEM's capability to predict variables like in-cylinder pressures and temperatures while preserving fast execution times. This technique is especially beneficial for performance prediction in studies on control system design, where simplicity and speed are critical [70]. This combined MVEM and 0D approach has already demonstrated its effectiveness in research exploring the feasibility of using ammonia as an alternative fuel in two-stroke marine engines [72].

Advanced modelling methods

More advanced modelling methods, such as computational fluid dynamics (CFD), offer detailed spatial and temporal resolutions of in-cylinder processes, capturing complex phenomena such as turbulence, fuel spray dynamics, and pollutant formation [19]. While CFD provides unmatched fidelity, it demands substantial computational resources, extensive input data, and long calculation times. Consequently, CFD is primarily used in research and development applications where high precision is necessary, rather than in feasibility studies requiring rapid execution.

Project approach

As demonstrated, the complexity and computational demands of a model generally increase with its level of detail, making it crucial to match the model type with the study's objectives. Since this study primarily focuses on evaluating critical engine limits (such as peak pressure, maximum temperature, air excess ratio, and combustion speed), the choice of a 0D model, potentially combined with MVEM, is well-suited to achieve a balance between computational efficiency and accuracy. This combination enables sufficient insight into combustion dynamics while allowing for feasible execution times, making it ideal for assessing the potential of hydrogen as a viable fuel for large two-stroke engines.

5.2. Seiliger model

Among the 0D modelling approaches, the Seiliger model is frequently used for its ability to represent key stages of the combustion cycle, namely, isentropic compression, constant volume heat addition, constant pressure heat addition, constant temperature heat addition, and isentropic expansion. This structure provides a versatile framework for simulating different combustion profiles with reasonable computational demands. The Seiliger model has been successfully applied in multiple studies to evaluate combustion performance and emissions in internal combustion engines [19, 73]. Given these advantages, the Seiliger approach was selected as the primary modelling framework for this study. It allows for flexible adjustment of combustion parameters, making it particularly well-suited for exploring the effects of varying hydrogen energy shares, combustion phasing, and air excess ratios in large two-stroke marine engines.

6

Conclusion

6.1. Conclusion and summary

This section provides a structured summary of the literature review, organized to address the primary research question and sub-questions presented in Chapter 2.

The central research question guiding this study is: *"How can an in-cylinder combustion model be used to evaluate the feasibility and technical implications of hydrogen operation with LPDI in large two-stroke marine engines?"*

Below, we address the first three sub-questions based on insights derived from the literature review, examining critical aspects of hydrogen combustion, marine two-stroke engines, and engine modelling approaches relevant to this application.

What key parameters are found to be of influence on the reliable combustion of hydrogen in existing hydrogen internal combustion engines?

To answer this first sub-question, we focus on the primary factors affecting hydrogen combustion stability. Research consistently identifies several combustion challenges particularly prominent in hydrogen engines, including pre-ignition and knocking, both of which arise due to hydrogen's high reactivity and low ignition energy. Although backfiring is another common issue in hydrogen engines, it is predominantly associated with four-stroke engines and will not be considered further in this study.

The main strategies applied to obtain reliable combustion in hydrogen engines include fuel-air mixture ratio, ignition method, and injection strategy. A lean combustion approach is widely adopted to prevent abnormal combustion events, as the lower reactivity and slower flame speed of lean mixtures reduce the likelihood of pre-ignition and knocking. By keeping the air-to-fuel ratio lean, engine stability improves, and NOx emissions are simultaneously minimized.

The ignition method is an essential factor in achieving stable combustion in hydrogen engines, due to hydrogen's high auto-ignition temperature, which is too high to reliably support compression ignition. As a result, hydrogen combustion generally requires an external ignition source. In smaller engines, a spark plug is often sufficient to initiate combustion. However, in larger engines, the energy provided by a single spark plug may not be adequate to ignite the entire mixture, particularly in lean conditions. To address this, alternative methods such as prime fuel injection can be used in larger engines. This prime fuel creates localized ignition that subsequently triggers the combustion of hydrogen, providing a more reliable start for the hydrogen combustion process.

Finally, the fuel injection strategy is critical. DI has demonstrated superior performance for hydrogen engines. By introducing hydrogen directly into the cylinder, DI reduces the risk of pre-ignition and avoids the volumetric efficiency losses that are common with port fuel injection systems. Direct injection also allows more precise control over the fuel's exposure to hot spots, which can help prevent knocking and enhance combustion efficiency.

How are the main characteristics of combustion in large two-stroke diesel engines generally modelled to determine the feasibility of reliable running?
To address this second sub-question, we examine both the unique operational characteristics of large two-stroke engines and the modelling strategies employed to represent their combustion processes.

Large two-stroke diesel engines operate on a cycle that requires the gas exchange process to occur within a limited time frame, with minimal assistance from the piston's motion during this phase. During the scavenging phase, both the intake ports and the exhaust valve are open, allowing burned gases to exit while fresh air is introduced. This simultaneous opening creates a flow in which a certain amount of fresh air slips through the engine without contributing to combustion. Managing this slip is particularly important when using LPDI, as unburned fuel could be lost during scavenging if the injection timing is not carefully controlled.

For modelling the combustion characteristics in these engines, three main strategies are commonly used: MVEM, 0D models, and advanced modelling techniques.

- MVEMs are often used for simplified, system-level analysis of engine performance. They approximate the engine as a continuous flow system, providing insights into average parameters like engine speed and torque without the need to model every crank angle. Due to their simplicity and efficiency, MVEMs are suitable for applications where real-time predictions are needed, such as in control system design, but are less precise in capturing detailed in-cylinder processes.
- 0D models operate on a per-crank-angle basis, using differential equations to simulate parameters like in-cylinder pressure, temperature, and gas composition over the engine cycle. These models can capture some aspects of combustion dynamics and are more detailed than MVEMs while remaining computationally efficient. They are commonly employed to predict feasibility and performance in scenarios where detailed in-cylinder data is required, such as in analysing peak pressures and temperatures.
- Advanced models, such as multi-zone and CFD simulations, provide highly detailed representations of in-cylinder processes, accounting for fluid dynamics, temperature gradients, and chemical reactions at each crank angle. Although these models offer the most accurate insights, they are computationally intensive and generally reserved for high-precision studies or specific sections of the engine cycle rather than full-cycle simulations.

For studies focusing on the feasibility of combustion in two-stroke engines, a combination of MVEM and 0D modelling often provides an effective balance, allowing reasonable accuracy in representing in-cylinder processes without excessive computational demands.

How does an in-cylinder combustion model need to be adapted to represent hydrogen combustion in a large two-stroke engine
The choice of a combustion model must align with the study's objectives, as the level of model detail directly affects both complexity and computational demands. This study primarily seeks to evaluate key engine limits, such as peak pressure, maximum temperature, air excess ratio, and combustion speed. Given these goals, a 0D model, potentially combined with a MVEM, offers an ideal balance of accuracy and computational efficiency.

In this project, a Seiliger-based model was selected as the main combustion framework, due to its relative simplicity and effectiveness in capturing the main stages of combustion, namely isentropic compression, isochoric, isobaric and isothermal combustion, and isentropic expansion. This model offers sufficient control over the distribution of energy input across different phases of combustion while maintaining low computational demands. It is particularly well-suited to evaluating engine performance over a wide range of operating conditions.

6.2. Gap analysis

The literature gap analysis identifies where existing research on hydrogen as a fuel for large two-stroke marine engines falls short. This research part of this study seeks to address part of this gap.

Firstly, a vast amount of information is available on hydrogen as a fuel, particularly in smaller four-stroke engines. Research into hydrogen's use in engines, also specifically in diesel-type engines, has

been ongoing for decades [47, 48, 57, 63]. Recent studies continue to provide insights into hydrogen's specific combustion properties and methods for managing challenges associated with hydrogen combustion [11, 42, 54]. This ongoing research establishes a solid foundation on hydrogen combustion fundamentals in smaller engines.

Additionally, the literature provides a thorough understanding of large, slow-turning marine two-stroke engines [23–26, 28]. These sources outline the combustion dynamics, mechanical configuration, and operational principles of large marine two-stroke diesel engines, offering an essential base for adapting this technology to alternative fuels.

Significant research has also been conducted on the use of alternative fuels in two-stroke marine engines, notably LNG [33, 34]. LNG-powered two-stroke engines have been implemented in real-world applications, showcasing the viability of alternative fuels in marine engines [35, 36]. Studies on using ammonia as a fuel for this engine type also show promising avenues for adaptation to low-carbon fuels [72].

Despite the promising outlook for hydrogen as a marine fuel, there is limited research specifically on its application in large two-stroke engines. The literature contains only a few studies directly examining this topic. Notably, Qu [21] offers a detailed analysis of hydrogen injection parameters for marine two-stroke engines, providing valuable data for injection system design but offering limited insights into the combustion process itself. In addition, Serrano [30] has modelled hydrogen combustion in a two-stroke marine engine but used unique injection methods that may not align with this project's LPDI approach. Nevertheless, his modelling approach will be reviewed as a potential resource.

This clearly highlights a gap in the literature regarding the feasibility of hydrogen combustion in large two-stroke marine engines. To fill part of this gap, the research part of this study will be focussed on developing a combustion model that evaluates the feasibility and challenges of using hydrogen as a fuel in large marine two-stroke engines, providing a basis for further technical development in this area.

6.3. Project approach

This section outlines the research plan developed to meet the project objectives. Following the completed literature review on hydrogen combustion, particularly focusing on in-cylinder processes in large two-stroke engines, this study now proceeds to the model development phase.

The primary aim of this phase is to construct a closed-cylinder combustion model using the Seiliger process, as previously discussed. This model will represent the combustion characteristics of hydrogen in large two-stroke engines, capturing key parameters such as peak pressure, maximum temperature, air excess ratio, and combustion speed. MATLAB Simulink is selected as the modelling environment, given its use for existing engine models at the TU Delft. The choice of MATLAB Simulink makes it possible to implement this combustion model within more comprehensive engine models as the research progresses.

This closed-cylinder model will use a 0D approach, focusing on efficient computation to facilitate parameter testing under various engine conditions. The parameters for the Seiliger process will initially be estimated using data from existing hydrogen combustion research and analogous fuels, with refinements achieved through sensitivity analysis. Ultimately, this model will serve as a practical tool to assess the feasibility of hydrogen combustion in large two-stroke marine engines, offering insights into the potential operational limits and modifications required for safe and efficient performance.

Research

7

Modelling approach

This chapter introduces the modelling approach employed in this research. It outlines the rationale behind selecting a Mean Value First Principle (MVFP) Seiliger model as the basis for evaluating hydrogen combustion in large two-stroke marine engines. The MVFP Seiliger model provides a balance between computational simplicity and the ability to accurately predict key engine parameters, such as maximum cylinder pressure, temperature, air-fuel ratio, and engine brake power. The choice of this modelling technique is justified by its effectiveness in rapidly assessing engine feasibility under varying operational conditions, thus providing valuable insights relevant to evaluating the feasibility of new engine concepts.

7.1. The diesel engine A-model

MVFP models provide an effective balance between computational efficiency and accurate representation of key thermodynamic parameters. Originally developed by Delft University of Technology and the Netherlands Defence Academy, MVFP models based on the Seiliger process have successfully been applied to simulate essential engine parameters under dynamic conditions, effectively capturing the interactions between engines, ships, and propellers during manoeuvring [74].

The MVFP modelling approach developed at TU Delft comprises two main variants: the Diesel A and Diesel B models, each serving a distinct purpose. Both models utilise the Seiliger cycle to simulate the engine combustion processes. The Diesel A model is intended as a lower level entry model, simulating general engine performance parameters based primarily on readily available manufacturer data and standard thermodynamic assumptions [75]. In contrast, the Diesel B model integrates more detailed representations of engine systems, especially advanced turbocharging strategies, requiring additional turbocharger maps and proprietary manufacturer data [76].

The Diesel A model has been chosen for this project due to its suitability for preliminary feasibility studies, the limited and readily available input data required, and its proven applicability to various configurations of marine diesel engines. It provides sufficient accuracy to assess key parameters, such as pressures, temperatures, and power, without requiring detailed data of the engine, which is not known for the specific engine considered in this project.

In the subsequent sections of this chapter, the specific implementation and functionality of the Diesel A model within the Simulink environment will be described. Attention will be given to detailing the modifications made to tailor the A-model to represent the particular two-stroke engine analysed in this study, and to enable simulations incorporating hydrogen as fuel.

Working principle of the A-model

The Diesel A-model implemented in MATLAB Simulink operates by calculating the load on the engine based on external conditions and system demands, as depicted on the right-hand side of Figure 7.1. Together with the torque output generated by the engine model, the load determines the resulting

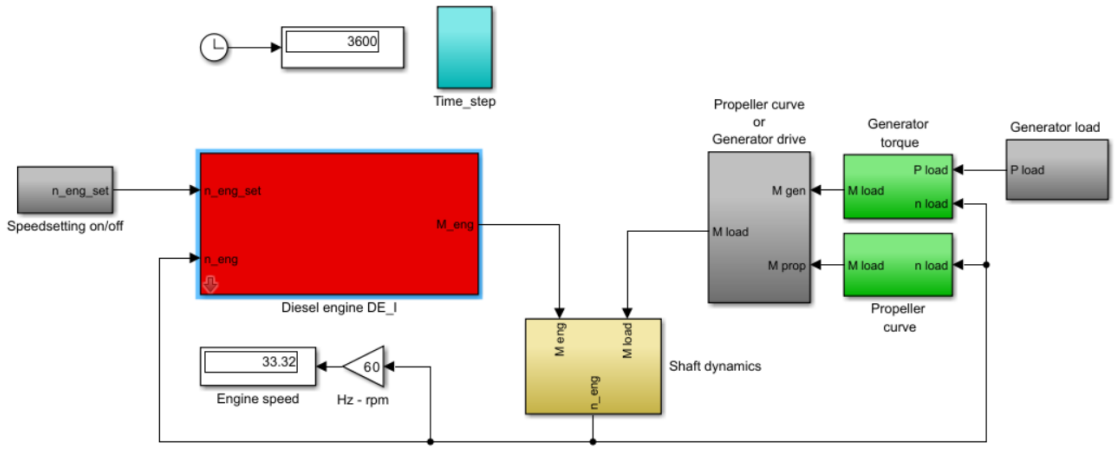

Figure 7.1: Diesel A model overview in Simulink

engine speed. This calculated engine speed subsequently feeds back as an input for both the load computations and the engine model itself, enabling dynamic interaction between these components.

In the original implementation of the Diesel A-model, the engine's fuel input is represented by a constant nominal fuel mass per cycle, based on the brake specific fuel consumption (bsfc), a standard value typically provided by the engine manufacturer. However, this value is not directly applicable when hydrogen is used as an alternative fuel, as no predefined fuel mass per cycle is available.

Consequently, the current model has been adapted to accommodate simulations involving both hydrogen and diesel simultaneously in varying proportions. Instead of the nominal fuel mass per cycle, the modified model uses the energy input per cycle along with an additional parameter known as the Hydrogen Energy Share (HES). This parameter specifies the proportion of total fuel energy supplied by hydrogen. Using the HES, the model calculates the individual fuel masses of hydrogen and diesel injected into the engine cylinder, thus enabling the determination of the air excess ratio. This approach exploits the strengths of the Diesel A-model, providing a robust basis for exploring various hydrogen-diesel fuel blends and their combustion characteristics.

In addition to the aforementioned adaptations, the model includes a configurable setting that allows the user to define whether the simulated engine operates on a two-stroke or four-stroke cycle. For the purpose of this study, the engine mode has been set to two-stroke operation. A thorough verification was conducted to ensure that all compression-related calculations were appropriately adjusted to reflect this configuration. Unlike in four-stroke engines, where the compression stroke typically spans the entire piston travel from BDC to TDC, compression in a two-stroke engine only begins after the intake ports and exhaust valves have closed. As a result, a smaller fraction of the upward piston stroke contributes to effective compression. These differences have been carefully accounted for in the model to ensure accurate simulation of compression processes specific to large low-speed two-stroke engines.

Air intake requirements

An interesting observation emerges when comparing hydrogen and diesel in terms of their respective air requirements for delivering equal amounts of combustion energy. The mass of air needed for combustion can be determined based on the stoichiometric air/fuel ratio (σ) of each fuel. For diesel this is generally assumed at 14.5, while the precise value can vary depending on the exact composition of the fuel.

$$m_{a,diesel} = m_{f,diesel} \cdot \sigma_{diesel} \tag{7.1}$$

In this equation, $m_{a,diesel}$ is the amount of air in kilogram that is required for the stoichiometric combus-

tion of the amount of fuel, $m_{f,diesel}$ is the amount of diesel fuel in kilogram, and σ_{diesel} is the stoichiometric air/fuel ratio of the fuel which is set at 14.5 for diesel fuel. Thus, to stoichiometrically combust 1 kg of diesel fuel, 14.5 kg of air is required at a minimum.

To compare this to the air requirements for hydrogen combustion, first we have to determine the amount of hydrogen that contains exactly the same amount of energy as the 1 kg of diesel. This is calculated using the lower heating value (h^L) of the fuels. For diesel, the lower heating value can be assumed to be 42.5 MJ/kg, resulting in an energy content of 42.5 MJ in 1 kg of diesel. The lower heating value for hydrogen is approximately 119.9 MJ/kg.

$$\frac{h^L_{diesel}}{h^L_{hydrogen}} = 0.354 \tag{7.2}$$

By dividing these lower heating values, it follows that 0.354 kg of hydrogen contains the same amount of energy as 1 kg of diesel. When we calculate the required amount of air to combust this amount of hydrogen, using the stoichiometric air/fuel ratio for hydrogen, which is 34.4, this results in a required air amount of 12.19 kg.

$$m_{f,hydrogen} \cdot \sigma_{hydrogen} = m_{a,hydrogen} \tag{7.3a}$$
$$0.354 \cdot 34.4 = 12.19 \tag{7.3b}$$

Interestingly, despite the substantial differences in the physical and combustion properties of hydrogen and diesel, the stoichiometric air requirements for generating equivalent energy outputs from both fuels are relatively similar, approximately 14.5 kg of air per kilogram of diesel compared to 12.19 kg of air per equivalent hydrogen mass. It should, however, be emphasised that these values represent stoichiometric conditions, which are rarely applied in practical engine operations. In actual practice, engines typically run lean, employing an air excess ratio greater than one, to ensure complete combustion and minimise undesirable emissions. For hydrogen engines specifically, operating conditions are typically set even leaner than those for diesel, to mitigate the risks associated with abnormal combustion events such as pre-ignition and knocking. Nonetheless, despite these higher practical air excess ratios, the required air mass for hydrogen combustion remains within a similar order of magnitude to that for diesel. This similarity implies that the existing engine air intake systems designed for diesel operation can largely remain unchanged when transitioning to hydrogen.Consequently, within the modelling approach, no fundamentally different air intake configuration needs to be implemented.

Initial pressure in the combustion cycle

The model requires the pressure at the start of the compression stroke as an input parameter. For conventional diesel combustion, only air is present in the cylinder during compression, and thus the charge air pressure which is typically provided by the engine manufacturer serves as a suitable estimate for this initial pressure. In the specific context of this project, however, an LPDI system is employed for hydrogen fuel injection, meaning that hydrogen is injected during the compression stroke and is therefore subject to compression alongside the air.

In reality, the hydrogen is gradually introduced during the early phase of compression, as detailed by Jiao [22]. Modelling the exact timing and rate of hydrogen injection throughout the stroke is complex and of limited relevance for a combustion model of this nature. Consequently, a simplifying assumption is made: the entire mass of hydrogen injected per cycle is considered to be present in the cylinder from the start of the compression process, at Stage 1 of the Seiliger cycle. It is important to note that this assumption does not imply a displacement of intake air. In practice, the closed cycle begins with a cylinder full of air, and hydrogen injection only starts thereafter. The model thus preserves the full charge air mass and superimposes the hydrogen mass without reducing the oxygen available for combustion.

This modelling approach differs significantly from the injection strategy described by Serrano [30], who assumes premixing of hydrogen and air in the engine plenum prior to scavenging. In such a configu-

ration, hydrogen displaces part of the intake air, thereby reducing the available oxygen for combustion. Additionally, unburned hydrogen is likely to escape during the scavenging phase, which reduces the overall efficiency due to the loss of uncombusted fuel prior to ignition. By contrast, the LPDI configuration considered in this study enables better control of mixture formation and avoids hydrogen losses prior to compression.

Added pressure during compression from hydrogen addition

When the model is operated with a HES of 0.8, meaning that 80% of the fuel energy input originates from hydrogen, the resulting hydrogen mass fraction in the cylinder relative to the total in-cylinder mass is approximately 0.6%. At first glance, this appears negligible and might be assumed to have a minimal effect on the thermodynamic properties of the gas mixture. However, due to the exceptionally low molar mass of hydrogen, this small mass fraction corresponds to a substantial share of the total number of mol present in the cylinder.

For reference, the molar mass of air is approximately $0.02897\ \mathrm{kg/mol}$, whereas the molar mass of hydrogen is only $0.002016\ \mathrm{kg/mol}$. As a result, the hydrogen introduced at HES = 0.8 constitutes roughly 8% of the total mol count in the cylinder. Assuming ideal gas behaviour, this proportion directly translates into an approximate 8% increase in the in-cylinder pressure at the start of compression due to the additional number of mol.

This pressure increase is accounted for within the Simulink implementation of the model. Specifically, an additional pressure contribution is added to the base value of p_1, the scavenging pressure input, based on the selected HES. In this way, the model dynamically adjusts the initial pressure to reflect the presence of hydrogen in the cylinder and its influence on the early stages of compression.

7.2. Seiliger process

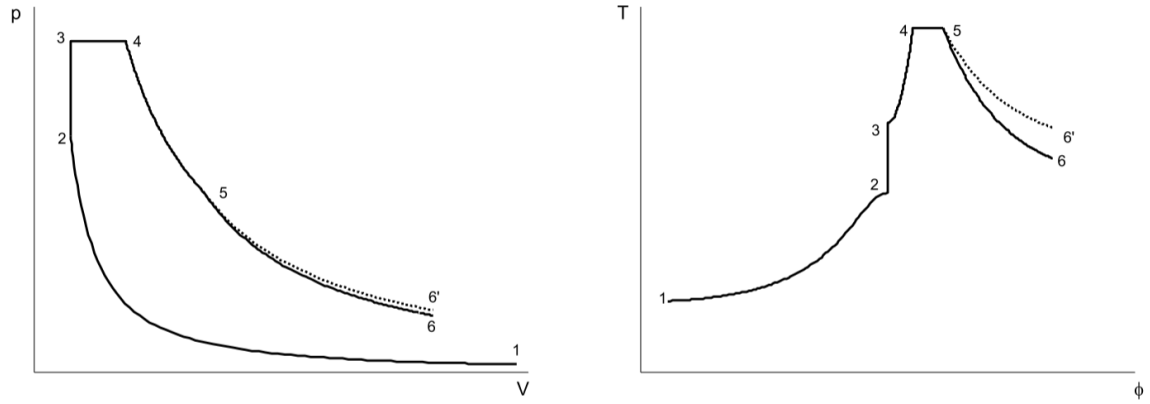

Figure 7.2: six-point Seiliger process $p - V$ diagram and $T - \phi$ diagram

The Seiliger model approximates the thermodynamic processes within internal combustion engines through a simplified idealised cycle. Originally proposed by Seiliger in 1922, this approach divides the closed-cylinder combustion process into distinct, idealised stages, each representing specific thermodynamic processes occurring within the cylinder [23, 77]. By parameterising these stages, the model provides insights into engine performance with relatively modest computational effort, making it especially suitable for mean-value first principle modelling [73, 78].

The Diesel A-model was initially constructed using a five-stage Seiliger process, in which the isothermal combustion stage (Stage 4–5) is omitted. The isothermal stage, which theoretically accounts for heat addition at constant temperature, is sometimes excluded on the grounds that its physical relevance in high-speed combustion processes is limited, or for the sake of model simplicity and numerical robustness.

However, the inclusion of an isothermal stage can offer increased modelling flexibility, particularly when simulating fuel mixtures or advanced combustion strategies that do not align well with the assumptions

of purely isochoric or isobaric combustion. For this reason, and to enhance the adaptability of the model for hydrogen-diesel dual-fuel scenarios, the sixth stage has been incorporated into the Simulink model. As a result, the current model utilises a six-stage Seiliger process, allowing more nuanced representation of heat release characteristics across a broader range of operating conditions.

Stage	Volume ratio	Pressure ratio	Temperature ratio
1–2	$\frac{V_1}{V_2} = r_c$	$\frac{p_2}{p_1} = r_c^{n_c}$	$\frac{T_2}{T_1} = r_c^{n_c-1}$
2–3	$\frac{V_3}{V_2} = 1$	$\frac{p_3}{p_2} = a$	$\frac{T_3}{T_2} = a$
3–4	$\frac{V_4}{V_3} = b$	$\frac{p_4}{p_3} = 1$	$\frac{T_4}{T_3} = b$
4–5	$\frac{V_5}{V_4} = c$	$\frac{p_4}{p_5} = c$	$\frac{T_5}{T_4} = 1$
5–6	$\frac{V_6}{V_5} = r_{\text{exp}}$	$\frac{p_5}{p_6} = r_{\text{exp}}^{n_{\text{exp}}}$	$\frac{T_6}{T_5} = r_{\text{exp}}^{1-n_{\text{exp}}}$

Table 7.1: Seiliger process definition and parameters [73]

Stage	specific work w [J/kg]	specific heat q [J/kg]
1–2	$-\,c_{v,12}\,T_1\,\frac{\gamma_{12}-1}{n_c-1}\left(r_c^{n_c-1}-1\right)$	$c_{v,12}\,T_1\,\frac{\gamma_{12}-1}{n_c-1}\left(r_c^{n_c-1}-1\right)$
2–3	0	$c_{v,23}\,T_1\,r_c^{n_c-1}\,(a-1)$
3–4	$c_{v,34}\,T_1\,(\gamma_{34}-1)\,r_c^{n_c-1}\,a\,(b-1)$	$c_{v,34}\,T_1\,(\gamma_{34}-1)\,r_c^{n_c-1}\,a\,(b-1)$
4–5	$c_{v,45}\,T_1\,(\gamma_{45}-1)\,r_c^{n_c-1}\,a\,b\,\ln(c)$	$c_{v,45}\,T_1\,(\gamma_{45}-1)\,r_c^{n_c-1}\,a\,b\,\ln(c)$
5–6	$c_{v,56}\,T_1\,\frac{\gamma_{56}-1}{n_{\text{exp}}-1}\,r_c^{n_c-1}\,a\,b\left(1-\frac{1}{r_{\text{exp}}^{n_{\text{exp}}-1}}\right)$	$-\,c_{v,56}\,T_1\,\frac{\gamma_{56}-1}{n_{\text{exp}}-1}\,r_c^{n_c-1}\,a\,b\left(1-\frac{1}{r_{\text{exp}}^{n_{\text{exp}}-1}}\right)$

Table 7.2: Overzicht van de specifieke arbeid en warmte per stadium.

Seiliger stages

The six stages of the cycle are discussed in detail below, referring to Figure 7.2 and Tables 7.1 and 7.2 for their schematic visual representation and mathematical definitions.

Stage 1–2: Polytropic compression

$$\frac{p_2}{p_1} = r_c^{n_c}, \quad \frac{T_2}{T_1} = r_c^{n_c-1} \tag{7.4}$$

During this initial stage, air trapped in the cylinder is compressed polytropically. The polytropic exponent (n_c) accounts for heat transfer effects, primarily due to cylinder wall cooling. This exponent typically varies between the limits of an adiabatic process (no heat exchange, $n_c = \gamma$) and an isothermal process (maximum heat exchange, $n_c = 1$), depending on cylinder geometry and thermal boundary conditions [23]. As a result of compression, both the pressure and temperature of the gas increase.

Stage 2–3: Isochoric combustion

$$\frac{p_3}{p_2} = a, \quad \frac{T_3}{T_2} = a \tag{7.5}$$

Isochoric (constant-volume) combustion represents rapid, nearly instantaneous combustion that occurs immediately after compression when the piston is near top dead centre. In this stage, the volume remains unchanged, but the pressure and temperature sharply increase due to combustion heat release. The parameter a indicates the pressure and temperature ratio increase caused by combustion at constant volume [73, 78].

Stage 3–4: Isobaric combustion and expansion

$$\frac{V_4}{V_3} = b, \quad \frac{T_4}{T_3} = b \tag{7.6}$$

This stage models the subsequent slower combustion phase, which occurs at nearly constant pressure as the piston starts to move downwards. Fuel continues to combust, expanding the combustion gases and delivering mechanical work to the piston. The parameter b describes the volume and temperature increase during this phase, accounting for slower, diffusion-controlled combustion commonly observed in diesel engines [23, 78].

Stage 4–5: Isothermal combustion and expansion

$$\frac{V_5}{V_4} = c, \quad \frac{p_4}{p_5} = c, \quad \frac{T_5}{T_4} = 1 \tag{7.7}$$

The isothermal combustion and expansion stage maintains constant temperature, reflecting late-stage combustion where heat addition balances the temperature drop due to expansion. This phase models prolonged combustion processes and afterburning phenomena, where fuel continues to burn slowly at lower pressures, maintaining cylinder temperature relatively constant. Parameter c quantifies this additional expansion and heat release at constant temperature [23, 73].

Stage 5–6: Polytropic expansion

$$\frac{p_6}{p_5} = r_{\text{exp}}^{n_{\text{exp}}}, \quad \frac{T_6}{T_5} = r_{\text{exp}}^{1-n_{\text{exp}}} \tag{7.8}$$

In this stage, the gases undergo a polytropic expansion with significant heat loss due to cylinder cooling. The polytropic exponent (n_{exp}) accounts for heat transfer and losses to the cylinder walls. Expansion continues until the exhaust valve opens, contributing further mechanical work to the piston, while the pressure and temperature decrease significantly [73, 74].

Stage 6–1: Isochoric heat rejection

This final stage occurs at constant volume and represents the idealised replacement of hot exhaust gases by fresh, cooler intake air. In practical engines, this phase does not physically occur inside the cylinder, as exhaust gases are expelled through the exhaust system while fresh air enters. However, in the Seiliger cycle, this stage closes the loop by resetting the thermodynamic state to the initial conditions, making the cycle continuous and thermodynamically consistent [23, 78].

By clearly defining and parameterising each stage, the 6-stage Seiliger model provides a reliable yet computationally efficient framework for simulating diesel engine performance, ideal for preliminary feasibility studies and comparative analyses of different combustion strategies.

Determining the Seiliger parameters

The accuracy and effectiveness of the Seiliger model are highly dependent on the correct determination of its parameters. The Seiliger parameters a, b, c, r_c, r_{exp}, n_c, and n_{exp} must be appropriately chosen or calculated to accurately simulate the combustion and expansion processes within a cylinder. These parameters can be established through direct measurements, empirical relationships, estimation from analogous engines, or sensitivity analyses. Below, each parameter is discussed in detail.

Effective compression ratio (r_c)

The effective compression ratio, r_c, is defined as:

$$r_c = \frac{V_1}{V_2} \tag{7.9}$$

Here, V_1 represents the volume at the start of the compression stroke, and V_2 the volume at TDC. r_c is predominantly determined by the engine's physical geometry and valve timing, particularly the exhaust valve closing angle. For the engine considered in this project, the value of r_c is determined in Chapter 8.

Polytropic compression exponent (n_c)

The polytropic exponent during compression, n_c, describes the thermodynamic nature of the compression process, specifically how heat exchange between the gas and the cylinder walls is represented. It is defined by the general polytropic relation:

$$pV^{n_c} = \text{constant} \tag{7.10}$$

The value of n_c can vary depending on the extent of heat exchange and other irreversibilities in the process. In the limiting case of completely isothermal compression, where temperature remains constant throughout the process, the exponent equals exactly $n_c = 1.0$. Conversely, in a perfectly isentropic (adiabatic and reversible) process, the exponent equals the ratio of specific heats, $\gamma = c_p/c_v$. For air at room temperature, this value is typically $\gamma = 1.4$.

Real engine behaviour generally falls between these two extremes. Thus, n_c is often in the range 1.30 to 1.36 for diesel engines, depending on design and operating conditions [23]. When experimental cylinder pressure data is available, n_c can be determined empirically by fitting pressure-volume measurements during the compression stroke.

In many practical implementations of the Seiliger cycle, including the original A-model used as the basis for this project, compression and expansion are modelled as isentropic processes. In such cases, a constant value of $\gamma = 1.4$ is assumed. However, this simplification neglects the fact that c_p and c_v vary significantly with temperature and gas composition, particularly in hydrogen-air mixtures. As a result, the assumption of a constant γ introduces inaccuracies, especially under high-temperature conditions. A more refined modelling approach that incorporates temperature-dependent heat capacities and recalculates the effective γ at several steps of the Seiliger cycle is therefore explored in Chapter 9.

Isochoric combustion parameter (a)

Parameter a is defined as the pressure and temperature increase ratio during the isochoric combustion stage:

$$a = \frac{p_3}{p_2} = \frac{T_3}{T_2} \tag{7.11}$$

This parameter is ideally determined using experimental in-cylinder pressure data at the onset of combustion. If this data is not available, parameter a can be estimated through empirical correlations based on fuel type, fuel-air ratio, and ignition timing. Typically, values of a for diesel combustion range from about 1.5 to 2.5, depending heavily on the fuel injection timing and combustion efficiency.

In the standard implementation of the A-model, it is assumed that p_3, the cylinder pressure immediately after isochoric combustion, is known from experimental data, allowing direct calculation of a. However, for the engine considered in this study, no experimental pressure data is available. As a result, certain modelling assumptions are required. For the case of pure diesel operation, with a HES of 0, it is

assumed that p_3 reaches 160 bar. This assumed value is used to establish the corresponding parameter a under full-diesel conditions. For simulations involving other fuel mixtures, the value of p_3 is varied accordingly to reflect realistic pressure levels associated with the specific combustion scenario.

Isobaric combustion and expansion parameter (b)
The parameter b represents the volume and temperature increase during the isobaric combustion stage:

$$b = \frac{V_4}{V_3} = \frac{T_4}{T_3} \tag{7.12}$$

The b parameter characterises the extent of slow, diffusion-controlled combustion typical in diesel engines. Its value depends on combustion speed, fuel injection characteristics, and the air-fuel mixing rate. Experimental data from cylinder pressure measurements, along with engine displacement data, typically determine this parameter. In absence of such data, typical values can be sourced from literature on similar engine types, generally ranging from 1.3 to 2.0 [73, 78].

Isothermal combustion and expansion parameter (c)
The parameter c denotes the isothermal expansion and combustion stage:

$$c = \frac{V_5}{V_4} = \frac{p_4}{p_5} \tag{7.13}$$

Parameter c is typically the most challenging to define, as it represents late-stage combustion or afterburning, which is influenced by incomplete combustion and ongoing heat release. The accurate determination of c generally requires careful analysis of cylinder pressure data collected near the expansion stroke. Often, if no detailed measurements are available, c may initially be set close to 1 (indicating negligible late combustion) or adjusted slightly above 1 based on similar engine configurations.

Expansion ratio (r_{exp})
The expansion ratio, r_{exp}, describes the volumetric expansion during the expansion stroke:

$$r_{\text{exp}} = \frac{V_6}{V_5} \tag{7.14}$$

This parameter is typically derived from the engine geometry and the timing of exhaust valve opening. It can be calculated from known geometric parameters of the engine cylinder and piston positions, analogous to the compression ratio.

Polytropic expansion exponent (n_{exp})
Similar to the compression exponent, the polytropic expansion exponent n_{exp} characterises the heat exchange during the expansion phase:

$$pV^{n_{\text{exp}}} = \text{constant} \tag{7.15}$$

Experimental in-cylinder pressure and volume data during expansion ideally determine this parameter. Typical values for diesel engines lie between 1.2 and 1.3, reflecting the heat loss to cylinder walls and surroundings. When such measurements are unavailable, reference values from similar engine configurations are commonly adopted.

7.3. Limitations of the Seiliger process

Throughout the course of this project, several inherent limitations of the Seiliger process became apparent, which stem directly from the fixed assumptions underlying the method. Despite its many advantages, such as conceptual simplicity, low computational cost, and its ability to parametrise key thermodynamic stages within the closed portion of the engine cycle, the Seiliger process also imposes constraints that limit its applicability under certain operating conditions.

One such limitation lies in its assumption of an isochoric (constant-volume) heat addition phase at the start of combustion. In the Seiliger model, the combustion process always begins at TDC, with an instantaneous pressure rise while the cylinder volume remains constant. For conventional diesel engines, this is generally a reasonable approximation: combustion initiates shortly before or near TDC, when the piston velocity is low, and the cylinder volume changes minimally. Thus, the early phase of diesel combustion can be effectively captured by an isochoric heat addition stage.

However, when modelling hydrogen combustion, especially in dual-fuel configurations with high hydrogen content, this assumption becomes more problematic. Hydrogen-air mixtures typically exhibit very rapid combustion, which poses the risk of an excessive pressure rise if ignition occurs at or near TDC. In such cases, the maximum cylinder pressure may exceed mechanical design limits of the engine. One strategy to mitigate this risk is to delay the start of combustion until after TDC, when the piston has already begun its downward stroke and the cylinder volume is increasing. This moderates the pressure rise while still allowing complete combustion of the hydrogen charge.

An illustration of this effect is provided in Figure 7.3. The black line represents cylinder pressure as a function of crank angle for standard diesel combustion, while the green lines show simulated pressure traces for a hydrogen-diesel dual-fuel mode with HES = 0.8, under various valve timing scenarios. In these simulations, the hydrogen combustion is deliberately initiated later in the cycle, resulting in peak pressures that remain comparable to those observed in conventional diesel operation.

Unfortunately, such a delayed start of combustion cannot be directly represented within a Seiliger process, which enforces the start of combustion at TDC via the isochoric stage. While it was considered whether the isochoric stage could be minimised or even eliminated entirely in favour of transferring the combustion process entirely to the isobaric and isothermal phases, this approach proved insufficient. Aside from potentially misrepresenting the actual combustion dynamics, it also results in a significantly reduced work output. The work produced by the cycle, as derived from the Seiliger model, corresponds to the enclosed area beneath the pressure–volume (p–V) diagram. Eliminating the isochoric pressure rise leads to a smaller enclosed area, and thus to an under prediction of indicated work.

Accurately modelling a delayed start of combustion therefore requires a different modelling approach. A Wiebe function-based combustion model, such as the one employed by Serrano [30], offers greater flexibility in specifying the timing and rate of heat release as a function of crank angle. This alternative methodology is further explored in Chapter 11.

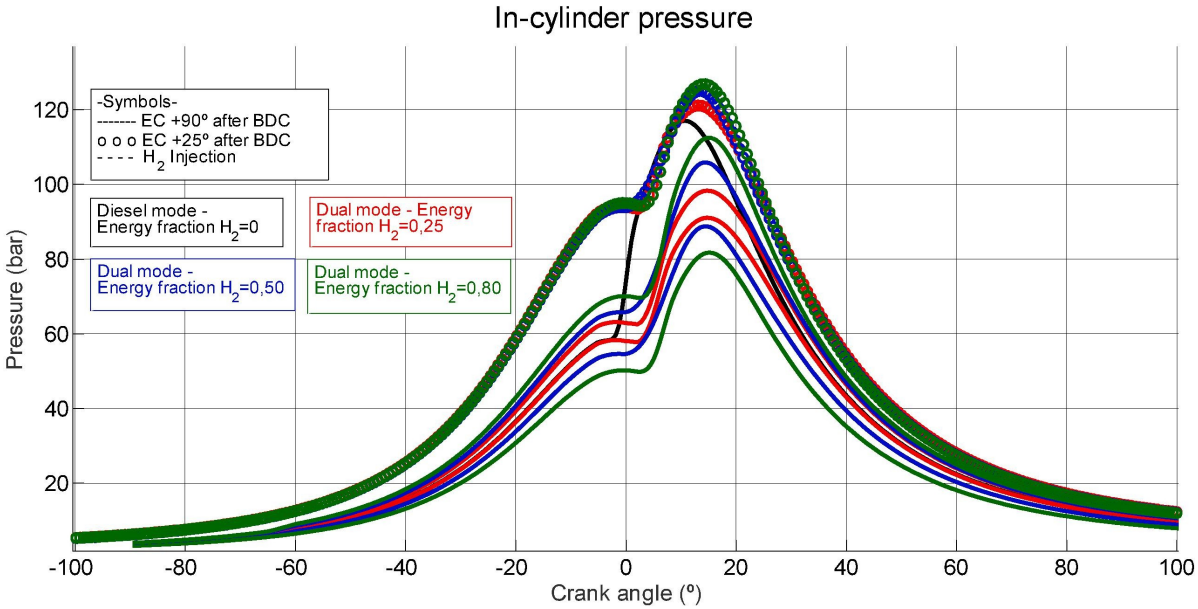

Figure 7.3: Pressure-crankangle diagram for various timing settings, determined using a Wiebe function based approach [30]

8

Engine and modelling parameters

To enable accurate simulation of the Seiliger cycle for the WinGD X92DF engine, a reliable set of engine and modelling parameters must first be established. While some specifications are provided by the manufacturer, many essential values such as the precise timing of valve events and the in-cylinder volume at critical crank angles are not publicly disclosed. This chapter outlines the available engine specifications, the methods used to estimate missing data, and the derivation of parameters required to define the compression ratio, cylinder volume evolution, and other key characteristics necessary for thermodynamic modelling.

8.1. Engine specifications

Several detailed specifications of the WinGD X92DF engine that are essential for accurate combustion modelling are not publicly disclosed by the manufacturer. Critical parameters such as the precise TDC volume, inlet port positions, and exhaust valve timing are proprietary information and thus unavailable. However, these parameters are crucial for reliable modelling, particularly in predicting in-cylinder pressures and evaluating engine performance characteristics such as efficiency and output power.

The engine specifications that are publicly available from the manufacturer are listed in Table 8.1. These key parameters form the basis for subsequent calculations and approximations made throughout this study to develop a representative combustion model of the X92DF engine.

Parameter	Value
Cylinder bore	920 mm
Piston stroke	3468 mm
Engine nominal speed	80 rpm
Mean effective pressure	17.3 bar
Number of cylinders	12
Nominal output power	63840 kW
Geometric compression ratio ε	12.4
Scavenge air pressure (p_1)	4.0 bar
Scavenge air temperature (T_1)	32.8 °C

Table 8.1: Engine specifications for X92DF

The schematic cross-section shown in Figure 8.1 serves as the basis for estimating the remaining engine parameters not disclosed by the manufacturer. This image represents a typical cross-sectional layout of a WinGD dual-fuel two-stroke engine equipped with LNG LPDI. Given the lack of publicly available detailed dimensional data, this schematic provides the best available reference for making reasonable assumptions about port positions, crank angles, and combustion chamber geometry.

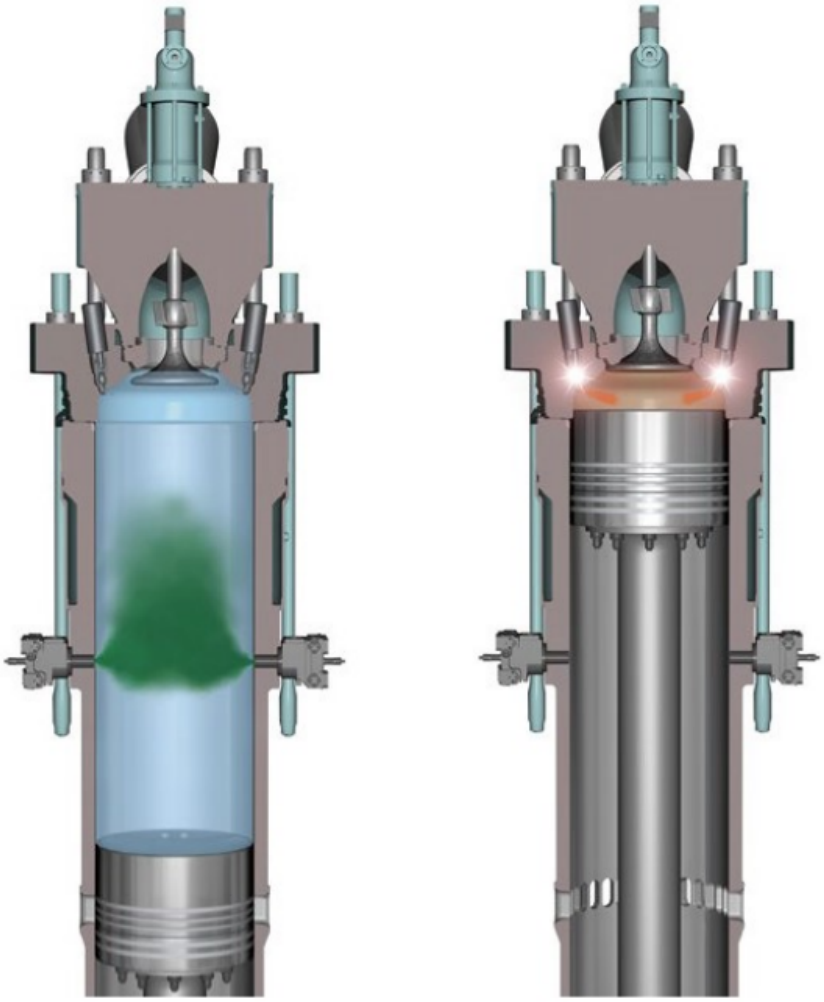

Figure 8.1: Cylinder cross-section of the WinGD X92DF engine [68]

Cylinder volume as a function of crank angle

For large crosshead two-stroke marine engines, such as the WinGD X92DF, the instantaneous cylinder volume during engine operation depends on the crank angle. Accurately determining cylinder volume as a function of crank angle is crucial for thermodynamic modelling, particularly for combustion simulations where the changing cylinder volume directly influences pressure and temperature.

Moreover, the volume–crank angle correlation is also utilised in this study to reverse-engineer specific crank angles corresponding to measured geometric features of the engine. By combining estimated cylinder volumes obtained from the schematic cross-section (Figure 8.1) with the analytical expression for piston motion, it becomes possible to approximate the crank angles at which inlet ports open or close, and to determine the effective compression and expansion phases for this specific engine design.

The relationship between cylinder volume and crank angle (θ) for a crosshead engine can be expressed by the following geometrical formula [26]:

$$V(\theta) = V_{TDC} + \frac{\pi D^2}{4}\left[L + R - \left(R\cos\theta + \sqrt{L^2 - R^2\sin^2\theta}\right)\right] \tag{8.1}$$

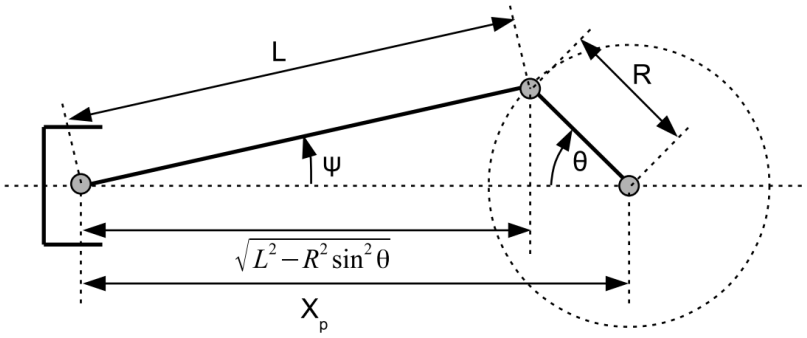

Figure 8.2: Schematic overview of a crank-slider mechanism [79]

In this equation, $V(\theta)$ represents the instantaneous cylinder volume, V_{TDC} is the clearance volume at TDC, D is the cylinder bore, L denotes the connecting rod length, and R is the crank radius (half of the stroke length). The crank angle θ is defined as 0° at TDC and 180° at BDC. In the absence of exact manufacturer data, the connecting rod length L has been estimated using guidelines from literature and data from published research, setting the ratio L/R to 3.5 [26, 30, 80].

This equation is particularly suitable for crosshead two-stroke marine engines due to their relatively long stroke and connecting rod configurations. Accurate use of equation (8.1) provides essential inputs to the combustion model, influencing the accuracy of calculations related to pressure, heat release, and combustion timing within the cylinder. A visual representation of the crank-slider geometry, as described by the equation, is shown in Figure 8.2.

Derivation of additional engine parameters

In this section, the remaining parameters are derived through analytical expressions, engineering assumptions, and approximations based on schematic representations of the engine. Each parameter is discussed in the following sections.

Volume at top dead centre

Before analysing the timing of inlet and exhaust events, the volume at TDC, denoted V_{TDC}, must be determined. This can be calculated using the geometric compression ratio ε, defined as:

$$\varepsilon = \frac{V_{\text{TDC}} + V_s}{V_{\text{TDC}}} \tag{8.2}$$

Rearranging this yields:

$$V_{\text{TDC}} = \frac{V_s}{\varepsilon - 1} \tag{8.3}$$

For the X92DF engine, the stroke volume per cylinder V_s is approximately 2.304 m^3, and the geometric compression ratio is reported as $\varepsilon = 12.4$. Substituting these values gives:

$$V_{\text{TDC}} = \frac{2.304}{12.4 - 1} = 0.2022 \text{ m}^3 \tag{8.4}$$

Location of inlet ports

Based on the schematic cross-sectional drawing of the engine, it was determined that the inlet ports are located at a height of approximately 0.71 metres above the piston position at BDC. When the piston reaches this position during the upward stroke and closes the inlet ports, the corresponding in-cylinder volume is calculated to be 2.04 m^3.

By applying the crank-slider mechanism described in Figure 8.2 and governed by equation (8.1), this volume can be used to determine the associated crank angle. Substituting the known values for bore, stroke, TDC volume, and connecting rod-to-crank radius ratio into the expression yields a crank angle of approximately 48° after BDC at the moment the inlet ports close.

Exhaust valve timing

No official information is available regarding the exhaust valve timing of the X92DF engine. However, it is standard practice in large two-stroke crosshead engines that the exhaust valve closes shortly after the inlet ports close, and reopens before the inlet ports open again. This overlap allows for efficient scavenging and minimises pressure losses during gas exchange.

Based on assumptions consistent with typical two-stroke engine operation and supported by literature [30], the exhaust valve closing angle is set to 60° after BDC, while the exhaust valve opening angle is assumed to be 60° before BDC.

Using this assumed exhaust valve closing angle and the crank-slider mechanism described earlier, the corresponding in-cylinder volume is calculated to be $V_1 = 1.8080$ m^3

This volume marks the start of the closed cylinder process and is therefore taken as V_1 in the Seiliger model.

With both V_1 and the TDC volume V_{TDC} known, the effective compression ratio r_c can be calculated as:

$$r_c = \frac{V_1}{V_{\text{TDC}}} \tag{8.5}$$

Substituting the known values:

$$r_c = \frac{1.8080}{0.2022} = 8.94 \tag{8.6}$$

This value will be used in subsequent calculations related to the compression process in the Seiliger cycle.

Parameter	Value
Inlet port height from BDC	0.71 m
Crank angle when inlet closes	48° after BDC
Cylinder volume when inlet closes	2.04 m^3
Crank angle when exhaust closes	60° after BDC
Volume when exhaust closes (V_1)	1.8080 m^3
Crank angle when exhaust opens	60° before BDC
Volume at TDC (V_2)	0.2022 m^3
Effective compression ratio (r_c)	8.94
Connecting rod to crank radius ratio (L/R)	3.5

Table 8.2: Estimated and calculated specifications of the X92DF engine

All estimated and derived engine parameters used throughout the remainder of this project are summarised in Table 8.2. These values serve as the foundation for defining the Seiliger model parameters and for conducting subsequent combustion simulations.

To provide a clear visual representation of how the cylinder volume evolves throughout the engine cycle, the volume–crank angle relationship has been plotted in Figure 8.3. The crank angle is defined such that 0° corresponds to BDC and 180° to TDC. The timings of inlet port opening and closing and exhaust valve opening and closing are also indicated in the figure, providing insight into the effective gas exchange and compression phases of the cycle.

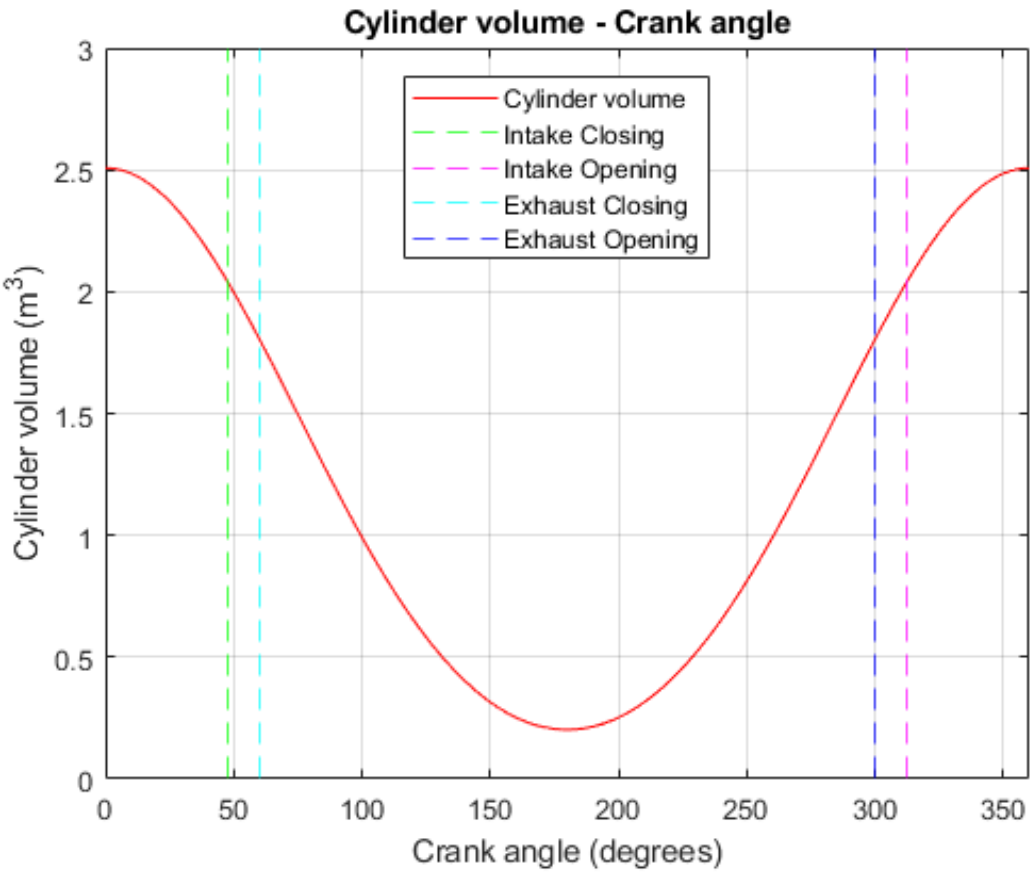

Figure 8.3: Cylinder volume - crank angle

9

Compression refinement

As discussed in Chapter 7, it is common practice in Seiliger process modelling to assume a constant compression exponent equal to the isentropic exponent γ at room temperature. The isentropic exponent is defined as the ratio of specific heats:

$$\gamma = \frac{c_p}{c_v} \tag{9.1}$$

For air under standard conditions, this value is typically taken as $\gamma = 1.4$. This simplification assumes that the compression and expansion processes are adiabatic and reversible, thus isentropic. However, this assumption becomes increasingly unrealistic as in-cylinder temperatures rise significantly during compression, especially in engines using hydrogen-air mixtures.

Both c_p and c_v are strongly dependent on temperature and gas composition, meaning that the ratio γ varies as well. This is illustrated in Figure 9.1, where the specific heat at constant pressure (c_p) for hydrogen is shown as a function of temperature. Consequently, using a constant γ in the Seiliger model can lead to inaccuracies in predicting in-cylinder temperature and pressure.

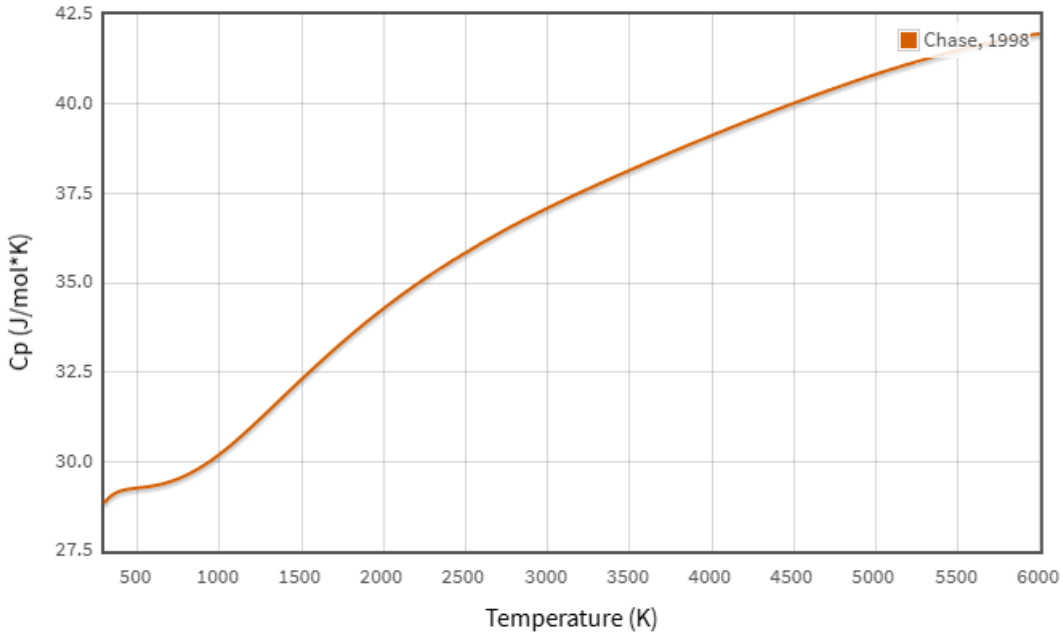

Figure 9.1: Evolution of c_p of pure H2 over temperature [81]

Previous research has shown that assuming a constant γ leads to discrepancies in the predicted thermodynamic behaviour during compression and expansion. Koekkoek [78] addressed this issue by proposing an alternative method for modelling compression in the Seiliger process, incorporating temperature-dependent values for c_p and c_v.

In this chapter, a modified version of Koekkoek's approach is developed and adapted for use in the context of this project. To illustrate the potential impact of this refinement, Figure 9.2 presents a typical comparison between the results of a Seiliger process simulation and experimental in-cylinder pressure data. It is evident that the Seiliger prediction deviates significantly from the measured values during the compression and expansion phases.

The aim of the refinement proposed in this chapter is to reduce this deviation and to bring the simulation results closer to the physical reality by accounting for the variable thermodynamic properties of the working gas.

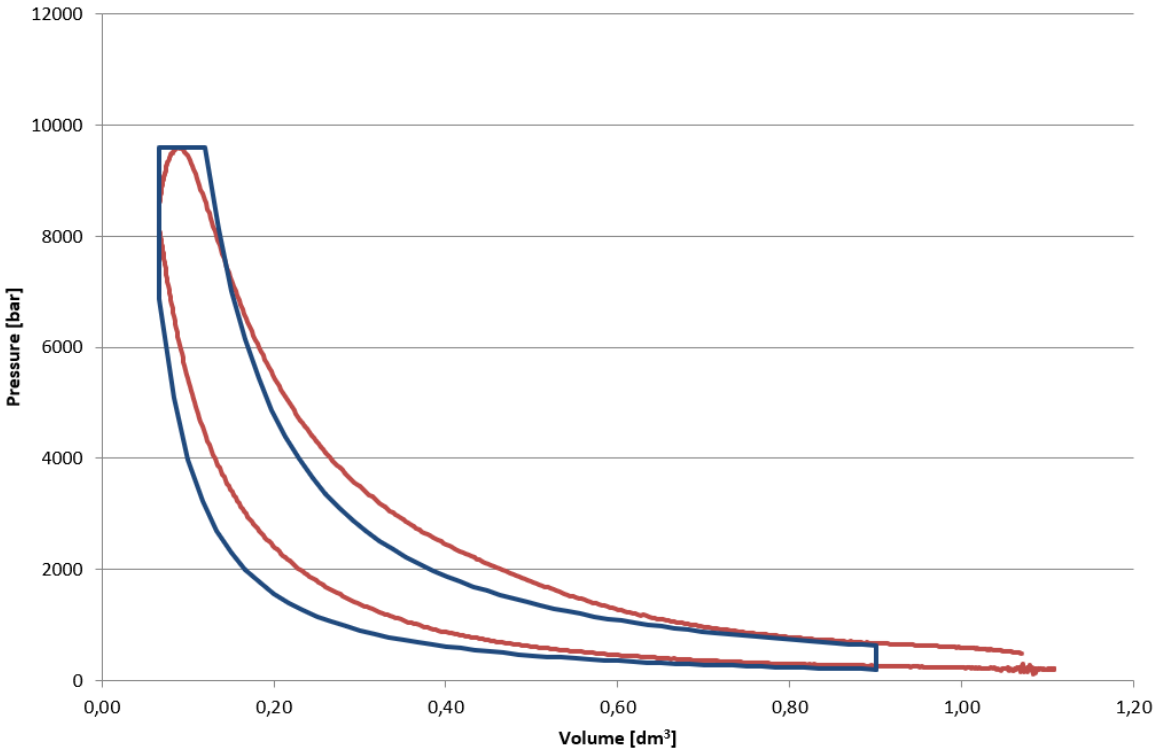

Figure 9.2: Typical representation of the difference between the result of a Seiliger analysis (blue line) and measurement data (orange line)

9.1. Temperature-dependent specific heat capacities

The specific heat capacities c_p and c_v represent the amount of energy required to raise the temperature of a unit amount of substance by one degree Kelvin. Specifically, c_v denotes the specific heat at constant volume, while c_p refers to the specific heat at constant pressure. Their physical meanings are directly tied to the internal energy and enthalpy changes of the gas during thermodynamic processes.

For combustion applications, this implies that the thermodynamic properties of the gas can vary significantly throughout the engine cycle, particularly in cases where the working gas contains hydrogen or other components with strong temperature-dependent behaviour.

Determination of c_p and c_v for gas mixtures

For an ideal gas, the molar heat capacity at constant pressure, c_p, is typically obtained from experimental data or empirical polynomial expressions. These polynomials, such as those provided by NIST, relate c_p to temperature and are expressed in the following general form:

$$c_p = A + B \cdot t + C \cdot t^2 + D \cdot t^3 + \frac{E}{t^2} \tag{9.2}$$

where $t = T/1000$, and the resulting unit is $\mathrm{J/molK}$. The coefficients A to E are substance-specific and determined empirically.

To compute the molar heat capacity at constant volume, c_v, the ideal gas relation is used:

$$c_v = c_p - R_u \tag{9.3}$$

where $R_u = 8.3145\,\mathrm{kJ/molK}$ is the universal gas constant.

The heat capacity ratio γ, which appears in the polytropic compression and expansion equations, follows from:

$$\gamma = \frac{c_p}{c_v} = \frac{c_p}{c_p - R_u} \tag{9.4}$$

When a gas mixture is considered, the total molar heat capacity at constant pressure is calculated using the mole-fraction-weighted sum:

$$c_{p,\text{mix}} = \sum_i x_i c_{p,i} \tag{9.5}$$

The same principle applies to c_v, and the mixture heat capacity ratio is then computed from:

$$\gamma_{\text{mix}} = \frac{c_{p,\text{mix}}}{c_{p,\text{mix}} - R_u} \tag{9.6}$$

This formulation allows for temperature-dependent and composition-dependent modelling of thermodynamic properties in ideal gas mixtures.

Temperature range (K)	100 to 500	500 to 2000
A	28.98641	19.50583
B	1.853978	19.88705
C	-9.647459	-8.598535
D	16.63537	1.369784
E	0.000117	0.527601

Table 9.1: NIST c_p polynomial parameters for $\mathrm{N_2}$ [82]

Temperature range (K)	100 to 700	700 to 2000
A	31.32234	30.03235
B	-20.23531	8.772972
C	57.86644	-3.988133
D	-36.50624	0.788313
E	-0.007374	-0.741599

Table 9.2: NIST c_p polynomial parameters for $\mathrm{O_2}$ [82]

Air modelling as a binary gas mixture

To obtain an accurate approximation of the temperature-dependent specific heat capacity at constant pressure (c_p) for air, the method described in the previous section is applied to a binary gas mixture consisting of 79% nitrogen and 21% oxygen by volume. This composition reflects the standard atmospheric air mixture commonly used in combustion modelling.

For each gas component, the NIST polynomial form of c_p as a function of temperature is employed. The coefficients A through E are specific to each species and temperature range, and are tabulated for both N_2 and O_2 in Tables 9.1 and 9.2, respectively.

By calculating the specific heat capacities of the individual components and taking a molar-weighted average, the mixture c_p can be determined. From this, the mixture value of $\gamma = c_p/c_v$ is calculated using the universal gas constant R. The resulting values for c_p and γ across a range of temperatures are shown in Table 9.4. These values serve as a more realistic representation of air properties under varying thermal conditions than the often-assumed constant $\gamma = 1.4$.

Extension to air–hydrogen mixtures under LPDI conditions

For the specific LPDI combustion strategy investigated in this project, hydrogen is injected during the compression phase. As a result, the gas composition during compression deviates from that of pure air and must be accounted for in the calculation of temperature-dependent thermodynamic properties. The methodology outlined in the previous section can be extended accordingly to include hydrogen in the gas mixture.

The NIST polynomial formulation is again used to calculate the specific heat capacity c_p of hydrogen as a function of temperature. The corresponding polynomial parameters for hydrogen are listed in Table 9.3. By applying the same approach, calculating the molar-weighted average of c_p for all species in the mixture, values for c_p and the corresponding ratio of specific heats γ can be determined.

For the case considered here, the hydrogen content is based on nominal power operation with a HES of 0.8. This results in a hydrogen molar fraction of approximately 8% of the total gas mixture, as also discussed in Chapter 7. The resulting temperature-dependent values for c_p and γ for this air–hydrogen mixture are shown in Table 9.4. These values provide a more accurate thermodynamic basis for modelling the compression process under LPDI conditions.

Temperature range (K)	298 to 1000	1000 to 2500
A	33.066178	18.563083
B	-11.363417	12.257357
C	11.432816	-2.859786
D	-2.772874	0.268238
E	-0.158558	1.977990

Table 9.3: NIST c_p polynomial parameters for H_2 [82]

It is worth noting that the molar specific heat capacity c_p of the air–hydrogen mixture is slightly lower than that of pure air, due to the relatively low c_p of hydrogen on a molar basis. However, hydrogen has a significantly lower molar mass than nitrogen and oxygen, which leads to a higher number of moles present in the cylinder at the same mass of gas. Consequently, the mass-based heat capacity c_p in units of J/kg·K would in fact be considerably higher for the hydrogen-containing mixture compared to pure air. This has important implications for the thermodynamic behaviour of the gas during compression and must be accounted for in accurate modelling approaches.

T (K)	c_p air (J/mol·K)	γ air	c_p mix (J/mol·K)	γ mix
300	29.18	1.398	29.15	1.399
400	29.43	1.394	29.41	1.394
500	29.90	1.385	29.84	1.386
600	30.52	1.374	30.43	1.376
700	31.23	1.363	31.08	1.365
800	31.92	1.352	31.74	1.355
900	32.57	1.343	32.35	1.346
1000	33.15	1.335	32.91	1.338
1100	33.67	1.328	33.42	1.331
1200	34.13	1.322	33.87	1.325
1300	34.54	1.317	34.28	1.320
1400	34.89	1.313	34.65	1.316
1500	35.20	1.309	34.97	1.312
1600	35.48	1.306	35.26	1.309
1700	35.73	1.303	35.51	1.306
1800	35.95	1.301	35.75	1.303
1900	36.15	1.299	35.97	1.301
2000	36.35	1.297	36.18	1.298

Table 9.4: Thermodynamic properties of air and a hydrogen-air mixture (HES 0.8) at 100 K intervals.

9.2. Integration of variable c_p and c_v in the Seiliger model

In order to improve the physical realism of the Seiliger cycle during the compression phase, a refinement is implemented that accounts for the temperature dependence of the specific heat capacities c_p and c_v. The refinement is based on an iterative segmentation of the compression phase and follows a step-by-step approach, described below:

1. The compression stage is subdivided into several sub-stages. The number and spacing of these stages are chosen to balance computational efficiency with accuracy.
2. The first refinement point (point 1) is placed halfway between the initial volume V_1 and the volume at the end of compression V_2. This represents the midpoint of the piston stroke. At the start of compression, the rate of temperature increase is relatively low, allowing for larger step sizes.
3. The second point (point 2) is placed halfway between point 1 and the end of compression, halfway through the remaining stroke. This approach is repeated iteratively: each new point is placed halfway through the remaining portion of the compression stroke, up to point 7. This results in a higher resolution near the end of the compression stroke, where temperature rises more steeply.
4. The eight point is placed at the end of compression, which corresponds to the start of the first combustion stage of the Seiliger process.
5. At each of these points, an initial estimate of the local temperature is obtained from the original Seiliger process.
6. Based on this estimated temperature, a value for c_p is determined using the temperature-dependent mixture polynomial, as described in the previous sections.
7. A new temperature is then calculated using the polytropic Seiliger relation for the given compression ratio, but now using the updated c_p value.
8. The difference between the original and updated temperature is evaluated. If the relative deviation is less than 2%, the updated temperature is accepted as sufficiently accurate.
9. With this refined temperature, the corrected value of c_p is used to calculate the corresponding pressure at that point using the polytropic relation.

This iterative method allows for a more accurate representation of the thermodynamic state during compression, especially in cases where the addition of hydrogen leads to significant variation in c_p with

temperature. This approach forms the basis for an improved fit between the Seiliger model and realistic pressure and temperature traces.

Figure 9.3 shows a comparison between the original Seiliger temperature profile and the refined profile, as a function of crank angle for a full engine cycle. Each dot in the refined curve represents one of the intermediate refinement points during the compression and expansion phases. The figure illustrates how the temperature evolution deviates from the idealised curve, particularly near the end of compression and beginning of expansion, where temperature sensitivity is highest.

Since pressure is directly coupled to temperature in the Seiliger relations, these differences also influence the computed pressure at each crank angle. Consequently, the refinement affects the resulting p–V diagram of the cycle. The impact of this refinement on pressure, temperature, and engine performance parameters is further analysed in Chapter 12.

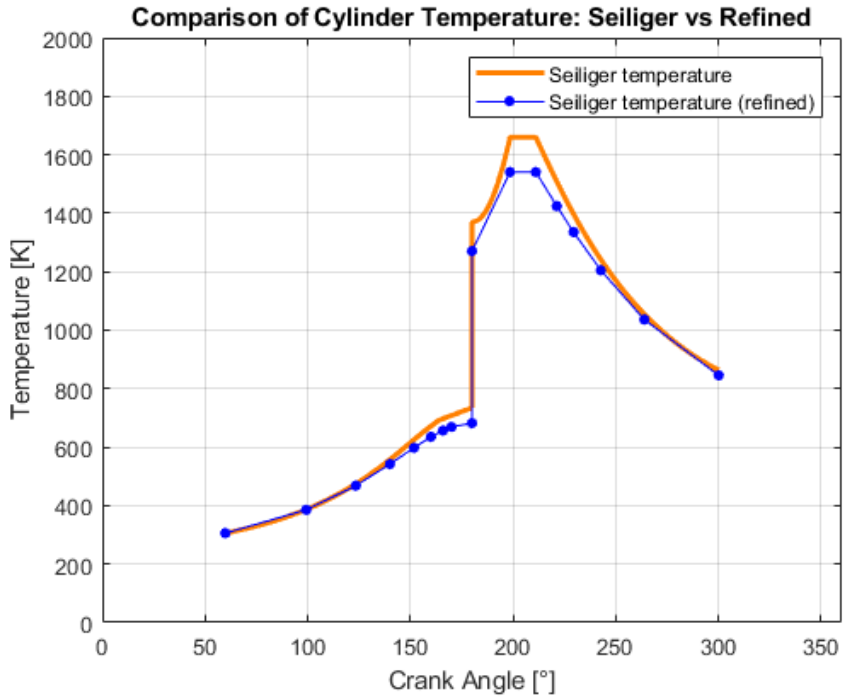

Figure 9.3: Comparison of cylinder temperature over the full cycle between the original and refined Seiliger process. The data shown corresponds to standard diesel operation at nominal power.

Although the method described above for integrating temperature-dependent values of c_p and c_v constitutes a significant improvement over the classical Seiliger approach, it remains a simplified representation. In reality, the thermophysical properties of the working gas, and therefore c_p and c_v, vary continuously throughout the compression and combustion stages. This is especially relevant with techniques such as LPDI, where the mixture composition changes during compression due to early hydrogen injection.

A more rigorous and physically accurate modelling approach would employ a *crank-angle resolved* framework, in which calculations are performed for each crank angle degree. This enables the use of instantaneous values for temperature and gas composition, and therefore allows c_p and c_v to be computed dynamically based on the evolving mixture properties.

In this project, however, a practical refinement of the conventional Seiliger process is proposed. The chosen method strikes a balance between physical realism and computational efficiency. It is specifically tailored to situations with limited measurement data, such as early-stage engine development or concept studies. Despite its simplified nature, the proposed approach provides a more realistic prediction of the pressure evolution during compression than the classical model based on a fixed value of γ.

10

Combustion physics

Although hydrogen is a promising alternative fuel due to its carbon-free combustion, its application in large two-stroke marine engines presents specific and significant challenges. While Section 4.3 provided a general overview of typical issues associated with hydrogen combustion such as pre-ignition, knocking, and backfiring, this chapter focuses more narrowly on how these phenomena manifest in the context of large low-speed marine engines.

The objective of this chapter is to examine combustion-physical constraints that are particularly relevant to this engine type. It aims to identify realistic operating boundaries for parameters such as the air excess ratio and compression ratio, based on available experimental data and findings from literature. Since large low-speed two-stroke hydrogen engines do not yet exist in practical applications, the available data is primarily derived from experimental studies on smaller hydrogen engines. These insights are used to evaluate whether full hydrogen operation in large engines is technically feasible and to support the assumptions made in this project's combustion modelling.

10.1. Pre-ignition and knocking risks

Two major limitations for using hydrogen as a fuel in large marine engines are pre-ignition and knocking. Hydrogen has an extremely low minimum ignition energy, significantly lower than that of typical hydrocarbon fuels. This makes it highly prone to early ignition in the presence of hot surfaces, residual gases, or minor local hotspots. In large two-stroke engines, this risk is further amplified due to the substantial thermal mass of engine components and the presence of larger quantities of residual lubricating oil in the combustion space. Regions near the exhaust valves and piston crown in particular, have been identified as critical zones for premature ignition events [39, 83].

Knocking, defined as the auto-ignition of the unburned fuel-air mixture ahead of the propagating flame front, is another abnormal combustion phenomenon of concern. Although hydrogen generally exhibits a high resistance to knock, especially under lean conditions, knock can still occur in specific operating scenarios. Larger engines are particularly sensitive to knocking due to their large bore diameters and the difficulty of achieving homogeneous mixture formation in the expansive combustion chamber [39, 45].

Both pre-ignition and knock are strongly influenced by the compression ratio and the fuel–air equivalence ratio. While increasing the compression ratio tends to improve thermal efficiency, it also raises the likelihood of abnormal combustion. For this reason, hydrogen-fuelled SI engines typically operate with conservative compression ratios. According to the literature, engines using PFI configurations are generally limited to compression ratios below 9, as higher values have been associated with increased pre-ignition risk [56]. In contrast, DI systems can allow for somewhat higher values, up to approximately 12, by injecting hydrogen later in the cycle and thereby reducing the residence time of the flammable mixture before ignition [18, 56].

Equivalence ratio effects

An important mitigating factor in both pre-ignition and knock tendency is the air excess ratio. Operating with a lean mixture significantly increases the ignition energy requirement and reduces the flame temperature, lowering the likelihood of abnormal combustion. Several studies confirm this stabilising effect under lean conditions [18, 84]. For instance, Mogi [84] demonstrated that a hydrogen Direct Injection (DI) engine with a compression ratio of 20:1 could be operated without knock or component damage when using an air excess ratio well above 3. This was attributed to the highly diluted mixture, which slows down the flame speed and reduces peak pressures and temperatures. Similar conclusions were drawn in [18], which noted that lean operation shifts the ϕ limit for stable combustion to lower values, thereby reducing the tendency for pre-ignition.

In line with these findings, a minimum air excess ratio of $\lambda = 3$ was adopted in this project's combustion model for hydrogen operation. This value reflects a conservative but realistic balance between combustion safety and engine performance, particularly in the absence of experimental data for hydrogen use in large marine two-stroke engines.

Compression ratio effects

CI diesel engines typically operate with compression ratios in the range of 14 to 22, depending on engine type and application [26]. These high values are necessary to achieve autoignition and ensure efficient combustion of diesel fuel across a wide operating range. For hydrogen-fuelled engines, however, such high compression ratios are not suitable.

Hydrogen cannot be ignited through compression alone due to its high autoignition temperature. In fact, at similar compression pressures, hydrogen is far more susceptible to abnormal combustion, such as pre-ignition and knocking. Rather than improving efficiency, increasing the compression ratio in hydrogen engines often increases the likelihood of combustion instability.

As discussed in literature [18, 39], the upper limit of the compression ratio in hydrogen engines is not defined by theoretical thermodynamic considerations, but rather by the point at which abnormal combustion or excessive heat losses begin to occur. While hydrogen has several beneficial combustion properties such as high flame speed and a wide flammability range, its sensitivity to surface ignition and its tendency to ignite prematurely in hot spots places firm constraints on the compression ratio, especially in larger engines with long residence times.

10.2. Efficiency considerations

The compression ratio plays a critical role in determining the thermodynamic efficiency of internal combustion engines. According to thermodynamic principles, increasing the compression ratio leads to a higher ideal cycle efficiency. This relationship is also observed in hydrogen-fuelled engines, although the maximum compression ratio that can be applied is more limited due to the onset of pre-ignition and knock, as discussed previously.

As a result, hydrogen engines often operate at lower compression ratios compared to diesel CI engines, which can contribute to their lower thermal efficiency. For instance, Yip [18] notes that combustion efficiency in hydrogen DI SI engines remains inferior to that of diesel CI engines, in part due to constraints on the compression ratio.

The experimental results of Mogi [84], shown in Figure 10.1, illustrate this relationship in practice. The figure presents the indicated thermal efficiency of a hydrogen-fuelled engine across a range of compression ratios. A clear increase in efficiency is observed with higher compression ratios. These results underline the fundamental trade-off: while higher compression ratios improve efficiency, they are constrained by combustion stability and abnormal ignition risks in hydrogen-fuelled engines.

10.3. Implications for this project

The WinGD X92DF engine, which serves as the reference engine in this study, operates with a geometric compression ratio of 12.4. When considering the effective compression ratio, defined from the moment the cylinder is fully closed at the end of scavenging, this value is approximately 9. Literature indicates that such compression ratios are generally acceptable for hydrogen combustion using DI un-

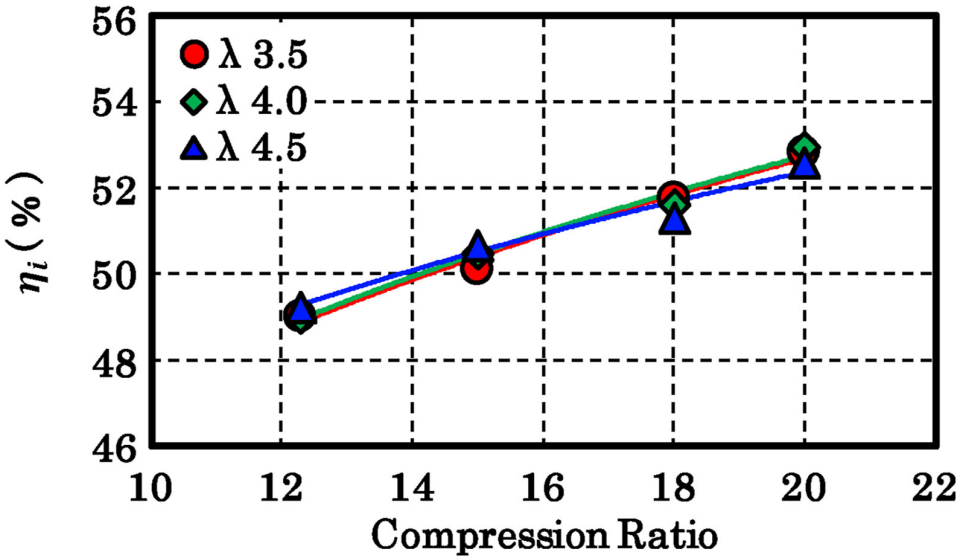

Figure 10.1: Change in indidated efficiency for various compression ratios [84]

der lean conditions [39, 56]. However, it is important to note that the LPDI configuration used in this project introduces additional challenges.

Similar to PFI, LPDI introduces hydrogen into the cylinder well before top dead centre, meaning the hydrogen–air mixture is present throughout the compression phase. This extended residence time under increasing pressure and temperature elevates the risk of pre-ignition. To mitigate this, the model employs a conservative strategy, maintaining an air excess ratio (λ) of at least 3.0 across all operating conditions. This is consistent with findings from literature showing that leaner mixtures significantly reduce the occurrence of knocking and surface ignition [18, 84].

Despite the effective compression ratio and lean operation being within safe limits, the lack of empirical combustion data for large two-stroke hydrogen engines justifies a cautious approach. Furthermore, lean hydrogen mixtures tend to ignite more slowly, especially in engines using spark ignition, where ignition can only begin from a very small localised region [18]. To address this, the study adopts a dual-fuel combustion strategy, using high-pressure diesel injection as a pilot fuel.

This pilot fuel improves ignition reliability by ensuring adequate penetration and initiating multiple ignition sites throughout the combustion chamber. In the context of this project, the HES is therefore limited to 80%, meaning that diesel contributes at least 20% of the total energy input. This dual-fuel configuration strikes a practical balance between maximising the benefits of hydrogen combustion and ensuring safe and reliable engine operation under conditions representative of a large two-stroke marine engine.

11

Wiebe

As outlined in Section 7.3, the Seiliger process, while useful for many general combustion modelling purposes, has inherent limitations. One key constraint is that it does not allow the user to shift the start of combustion beyond TDC, as it is fundamentally constructed around an isochoric heat addition phase centred at TDC. This becomes problematic in cases where delayed ignition is either desirable or necessary, which could be the case with hydrogen combustion under high load, where starting the combustion too early may result in excessive peak pressures.

In such cases, an alternative approach based on the Wiebe function offers a more flexible framework. The Wiebe model allows for a time-resolved description of the combustion rate as a function of crank angle, thereby enabling the study of scenarios in which the combustion onset is delayed past TDC.

This chapter provides a brief overview of the Wiebe function and demonstrates its application in a simplified form to the specific two-stroke hydrogen-fuelled engine under consideration in this project. The results are used to illustrate the impact of delayed combustion on the in-cylinder pressure evolution.

11.1. Wiebe function

The Wiebe function models the cumulative heat release, expressed as the fraction of fuel burned, as a function of the crank angle. This approach is widely adopted for engine cycle simulations across different combustion systems due to its empirical basis and adaptability. According to Ghojel [85], the Wiebe function is particularly valuable because it can be applied across various engine types, including DI diesel engines, SI engines, DI gasoline engines, and homogeneous charge compression ignition engines. This versatility makes it ideal for use in modelling combustion processes for unconventional fuels like hydrogen in large marine engines, as required in this study.

The Wiebe function is expressed mathematically as shown in Equation 11.1 [26], where the mass fraction burned is represented as a function of the crank angle:

$$x_b = 1 - \exp\left[-a\left(\frac{\theta - \theta_0}{\Delta\theta}\right)^{m+1}\right] \tag{11.1}$$

In this equation:

- θ is the crank angle
- θ_0 is the start of combustion
- $\Delta\theta$ represents the total combustion duration, over which the fraction burned increases from 0 to 1
- a and m are adjustable parameters that control the shape and steepness of the burn curve

By adjusting the parameters a and m, the Wiebe function can produce a variety of burn rate profiles, making it highly adaptable to different combustion conditions. This flexibility is especially important when modelling fuels with distinct combustion characteristics, as the shape of the curve can be tuned to match the desired combustion behaviour for hydrogen. The parameters a and m allow for significant changes in the curve's shape, as can be seen in Figure 11.1, which can closely represent the heat release patterns required in different combustion environments.

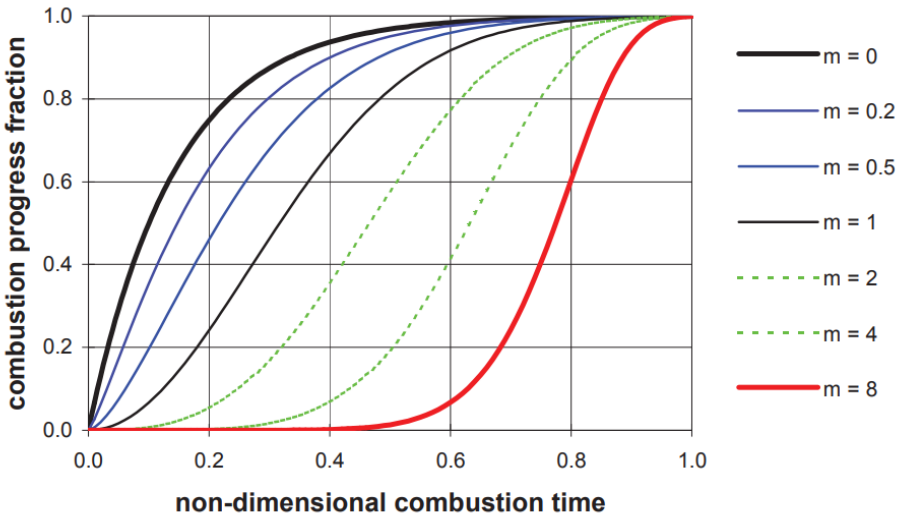

Figure 11.1: Combustion progress fraction plotted against combustion time for various values of Wiebe parameters [28]

For applications involving engines with complex combustion phases, such as those with a strong premixed combustion component, a single Wiebe function may be insufficient. In such cases, a combination of multiple Wiebe functions can be used to achieve a more accurate representation of the heat release characteristics, particularly for engines with layered combustion phases or direct injection systems [86]. However, given the focus of this project on evaluating engine limits rather than detailed pollutant formation, a single Wiebe function is expected to offer an adequate balance of accuracy and simplicity.

Determining Wiebe parameters

The accuracy of the Wiebe function in representing combustion behaviour depends heavily on the correct selection of its parameters, particularly a, m, θ_0, and $\Delta\theta$. Under ideal conditions, these parameters are calibrated based on experimental data specific to the engine and fuel being modelled. However, in cases where experimental data are unavailable, such as in this study, alternative methods must be employed to determine these parameters as accurately as possible.

When direct experimental data are lacking, a practical approach is to reference parameter values from similar studies on comparable engines or fuels. For instance, values from studies on natural gas or methane-fuelled large two-stroke engines can serve as a starting point, as well as values from studies on hydrogen combustion in smaller engines. This approach allows for an initial approximation that can later be refined.

In some cases, empirical correlations developed from a broad range of engine data can be used to estimate Wiebe parameters. These correlations often relate parameters like a and m to fundamental combustion properties or operating conditions, such as equivalence ratio, compression ratio, or fuel type.

11.2. Application of a simplified Wiebe model

To illustrate how a Wiebe model can be applied to analyse combustion phenomena that cannot be represented using a Seiliger approach, a simplified Wiebe model was implemented for the X92DF

engine. For this purpose, a MATLAB script from the book Internal Combustion Engines: Applied Thermosciences [87] was used to quickly establish the model framework.

The results are shown in Figure 11.2, where the blue curve simulates typical combustion with a peak pressure (p_{max}) occurring at TDC, while the orange curve represents an alternative timing scenario in which combustion starts 5 degrees after TDC. It is evident from this comparison that, although the same amount of fuel is burned in both cases, the timing of the combustion process significantly affects the magnitude of p_{max}.

If it were found that hydrogen combustion in this engine leads to a peak pressure exceeding the engine's design limits, it could be a viable strategy to initiate combustion slightly later in the cycle. A full investigation into this approach and its associated effects lies beyond the scope of this project. Nevertheless, this example effectively demonstrates how different modelling techniques serve different analytical purposes within engine simulation.

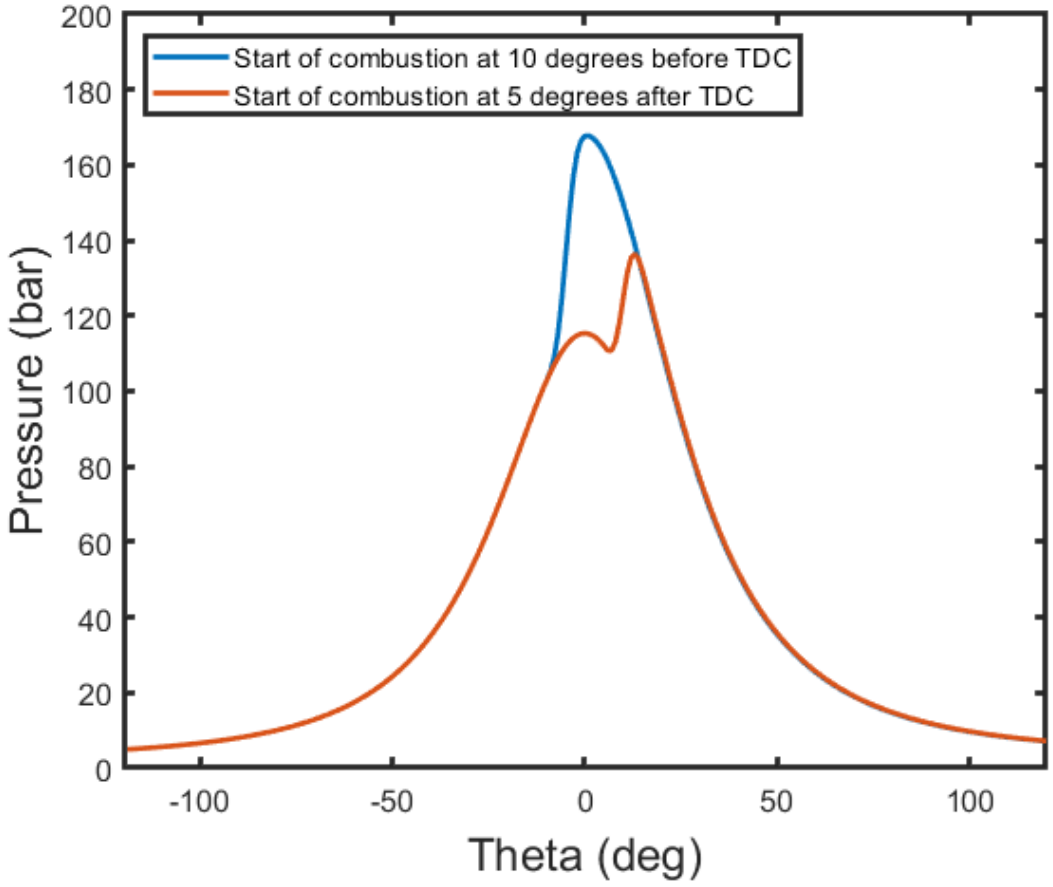

Figure 11.2: Representation of the difference in maximum pressure as a result of various combustion start moments

12

Results

Throughout this project, as described in Chapter 7 and using the parameters provided in Chapter 8, a fully functional closed-cycle combustion model has been developed for the WinGD X92DF engine. This model allows simulation of operation partially fuelled by hydrogen through LPDI. By means of a Seiliger process, the model calculates various thermodynamic parameters characterising the combustion cycle in detail.

The model includes functionality to specify the fraction of energy input derived from hydrogen. For each specified setting, the Seiliger process is computed over a full range of engine loads, from nominal power down to minimum operating power. The resulting outputs provide a rich dataset from which key parameters can be extracted and visualised through a series of plots.

In this chapter, the selection of several important model parameters is first justified. Subsequently, the results from a number of different combustion scenarios are presented and discussed.

12.1. Model parameters

In this section, several key model parameters are introduced and discussed. These parameters play a crucial role in shaping the outcomes of the combustion simulations and are therefore essential for the definition of the various scenarios considered. Where necessary, justification is provided for the chosen values or assumptions.

Maximum Hydrogen Energy Share

At the start of the project, the intention was to model a combustion process in which the engine would operate almost entirely on hydrogen, with at a maximum only a few percent of diesel used as a pilot fuel for ignition. However, as the project progressed, increasing evidence emerged suggesting that achieving reliable ignition of hydrogen in internal combustion engines is highly challenging, particularly for larger engines [39, 45, 83].

Moreover, most of the engines used in experimental research on hydrogen combustion are significantly smaller than the WinGD X92DF engine considered in this study. These findings raised doubts about the feasibility of fully replacing conventional fuels with hydrogen in such a large engine.

Consequently, and in alignment with the modelling approach of Serrano [30], who also simulates hydrogen combustion in a large, low-speed, two-stroke engine, it was decided to adopt a maximum HES of 0.8. The remaining 20% of the energy input is assumed to come from conventional diesel fuel, injected at high pressure. This quantity of diesel is expected to be more than sufficient to generate a penetrating fuel jet capable of initiating complete and reliable ignition of the hydrogen-air mixture throughout the cylinder.

Nevertheless, this configuration still allows for the substantial benefits of hydrogen combustion, including a significant reduction in harmful emissions.

Air excess ratio settings

As shown in Figure 12.1a, the air excess ratio λ for standard diesel operation is a direct output from the model. It is plotted against the relative power fraction. The air excess ratio is typically high at low power fractions, reaches a minimum value of 2.25 and goes to 2.66 at nominal power. As previously discussed in Section 4.4, hydrogen combustion typically requires a higher air excess ratio than diesel combustion to mitigate the characteristic combustion challenges associated with hydrogen.

Therefore, according to Section 10.3, the model has been adjusted so that the minimum air excess ratio for hydrogen operation is set to 3.00. The resulting curve for hydrogen operation across the same range of power fractions is shown in Figure 12.1b.

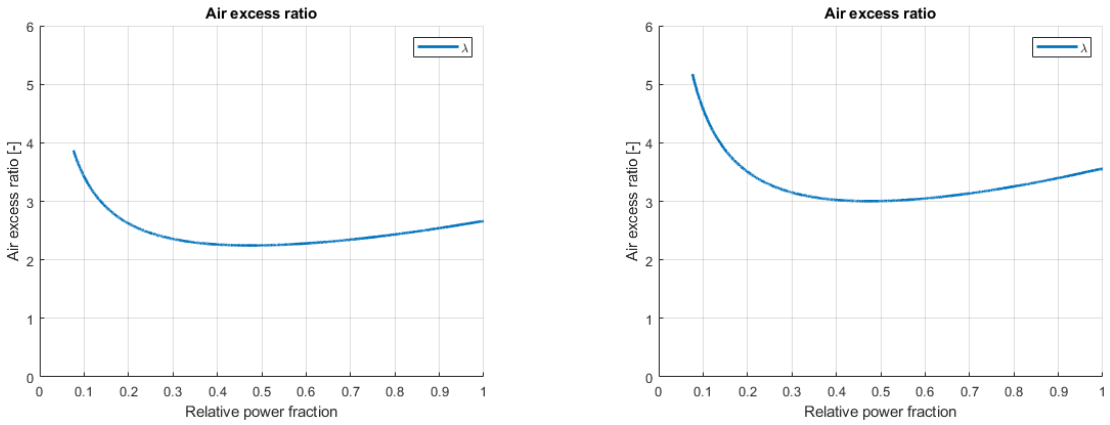

(a) Standard diesel operation (HES = 0)

(b) Normal hydrogen operation (HES = 0.8)

Figure 12.1: Air excess ratio λ plotted against the relative power fraction for both diesel and hydrogen operation

A direct consequence of applying a higher air excess ratio is a reduction in the maximum achievable power output. For the X92DF engine operating at a HES of 0.8, the nominal power decreases from 63,840 kW in standard diesel mode to approximately 57,300 kW. This represents a reduction of around 10% in nominal power. Similar reductions in maximum power output are frequently reported when switching from diesel to hydrogen combustion because of this need for a higher air excess ratio. The engine power in both cases is illustrated in Figure 12.2.

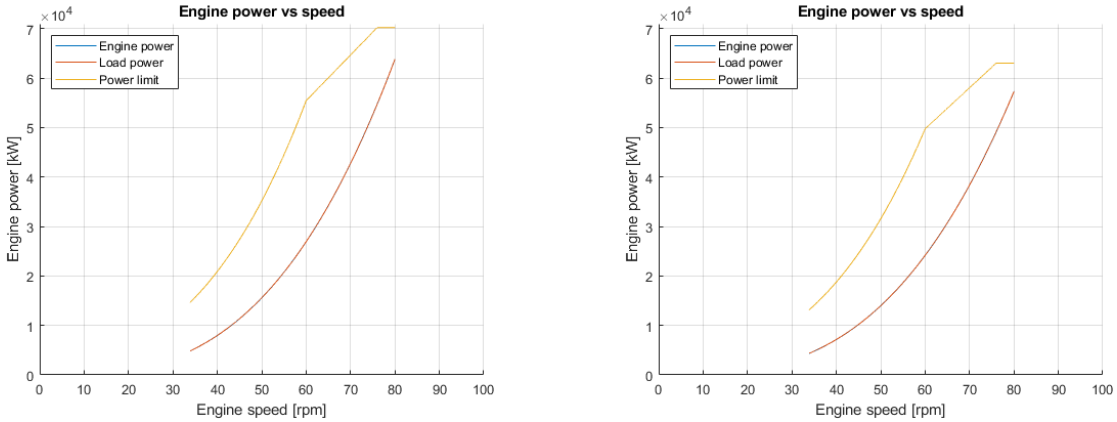

(a) Standard diesel operation (HES = 0)

(b) Normal hydrogen operation (HES = 0.8)

Figure 12.2: Engine power plotted against engine speed for both diesel and hydrogen operation

12.2. Model results

In this section, the outcomes of the combustion model are presented, focusing on the predicted values for peak pressure (p_{max}), peak temperature (T_{max}), and the resulting Seiliger p-V diagrams. These

outputs are shown for three distinct combustion scenarios to allow for comparison of different fuel strategies.

The first scenario reflects standard diesel combustion with a HES of 0.0, serving as the baseline. The second scenario represents normal hydrogen-assisted combustion with HES = 0.8, under the assumption that the fuel mixture burns at a similar rate as in fully diesel operation. The third scenario models fast hydrogen combustion, also at HES = 0.8, but assumes that 90% of the combustion occurs during the isochoric combustion stage and none during the isothermal stage. This effectively turns the process into a five-stage Seiliger cycle.

This distinction in combustion phasing is introduced to explore the sensitivity of the model results to combustion speed. Due to the limited technical specifications available for the engine and the absence of experimental validation data, it is difficult to precisely estimate the combustion characteristics of a hydrogen-diesel mixture. However, the two hydrogen combustion scenarios are expected to represent the realistic boundaries between which actual engine behaviour will fall.

12.2.1. Maximum pressure results

The figures below present the results from the model showing the pressure development at nominal engine power plotted against the crank angle during one full combustion cycle. Figure 12.3 displays the pressure curve for standard diesel operation (HES = 0), which reaches a peak pressure of 160 bar, which is also explained in the parameter determination outlined in Section 7.2.

When operating under the normal hydrogen combustion scenario (HES = 0.8), as shown in Figure 12.4, the model predicts only a modest increase in peak pressure, reaching approximately 166 bar. However, in the fast hydrogen combustion case, represented in Figure 12.5, a significantly higher peak pressure of around 215 bar is observed.

Such a considerable increase relative to the diesel baseline raises concerns about whether this pressure would exceed the mechanical limits for which the engine was designed. To better assess the implications of this result, it would be necessary either to determine more precisely where between 166 bar and 215 bar the actual peak pressure will occur for hydrogen combustion in this engine, or to establish the maximum allowable pressure according to the engine's design specifications. The latter is typically information only accessible via the engine manufacturer.

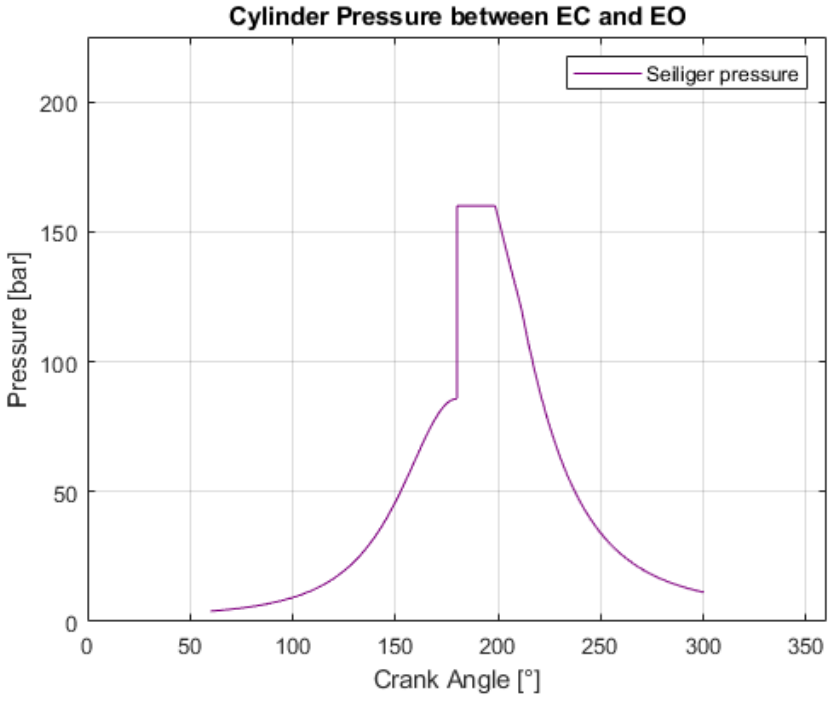

Figure 12.3: Pressure development at nominal power plotted against crank angle for standard diesel operation (HES = 0)

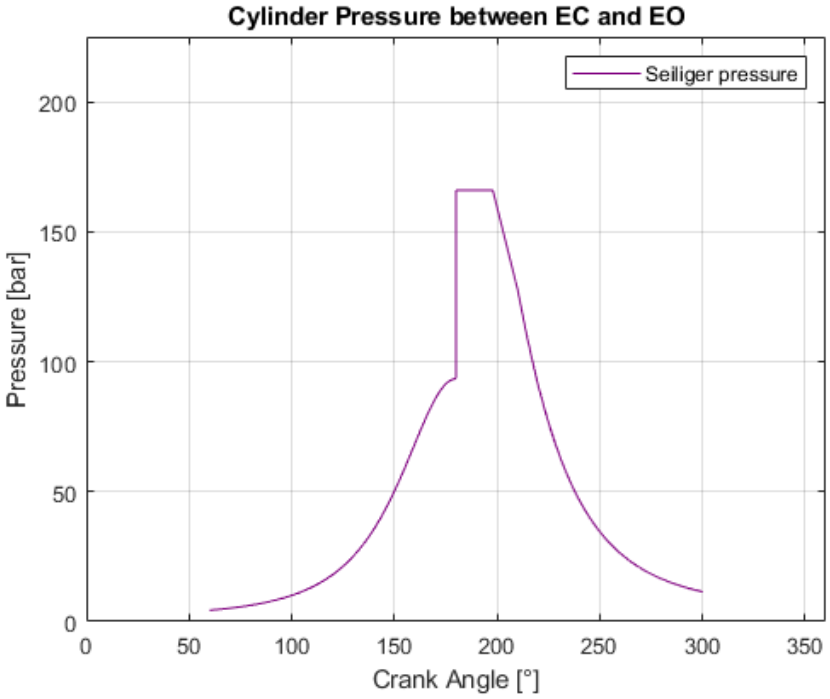

Figure 12.4: Pressure development at nominal power plotted against crank angle for normal hydrogen combustion (HES = 0.8)

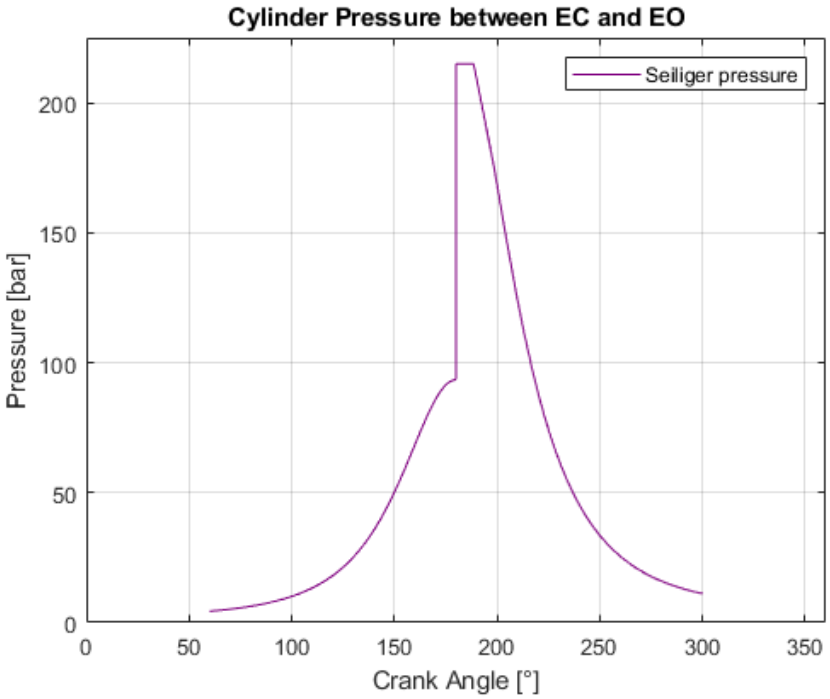

Figure 12.5: Pressure development at nominal power plotted against crank angle for fast hydrogen combustion (HES = 0.8)

12.2.2. Maximum temperature results

The figures below display the temperature profiles plotted against the crank angle during one full combustion cycle at nominal engine power. Figure 12.6 shows the temperature development for standard diesel operation, while Figures 12.7 and 12.8 show the same for normal and fast hydrogen combustion, respectively.

From these plots, it is evident that the peak temperature under normal hydrogen combustion is slightly lower than in the standard diesel case. This observation is consistent with the thermodynamic behaviour described in Section 9.1, where it was shown that the specific heat capacity of a hydrogen-air mixture is significantly higher than that of pure air. A higher specific heat capacity implies that a greater amount of energy is required to increase the temperature of one kilogram of the mixture by one kelvin, which results in a lower temperature rise for the same energy input.

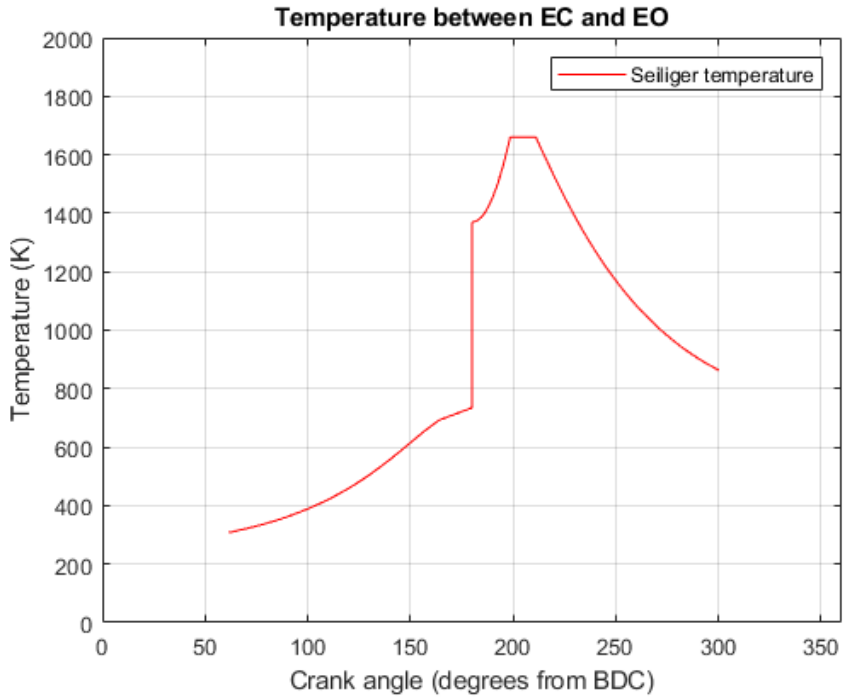

Figure 12.6: Temperature development at nominal power plotted against crank angle for standard diesel operation (HES = 0)

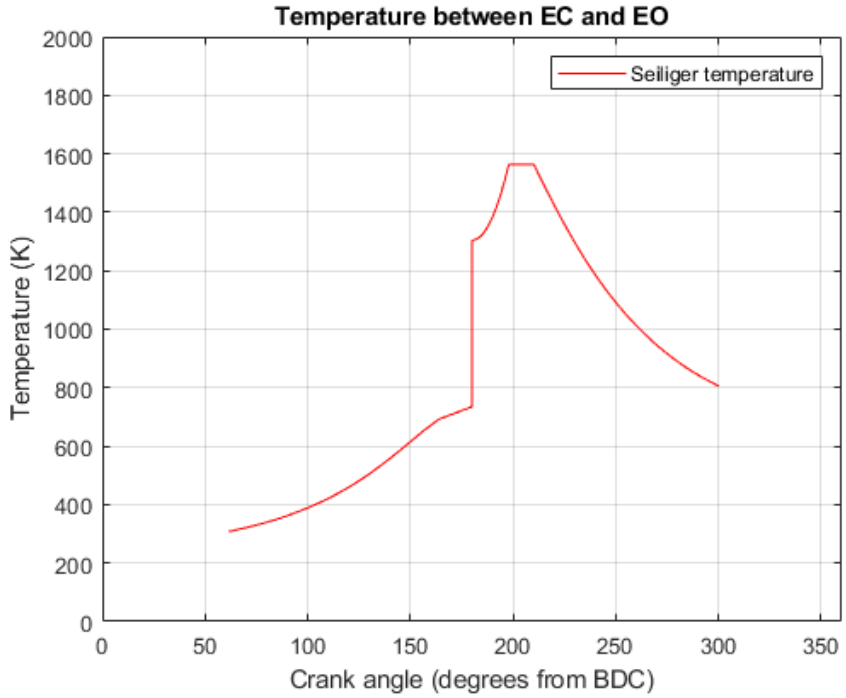

Figure 12.7: Temperature development at nominal power plotted against crank angle for normal hydrogen combustion (HES = 0.8)

In the case of fast hydrogen combustion, however, the temperature increases significantly. This is due to the higher in-cylinder pressure reached in this scenario, as discussed in Section 12.2.1. The elevated temperature in this case will also lead to an increase in NOx emissions, as elaborated in Section 4.1, which is an undesirable side effect.

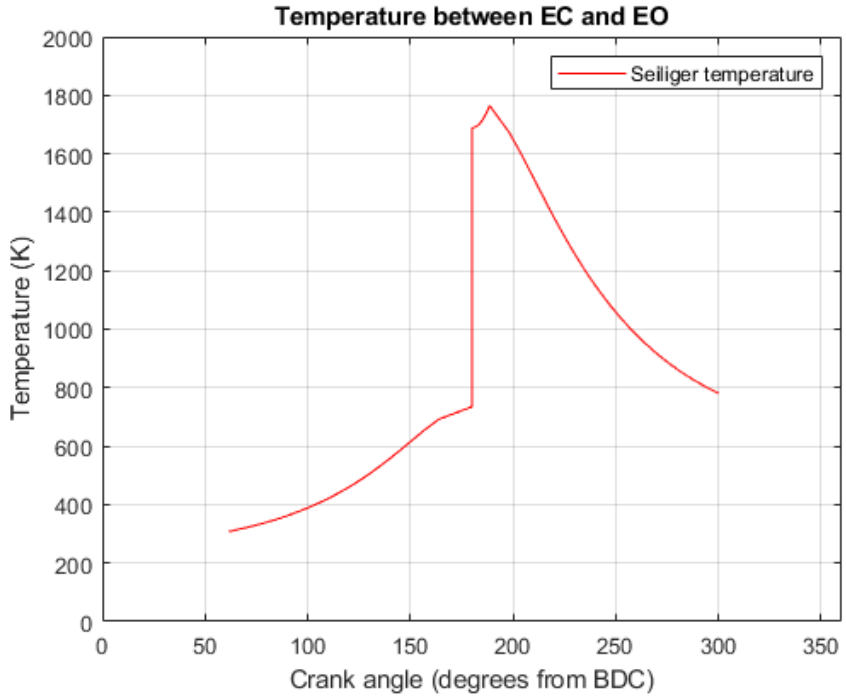

Figure 12.8: Temperature development at nominal power plotted against crank angle for fast hydrogen combustion (HES = 0.8)

12.2.3. Seiliger p−V diagrams

To provide a clear overview of the complete combustion cycles, the p–V diagrams for the three combustion scenarios are shown in Figures 12.9, 12.10, and 12.11. These diagrams offer valuable insight into how the pressure and volume evolve throughout the cycle and allow for an intuitive comparison of the different combustion strategies.

One notable observation is that the pressure at state point 2 in the hydrogen combustion diagrams is slightly higher than in the diesel case. This effect can be attributed to the addition of hydrogen during the compression phase through LPDI, as discussed in Section 7.1. The presence of additional fuel mass during compression increases the mixture pressure at the end of the compression stroke.

Furthermore, the diagram corresponding to the fast hydrogen combustion scenario shows a pronounced resemblance to that of a classic Otto cycle. This similarity arises due to the absence of significant combustion in the isothermal phase and the near-complete combustion within the isochoric phase, with minimal energy release occurring under isobaric conditions. As a result, the process deviates markedly from a typical Seiliger cycle and instead reflects the behaviour of an idealised Otto cycle.

In addition to pressure–volume behaviour, the Seiliger cycle enables the estimation of theoretical thermodynamic efficiency, which is defined as:

$$\eta_{\mathrm{td,th}} = \frac{w_{\mathrm{i,th}}}{q_{\mathrm{i,th}}} \tag{12.1}$$

where the specific work and specific heat input are determined by summing the work and heat contributions of the individual Seiliger stages:

$$w_{\mathrm{i,th}} = w_{12} + w_{34} + w_{45} + w_{56} \tag{12.2}$$

$$q_{\mathrm{i,th}} = q_{12} + q_{23} + q_{34} + q_{45} + q_{56} \tag{12.3}$$

The results from the model show that the thermodynamic efficiency for the standard diesel combustion case is approximately 57.95%. For normal hydrogen combustion, this efficiency increases slightly to 58.11%, while for the fast hydrogen combustion scenario it rises to 60.12%.

This improvement in efficiency for the fast hydrogen case is primarily a result of the more concentrated energy release during the iso-volumetric stage, which increases the peak pressure and expands the area enclosed in the p–V diagram, thereby increasing specific work output. However, this gain in efficiency comes at the cost of significantly higher peak pressures and temperatures, which may exceed mechanical limits and raise emissions concerns, as discussed in Sections 12.2.1 and 12.2.2.

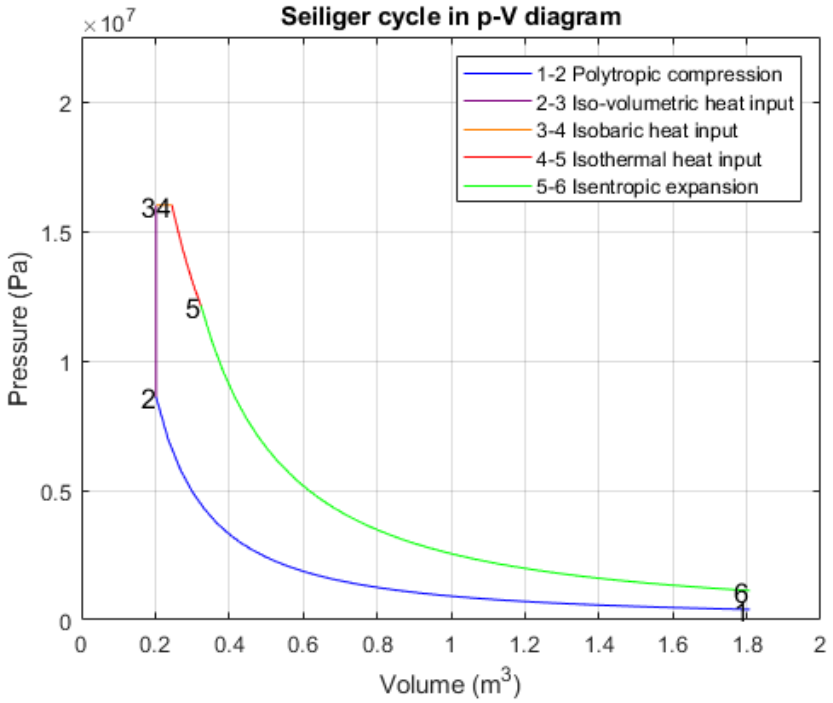

Figure 12.9: Seiliger p-V diagram at nominal power for standard diesel operation (HES = 0)

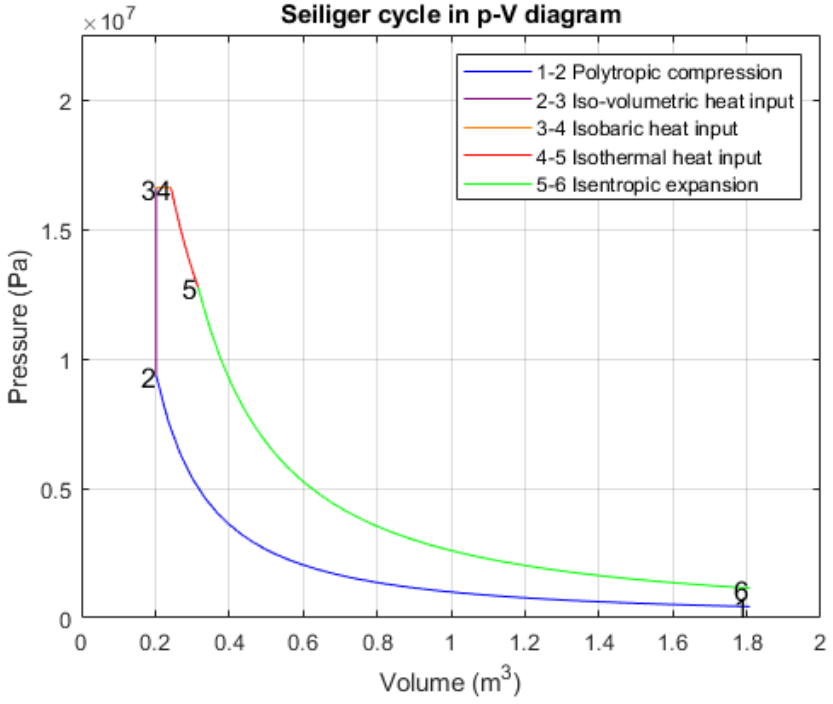

Figure 12.10: Seiliger p-V diagram at nominal power for normal hydrogen combustion (HES = 0.8)

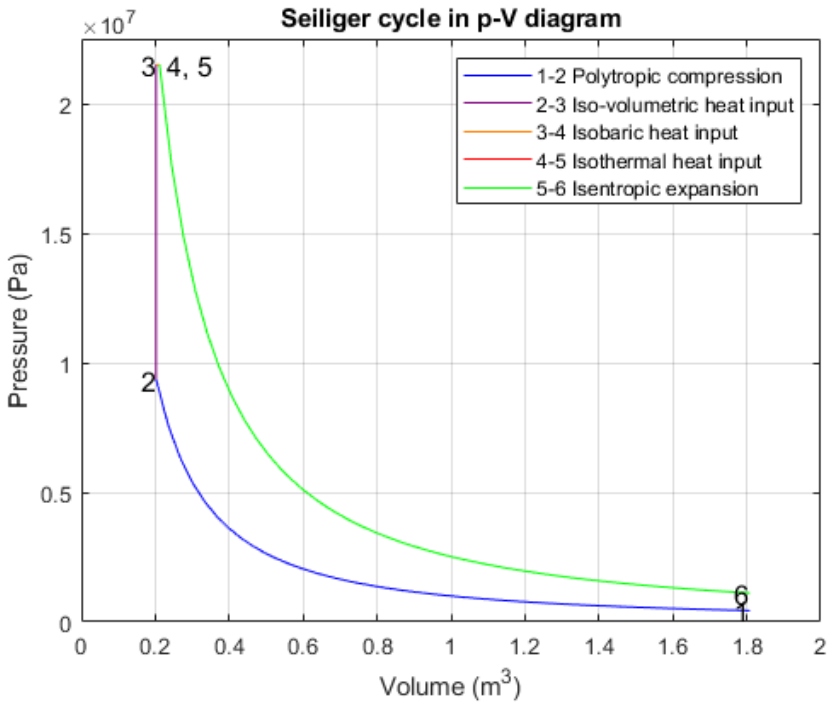

Figure 12.11: Seiliger p-V diagram at nominal power for fast hydrogen combustion (HES = 0.8)

12.2.4. Compression and expansion refinement results

This section presents the results obtained by implementing the refinement method described in Chapter 9, where the temperature-dependent variation of the specific heat capacities c_p and c_v was incorporated into the Seiliger process. The refinement was applied across all three combustion scenarios: standard diesel combustion (HES = 0), normal hydrogen combustion (HES = 0.8), and fast hydrogen combustion (HES = 0.8). For each case, the refined temperature, pressure, and p–V diagrams are plotted and compared to the original Seiliger output.

Diesel (HES = 0)

Figures 12.12, 12.13, and 12.14 show the results for standard diesel operation. As seen in the plots, the refined temperature and pressure curves (blue markers) deviate slightly from the standard Seiliger process (orange line), particularly in the latter stages of the compression and expansion phases. The correction results in a marginally lower peak pressure and temperature, due to the influence of increasing c_p at elevated temperatures. This effect results in a downward shift of the expansion curve in the p–V diagram, leading to a slight reduction in the area enclosed by the cycle and thus a marginal decrease in theoretical cycle efficiency.

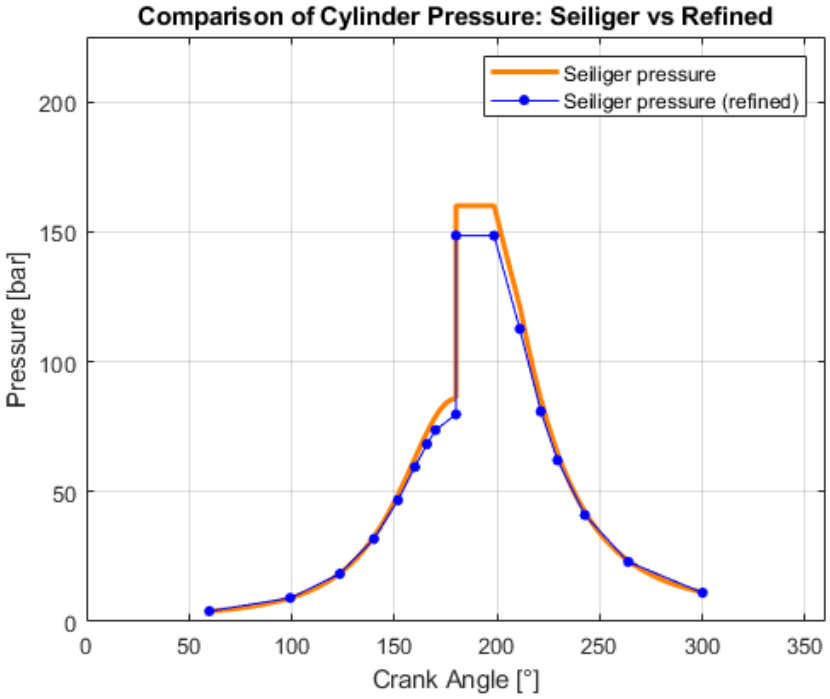

Figure 12.12: Comparison of cylinder pressure between nominal and refined Seiliger models at HES = 0 (standard diesel)

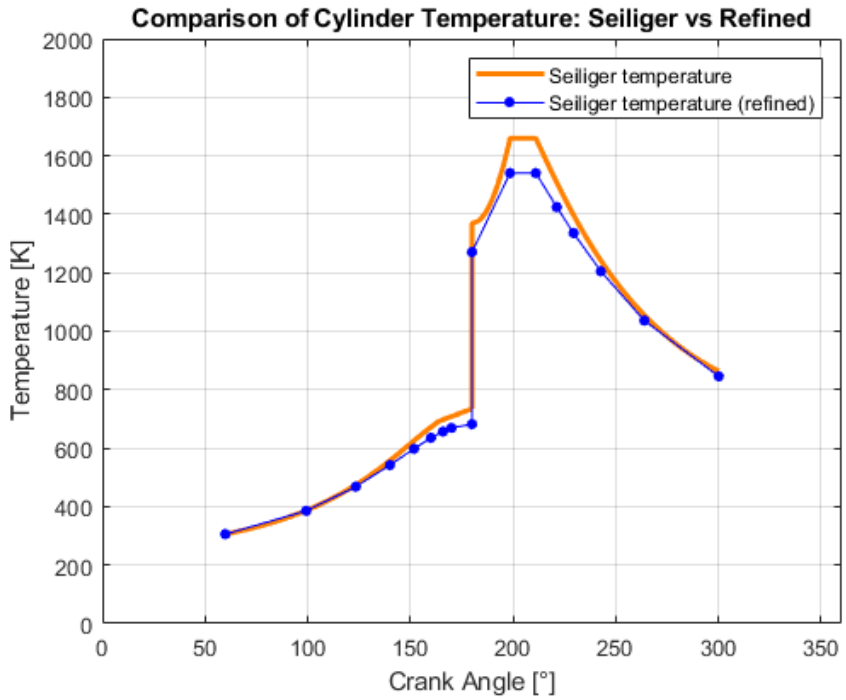

Figure 12.13: Comparison of cylinder temperature between nominal and refined Seiliger models at HES = 0 (standard diesel)

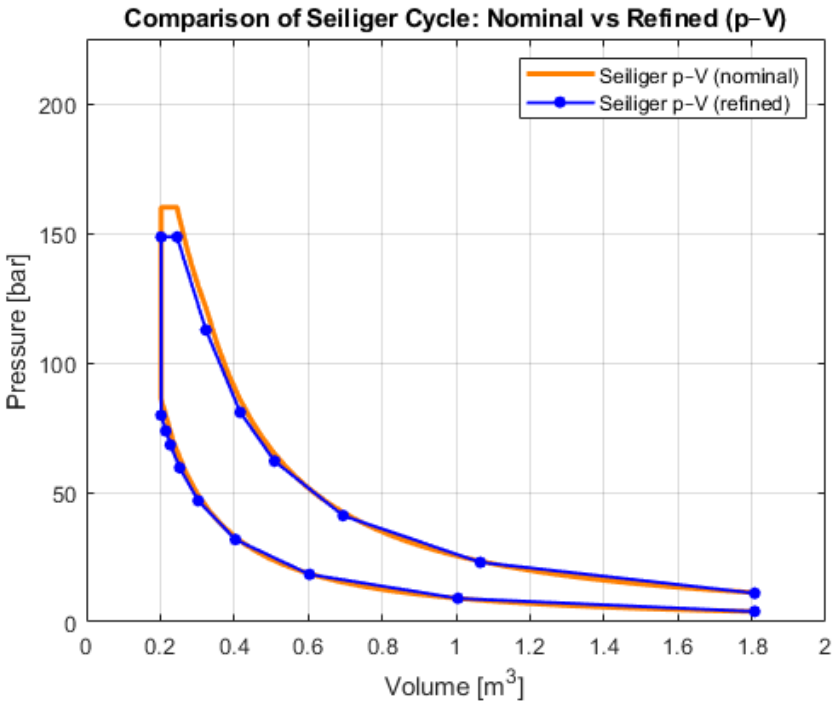

Figure 12.14: Comparison of p–V diagram between nominal and refined Seiliger models at HES = 0 (standard diesel)

Normal hydrogen combustion (HES = 0.8)

Figures 12.15, 12.16, and 12.17 show the results for the normal hydrogen combustion scenario. Compared to the diesel case, the difference between the nominal and refined model is of similar magnitude, despite the use of a different working gas composition.

This can be explained by the fact that, although the specific heat capacity c_p of the hydrogen–air mixture differs significantly from that of pure air, the ratio of specific heats $\gamma = c_p/c_v$ remains relatively similar across the relevant temperature range. As shown in Table 9.4, the values of γ for air and for the hydrogen–air mix converge closely, resulting in comparable behaviour during the compression and expansion phases when refinement is applied.

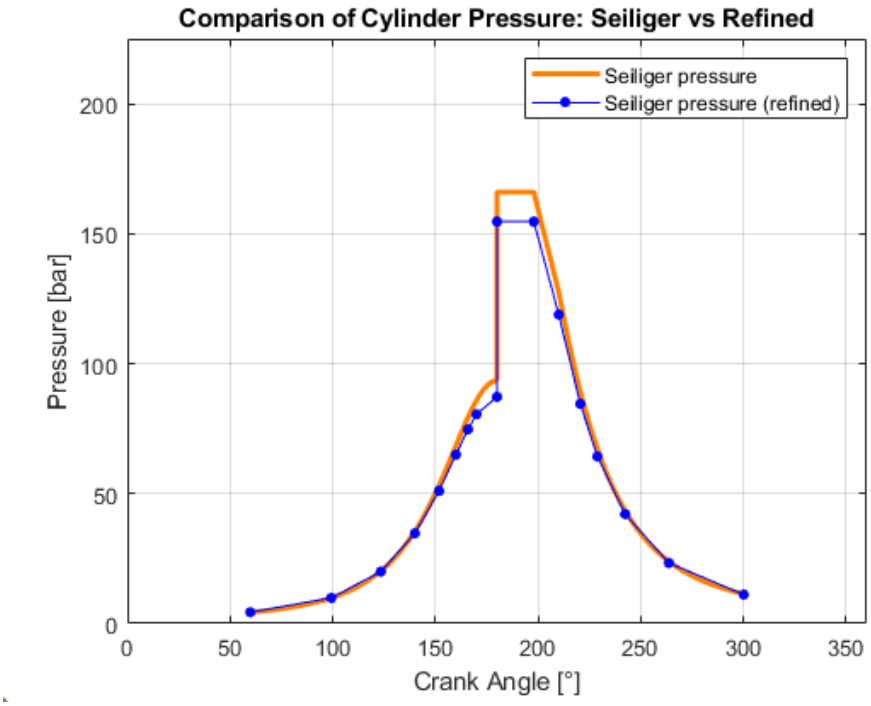

Figure 12.15: Comparison of cylinder pressure between nominal and refined Seiliger models at HES = 0.8 (normal hydrogen combustion)

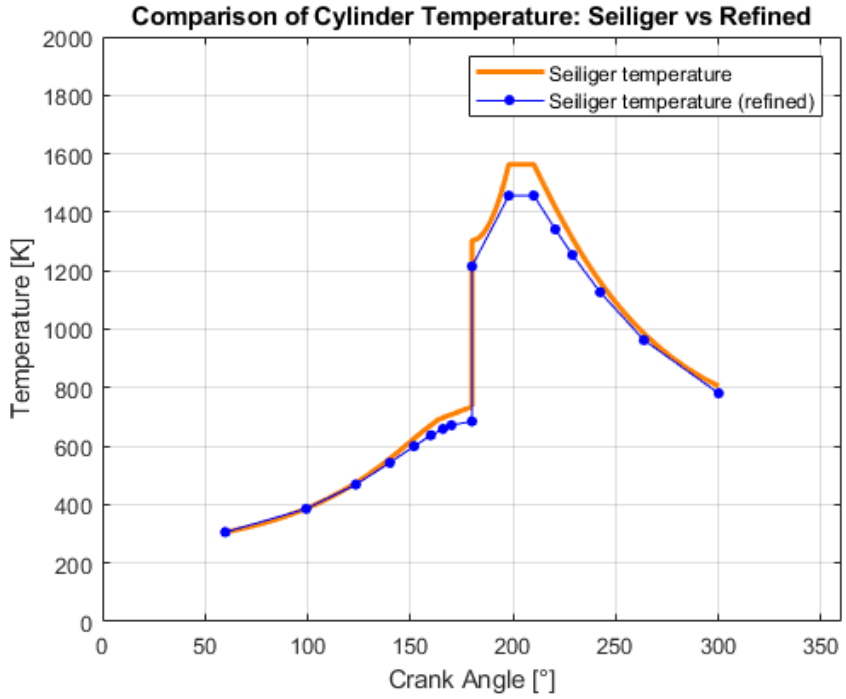

Figure 12.16: Comparison of cylinder temperature between nominal and refined Seiliger models at HES = 0.8 (normal hydrogen combustion)

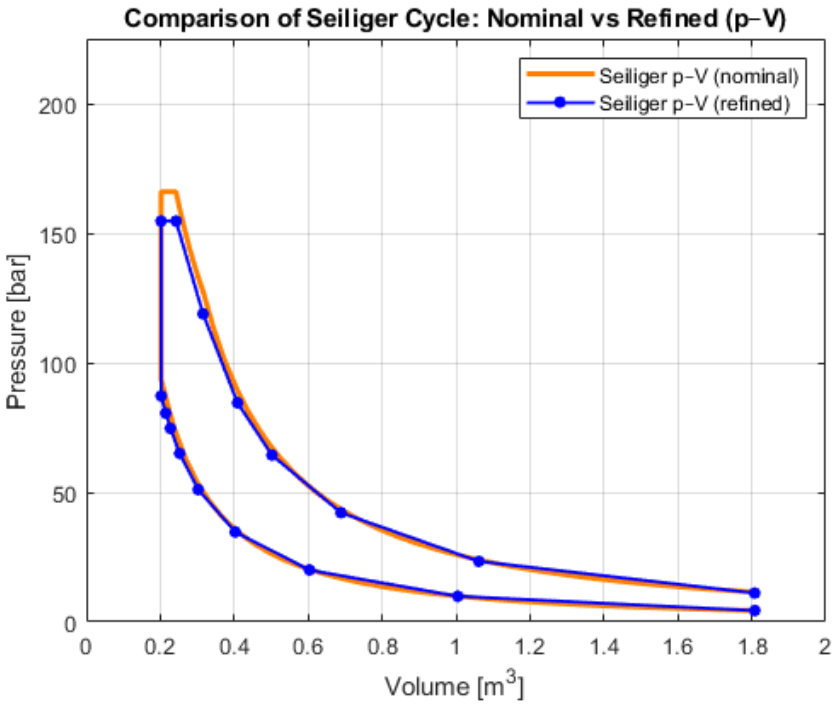

Figure 12.17: Comparison of p–V diagram between nominal and refined Seiliger models at HES = 0.8 (normal hydrogen combustion)

Fast hydrogen combustion (HES = 0.8)

Figures 12.18, 12.19, and 12.20 show the refinement results for the fast hydrogen combustion scenario. While the shape of the curves remains broadly similar to the nominal model, the refined temperature shows a slight reduction across the compression and expansion phases due to the temperature-dependent specific heat.

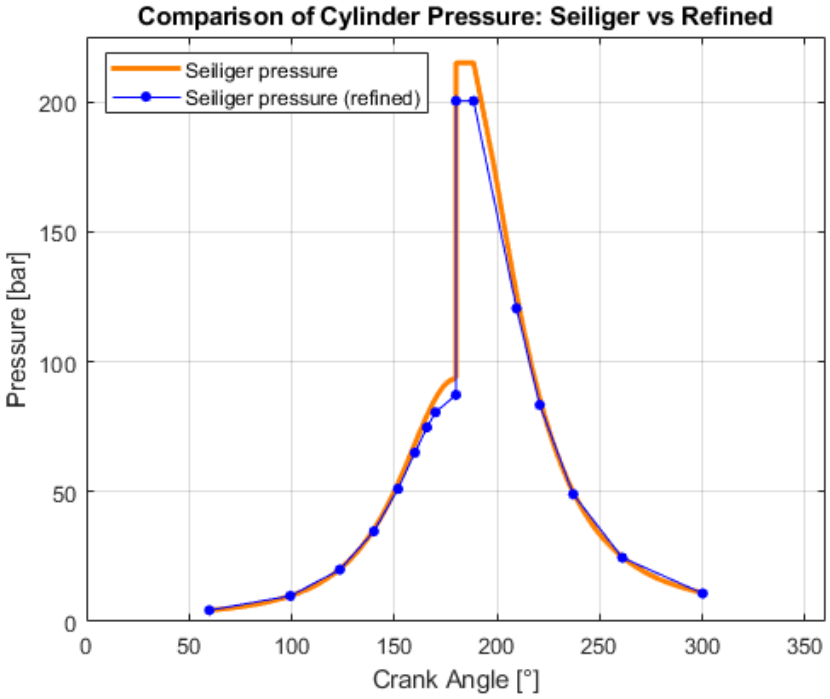

Figure 12.18: Comparison of cylinder pressure between nominal and refined Seiliger models at HES = 0.8 (fast hydrogen combustion)

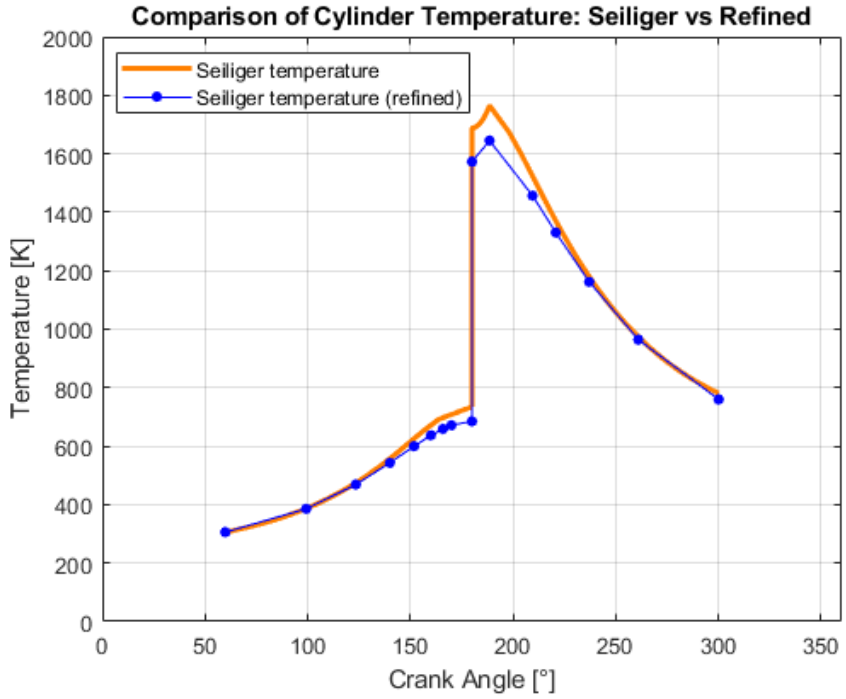

Figure 12.19: Comparison of cylinder temperature between nominal and refined Seiliger models at HES = 0.8 (fast hydrogen combustion)

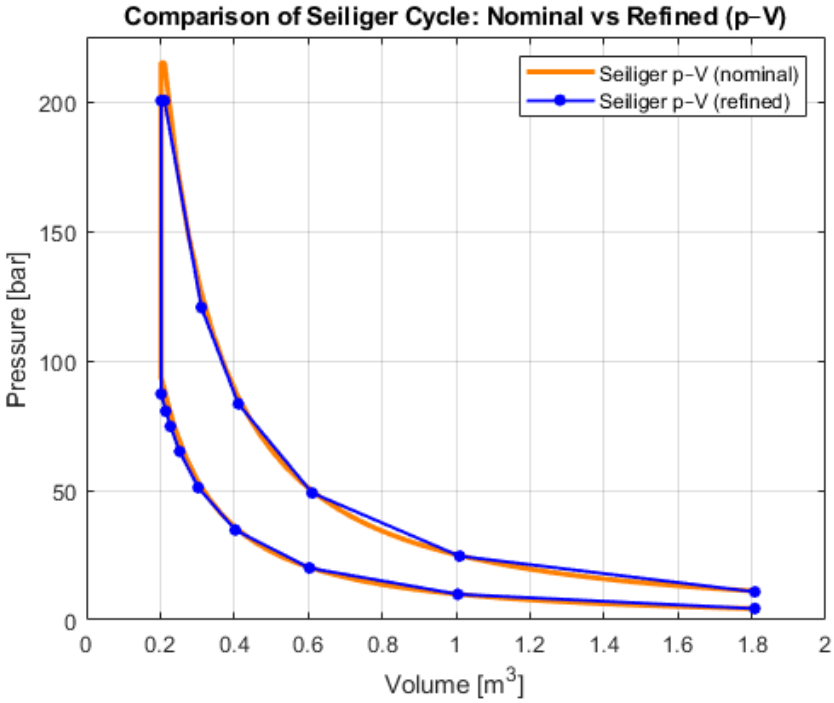

Figure 12.20: Comparison of p–V diagram between nominal and refined Seiliger models at HES = 0.8 (fast hydrogen combustion)

Conclusion on refinement

The integration of temperature-dependent thermodynamic properties into the Seiliger model demonstrably affects the predicted pressure and temperature development throughout the combustion cycle. While the overall shape of the combustion profiles remains similar, the refined model consistently yields lower peak temperatures and pressures compared to the classical model that assumes a constant γ. This indicates that the simplified approach may lead to systematic overestimations of thermal loads and in-cylinder conditions.

As a direct consequence of the altered temperature profile, the refinement also affects the calculated thermodynamic efficiency and work output of the cycle. Since both of these parameters are highly temperature-dependent, the refined model does not produce the same indicated power as the nominal model under identical boundary conditions. To reconcile this difference and match the same power output, the refined model would require further adjustment, for example by redistributing combustion phasing or by calibrating the model against experimental data, which falls outside the scope of this study.

Instead, the objective of the refinement presented here is to highlight the sensitivity of the Seiliger model to its thermodynamic assumptions, and to demonstrate how a more realistic representation of compression can influence model outcomes.

12.2.5. Conclusion of modelling results

The combustion model developed in this project provides an extensive and insightful dataset regarding the behaviour of hydrogen combustion in large two-stroke marine engines. Although many specific values within the model remain subject to validation by experimental data, the outcomes already offer a clear indication of the key phenomena that must be considered when introducing hydrogen as a fuel in this engine type.

The model allows for a structured exploration of how variations in combustion characteristics such as energy share, air excess ratio, and combustion timing affect important parameters including peak pressure, temperature, and the overall pressure–volume trajectory. This enables a more informed assessment of the feasibility and challenges of hydrogen implementation, highlighting the need for

careful optimisation of the combustion strategy to ensure both safe operation and favourable emission profiles.

13

Conclusions and recommendations

This chapter presents the overall conclusions of the study and addresses the research questions that were defined in Chapter 2. It begins with a summary of the conclusions drawn from the literature review, as previously outlined in Chapter 6. These findings are then expanded with the additional insights gained from the modelling work conducted during the research phase of this project.

Finally, this chapter offers several recommendations. These include suggestions on how to use the developed model effectively, as well as guidance for future research directions that could improve or build upon the results of this study.

13.1. Conclusion

The aim of this section is to formulate the best possible answer to the central research question that has guided this study:

> *"How can an in-cylinder combustion model be used to evaluate the feasibility and technical implications of hydrogen operation with LPDI in large two-stroke marine engines?"*

As outlined in Chapter 6, the literature review provided a strong foundation for answering this question.

Conclusions from literature review

The first sub-questions were addressed by examining existing research on hydrogen combustion, marine two-stroke engines, and applicable modelling techniques. These insights are summarised below.

What key parameters are found to be of influence on the reliable combustion of hydrogen in existing hydrogen internal combustion engines?

Hydrogen combustion is particularly sensitive to abnormal combustion phenomena such as pre-ignition and knocking, due to hydrogen's high reactivity and low ignition energy. While backfiring is frequently cited as a challenge, it is primarily relevant to four-stroke engines and was therefore not considered in this study.

Three main strategies emerge from the literature as essential for ensuring reliable hydrogen combustion: lean fuel-air mixtures, a suitable ignition method, and DI. Lean mixtures reduce the flame speed and lower the combustion temperature, mitigating the risk of knocking. The ignition method must account for hydrogen's high auto-ignition temperature; in larger engines, prime fuel injection is generally more reliable than spark ignition. DI is preferable for avoiding pre-ignition and improving combustion control, especially in large marine engines.

How are the main characteristics of combustion in large two-stroke diesel engines generally modelled to determine the feasibility of reliable running?

Large two-stroke engines present unique modelling challenges, particularly due to their scavenging phase in which fresh air and exhaust gases overlap. When using LPDI, this overlap necessitates precise control over fuel injection timing to minimise fuel loss.

Three modelling strategies were identified:

- **Mean Value Engine Models (MVEM):** useful for system-level trends and control applications, but lacking in detailed in-cylinder resolution.
- **Zero-dimensional (0D) models:** more detailed, suitable for crank-angle resolved simulations of pressure and temperature, and capable of assessing performance indicators such as $p_{\max}$ and $T_{\max}$.
- **Advanced CFD-based models:** highly accurate but computationally expensive, and typically not viable for full-cycle simulations in the early design stages.

For the purposes of this project, evaluating performance indicators for hydrogen combustion in a two-stroke marine engine, a 0D approach strikes a balance between detail and practicality.

The insights gained from the literature provided a strong basis for the development of the model used in this study. The following sections will now present the additional findings obtained through the application and extension of this model.

Conclusions from research part

The research part of the project provided insights to answer the remaining sub-questions, which are answered below.

Which type of combustion model is most suitable for predicting the feasibility of reliable hydrogen operation in large two-stroke marine engines?

The choice of combustion model depends on the objectives of the study and the level of detail required. For predicting the feasibility of hydrogen operation in large two-stroke engines, the model must strike a balance between physical realism and computational efficiency. Full CFD models, while highly accurate, are too resource-intensive for exploratory analysis without detailed geometry and experimental validation data. Conversely, simplified empirical models lack sufficient detail to capture thermodynamic effects specific to hydrogen.

In this project, a Seiliger-based 0D thermodynamic model was found to be the most suitable approach. This model provides the flexibility to represent different phases of the combustion process and to adjust key inputs, such as combustion phasing and fuel distribution. It also allows the effect of fuel-specific thermodynamic properties, particularly the temperature dependence of c_p and c_v, to be integrated in a manageable way. While it cannot capture all spatial and transient dynamics, it offers a useful middle ground that enables effective comparison between combustion scenarios and fuels.

How does an in-cylinder combustion model need to be adapted to represent hydrogen combustion in a large two-stroke engine?

To accurately represent hydrogen combustion, the model must account for the unique physical and chemical behaviour of hydrogen, which differs significantly from conventional diesel fuels. These include higher specific heat capacities, a lower ignition energy, higher diffusivity, and a broader flammability range.

The primary adaptation made in this project was to incorporate temperature-dependent heat capacities (c_p and c_v) into the Seiliger model. This enhancement addresses the fact that hydrogen-air mixtures require more energy to achieve a given temperature rise compared to air or diesel-air mixtures. By using a polynomial-based approach (derived from NIST data) for estimating c_p across temperature ranges, the model improves predictions of in-cylinder temperature and pressure, particularly during the compression phase.

In addition, a separate implementation of a Wiebe function was used to illustrate cases where combustion is delayed after TDC, which cannot be captured by the standard Seiliger approach. This reinforces the idea that different modelling approaches serve different purposes and that a combined modelling strategy may be needed to fully assess hydrogen combustion behaviour.

What is the effect of different combustion scenarios and model assumptions on key engine performance outcomes when simulating hydrogen operation?
The model developed in this study demonstrates that the choice of combustion scenario and modelling assumptions has a substantial impact on predicted engine performance outcomes. These outcomes include peak in-cylinder pressure, maximum temperature, thermodynamic efficiency, and net work output.

In particular, the results show that assumptions about combustion phasing are highly influential. The fast hydrogen combustion scenario, in which combustion occurs predominantly during the iso-volumetric stage, leads to a peak pressure of approximately 215 bar, significantly higher than the 160 bar baseline for diesel operation and the 166 bar for normal hydrogen combustion. This highlights the risk of exceeding mechanical design limits under aggressive combustion timing, even with the same fuel energy input.

Additionally, the refinement of the model to include temperature-dependent thermodynamic properties revealed that the common assumption of constant γ may overestimate both pressure and temperature. These refined calculations, while not altering the fundamental combustion scenario, influence thermodynamic efficiency and total work output, thereby affecting overall performance predictions.

Although the model cannot resolve all uncertainties in the absence of experimental data, it enables structured scenario analysis and sensitivity exploration. This makes it a valuable tool for identifying realistic operating windows and assessing the feasibility of hydrogen combustion strategies in large two-stroke engines.

In conclusion, this study has provided a detailed investigation into the feasibility and implications of using hydrogen as a fuel in large two-stroke marine engines through a tailored in-cylinder combustion model. By evaluating multiple scenarios, refining classical modelling techniques, and adapting thermodynamic assumptions to reflect hydrogen's properties, the model offers valuable insights into key parameters such as peak pressure, temperature development, and combustion phasing.

As identified in the literature gap analysis in Section 6.2, there exists a noticeable lack of dedicated research on hydrogen combustion specifically in large two-stroke marine engines. While prior studies have extensively addressed hydrogen combustion in smaller engines and examined the general behaviour of marine diesel engines, the intersection of these fields remains underexplored. This project contributes to narrowing this gap by presenting a practical modelling framework that can support further exploration and inform future experimental validation and engine development efforts.

13.2. Recommendations

Based on the outcomes of this study, several directions are recommended for further research and development:

- **Validation with experimental data:** The Seiliger-based combustion model developed in this project provides a good first approximation of in-cylinder hydrogen combustion behaviour. However, the accuracy of key output variables such as p_{max} and T_{max} could be significantly improved through validation with experimental data from large dual-fuel two-stroke engines operating with hydrogen.
- **Crank-angle resolved modelling:** For a more realistic prediction of combustion phasing and timing effects, future work should consider implementing a crank-angle resolved 0D or quasi-dimensional model. This would allow direct modelling of gradual hydrogen combustion, variable phasing, and effects such as pressure rise rate and knock tendency.
- **Investigation of hydrogen combustion phasing:** The most critical uncertainty in the current model lies in the assumed combustion duration and timing for hydrogen. Experimental or CFD-based studies on the phasing of hydrogen-diesel combustion in LPDI configurations would help constrain this assumption and improve model fidelity.
- **Coupling with emission models:** To better assess the environmental trade-offs of switching to hydrogen, it is recommended to couple the combustion model to basic NO_x emission formation models. This would enable more accurate analysis of the effect of combustion temperature and phasing on emissions.
- **Application to propulsion system design:** The model developed here can be used to support preliminary engine design choices for hydrogen-capable marine propulsion systems, such as derating, peak pressure control strategies, and fuel system dimensioning. It is recommended to explore its integration into broader ship energy system simulations.

References

[1] WinGD. *X92DF-2.0 Engine*. Accessed: 2025-04-12. Winterthur Gas & Diesel (WinGD). 2024. URL: https://staging.wingd.com/products-solutions/engines/x92df-20/.

[2] Iea - International Energy Agency. *World Energy Outlook 2023*. 2023. URL: www.iea.org/terms.

[3] V. Eyring et al. “Transport impacts on atmosphere and climate: Shipping”. In: *Atmospheric Environment* 44 (37 Dec. 2010), pp. 4735–4771. ISSN: 13522310. DOI: 10.1016/j.atmosenv.2009.04.059.

[4] Unctad. *Review of Maritime Transport*. 2019.

[5] IMO. *Fourth IMO GHG Study 2020 Full Report*. 2020.

[6] Xiao Tong Wang et al. “Trade-linked shipping CO2 emissions”. In: *Nature Climate Change* 11 (11 Nov. 2021), pp. 945–951. ISSN: 17586798. DOI: 10.1038/s41558-021-01176-6.

[7] G. P. Peters et al. “Carbon dioxide emissions continue to grow amidst slowly emerging climate policies”. In: *Nature Climate Change* 10 (1 Jan. 2020), pp. 3–6. ISSN: 1758-678X. DOI: 10.1038/s41558-019-0659-6.

[8] Steven J. Davis et al. *Net-zero emissions energy systems*. June 2018. DOI: 10.1126/science.aas9793.

[9] Evert A. Bouman et al. “State-of-the-art technologies, measures, and potential for reducing GHG emissions from shipping – A review”. In: *Transportation Research Part D: Transport and Environment* 52 (May 2017), pp. 408–421. ISSN: 13619209. DOI: 10.1016/j.trd.2017.03.022.

[10] International Maritime Organization. *RESOLUTION MEPC.304(72) (adopted on 13 April 2018) INITIAL IMO STRATEGY ON REDUCTION OF GHG EMISSIONS FROM SHIPS*.

[11] Dinçer Akal, Semiha Öztuna, and Mustafa Kemalettin Büyükakın. “A review of hydrogen usage in internal combustion engines (gasoline-Lpg-diesel) from combustion performance aspect”. In: *International Journal of Hydrogen Energy* 45 (60 Dec. 2020), pp. 35257–35268. ISSN: 03603199. DOI: 10.1016/j.ijhydene.2020.02.001.

[12] Wenjing Qu et al. “Optimization of injection system for a medium-speed four-stroke spark-ignition marine hydrogen engine”. In: *International Journal of Hydrogen Energy* 47 (44 May 2022), pp. 19289–19297. ISSN: 03603199. DOI: 10.1016/j.ijhydene.2022.04.096.

[13] Pavlos Dimitriou and Taku Tsujimura. *A review of hydrogen as a compression ignition engine fuel*. 2017. DOI: 10.1016/j.ijhydene.2017.07.232.

[14] Karsten Wittek, Vitor Cogo, and Geovane Prante. “Development of a pneumatic actuated low-pressure direct injection gas injector for hydrogen-fueled internal combustion engines”. In: *International Journal of Hydrogen Energy* 48 (27 Mar. 2023), pp. 10215–10234. ISSN: 03603199. DOI: 10.1016/j.ijhydene.2022.12.023.

[15] Gavin Dober et al. “Direct Injection Systems for Hydrogen Engines”. In: *MTZ worldwide* 82 (12 Dec. 2021), pp. 60–65. ISSN: 2192-9114. DOI: 10.1007/s38313-021-0720-5.

[16] Zhen Hu et al. “High-pressure injection or low-pressure injection for a direct injection hydrogen engine?” In: *International Journal of Hydrogen Energy* 59 (Mar. 2024), pp. 383–389. ISSN: 03603199. DOI: 10.1016/j.ijhydene.2024.02.018.

[17] Moritz Schumacher and Michael Wensing. “Investigations on an Injector for a Low Pressure Hydrogen Direct Injection”. In: *SAE Technical Papers*. Vol. 2014-October. SAE International, Oct. 2014. DOI: 10.4271/2014-01-2699.

[18] Ho Lung Yip et al. “A review of hydrogen direct injection for internal combustion engines: Towards carbon-free combustion”. In: *Applied Sciences (Switzerland)* 9 (22 Nov. 2019). ISSN: 20763417. DOI: 10.3390/app9224842.

[19] Congbiao Sui et al. “Mean value first principle engine model for predicting dynamic behaviour of two-stroke marine diesel engine in various ship propulsion operations”. In: *International Journal of Naval Architecture and Ocean Engineering* 14 (Jan. 2022). ISSN: 20926790. DOI: 10.1016/j.ijnaoe.2021.100432.

[20] Harsh Sapra et al. “Hydrogen-natural gas combustion in a marine lean-burn SI engine: A comparitive analysis of Seiliger and double Wiebe function-based zero–dimensional modelling”. In: *Energy Conversion and Management* 207 (Mar. 2020). ISSN: 01968904. DOI: 10.1016/j.enconman.2020.112494.

[21] Wenjing Qu et al. “Hydrogen injection optimization of a low-speed two-stroke marine hydrogen/diesel engine”. In: *Fuel* 366 (June 2024). ISSN: 00162361. DOI: 10.1016/j.fuel.2024.131352.

[22] Wenchao Jiao. *Simulating the low-pressure direct injection system of a hydrogen-fueled engine*. Aug. 2024.

[23] D Stapersma. *Diesel Engines Volume 1 Performance Analysis*. 2010.

[24] John B. Heywood and Eran Sher. *The Two-Stroke Cycle Engine*. Routledge, Nov. 1999. ISBN: 9780203734858. DOI: 10.1201/9780203734858.

[25] Gordon P.. Blair. *Design and simulation of two-stroke engines*. Society of Automotive Engineers, 1996, p. 623. ISBN: 1560916850.

[26] John B. Heywood. *Internal Combustion Engine Fundamentals*. 2nd ed. 2018.

[27] Robert Bosch GmbH. *Diesel-Engine Management*. 4th Edition. John Wiley Sons, 2005.

[28] D Stapersma. *Diesel Engines Volume 3 Combustion*. 2010.

[29] MAN Energy Solutions. *Managing methane slip on ME-GI installations Two-stroke*. 2024.

[30] J. Serrano, F. J. Jiménez-Espadafor, and A. López. “Prediction of hydrogen-heavy fuel combustion process with water addition in an adapted low speed two stroke diesel engine: Performance improvement”. In: *Applied Thermal Engineering* 195 (Aug. 2021). ISSN: 13594311. DOI: 10.1016/j.applthermaleng.2021.117250.

[31] MAN Energy Solutions. *ME-GI Dual Fuel MAN BW Engines A Technical, Operational and Cost-effective Solution for Ships Fuelled by Gas Content*. 2014.

[32] MAN Energy Solutions. *Introducing the upgraded MAN BW ME-GI Mk. 2 and the new low-pressure MAN BW ME-GA two-stroke dual-fuel engines. Whatever your vessel, we have a fuel solution that fits*. 2019.

[33] Zhen Lu et al. “Numerical research of the in-cylinder natural gas stratification in a natural gas-diesel dual-fuel marine engine”. In: *Fuel* 337 (Apr. 2023). ISSN: 00162361. DOI: 10.1016/j.fuel.2022.126861.

[34] Jinlong Liu. *Investigation of Combustion Characteristics of a Heavy-Duty Investigation of Combustion Characteristics of a Heavy-Duty Diesel Engine Retrofitted to Natural Gas Spark Ignition Operation Diesel Engine Retrofitted to Natural Gas Spark Ignition Operation*. 2018. URL: https://researchrepository.wvu.edu/etd.

[35] Stefan Goranov, Hybridisation Marcel Ott, and Patrik Printz. *WinGD 12X92DF, the Development of the Most Powerful Otto Engine Ever*. 2019. URL: www.tcpdf.org.

[36] MAN Energy Solutions. *MAN BW ME-GA The latest dual-fuel MAN BW two-stroke engine MAN Energy Solutions MAN BW ME-GA-The latest dual-fuel MAN BW two-stroke engine 2 Future in the making 3*. July 2022.

[37] Marcel Ott et al. “The 2-stroke Low-Pressure Dual-Fuel Technology: From Concept to Reality”. In: *CIMAC Congress, Product Development - Gas Dual Fuel Engines*. 2016. URL: www.tcpdf.org.

[38] C. M. White, R. R. Steeper, and A. E. Lutz. “The hydrogen-fueled internal combustion engine: a technical review”. In: *International Journal of Hydrogen Energy* 31 (10 Aug. 2006), pp. 1292–1305. ISSN: 03603199. DOI: 10.1016/j.ijhydene.2005.12.001.

[39] Sebastian Verhelst and Thomas Wallner. *Hydrogen-fueled internal combustion engines*. Dec. 2009. DOI: 10.1016/j.pecs.2009.08.001.

[40] Zbigniew Stępień. *A comprehensive overview of hydrogen-fueled internal combustion engines: Achievements and future challenges*. Oct. 2021. DOI: 10.3390/en14206504.

[41] L.M. Das. “HYDROGEN-OXYGEN REACTION MECHANISM AND ITS IMPLICATION TO HYDROGEN ENGINE COMBUSTION”. In: *International Journal of Hydrogen Energy* 21 (8 Aug. 1996).

[42] A. Onorati et al. *The role of hydrogen for future internal combustion engines*. Apr. 2022. DOI: 10.1177/14680874221081947.

[43] Rafael Sari et al. “Hydrogen Internal Combustion Engine Strategies for Heavy-Duty Transportation: Engine and System Level Perspective”. In: *SAE Technical Papers*. SAE International, Jan. 2024. DOI: 10.4271/2024-26-0175.

[44] Stephanie Frankl et al. “Investigation of ammonia and hydrogen as CO2-free fuels for heavy duty engines using a high pressure dual fuel combustion process”. In: *International Journal of Engine Research* 22 (10 Oct. 2021), pp. 3196–3208. ISSN: 20413149. DOI: 10.1177/14680874209678 73.

[45] G. Maio et al. “Experimental and numerical investigation of a direct injection spark ignition hydrogen engine for heavy-duty applications”. In: *International Journal of Hydrogen Energy* 47 (67 Aug. 2022), pp. 29069–29084. ISSN: 03603199. DOI: 10.1016/j.ijhydene.2022.06.184.

[46] ABC Engines. *BEH2YDRO Information Sheet*. 2023.

[47] B Haragopala Rao. “Hydrogen for dual fuel engine operation”. In: *International Journal of Hydrogen Energy* 8 (5 1983), pp. 381–384. ISSN: 03603199. DOI: 10.1016/0360-3199(83)90054-X.

[48] S LAMBE and H WATSON. “Low polluting, energy efficient C.I. hydrogen engine”. In: *International Journal of Hydrogen Energy* 17 (7 July 1992), pp. 513–525. ISSN: 03603199. DOI: 10.1016/0360-3199(92)90151-L.

[49] Xinyu Liu et al. “Performance and emissions of hydrogen-diesel dual direct injection (H2DDI) in a single-cylinder compression-ignition engine”. In: *International Journal of Hydrogen Energy* 46 (1 Jan. 2021), pp. 1302–1314. ISSN: 03603199. DOI: 10.1016/j.ijhydene.2020.10.006.

[50] René Heindl et al. “New and Innovative Combustion Systems for the H2-ICE: Compression Ignition and Combined Processes”. In: *SAE International Journal of Engines* 2 (1 2009), pp. 1231–1250.

[51] Pavlos G. Aleiferis and Martino F. Rosati. “Controlled autoignition of hydrogen in a direct-injection optical engine”. In: *Combustion and Flame* 159 (7 July 2012), pp. 2500–2515. ISSN: 00102180. DOI: 10.1016/j.combustflame.2012.02.021.

[52] Vinod Singh Yadav, S. L. Soni, and Dilip Sharma. “Engine performance of optimized hydrogen-fueled direct injection engine”. In: *Energy* 65 (Feb. 2014), pp. 116–122. ISSN: 03605442. DOI: 10.1016/j.energy.2013.12.007.

[53] Cheolwoong Park et al. “Effect of fuel injection timing and injection pressure on performance in a hydrogen direct injection engine”. In: *International Journal of Hydrogen Energy* 47 (50 June 2022), pp. 21552–21564. ISSN: 03603199. DOI: 10.1016/j.ijhydene.2022.04.274.

[54] Farzad Poursadegh et al. “Autoignition, knock, detonation and the octane rating of hydrogen”. In: *Fuel* 332 (Jan. 2023). ISSN: 00162361. DOI: 10.1016/j.fuel.2022.126201.

[55] Alberto Boretti. “Hydrogen internal combustion engines to 2030”. In: *International Journal of Hydrogen Energy* 45 (43 Sept. 2020), pp. 23692–23703. ISSN: 03603199. DOI: 10.1016/j.ijhydene.2020.06.022.

[56] Cemil Bekdemir, Erik Doosje, and Xander Seykens. “H2-ICE Technology Options of the Present and the Near Future”. In: *SAE Technical Papers*. SAE International, Mar. 2022. DOI: 10.4271/2022-01-0472.

[57] P C T De Boer, W J Mclean, and H S Homan. *PERFORMANCE AND EMISSIONS OF HYDROGEN FUELED INTERNAL COMBUSTION ENGINES?* 1976.

[58] Ghazi A Karim. *Hydrogen as a spark ignition engine fuel*. 2003. URL: www.sciencedirect.comwww.elsevier.com/locate/ijhydene.

[59] Yi-Hao Pu and Sebastian Verhelst. *Performance and Emissions of a Virtual Medium-Speed Spark-Ignited Engine on Methanol*. Aug. 2024.

[60] Pedro Orbaiz et al. “A comparative study of a spark ignition engine running on hydrogen, synthesis gas and natural gas”. In: *SAE International Journal of Engines* 6 (1 2013), pp. 23–44. ISSN: 19463936. DOI: 10.4271/2013-01-0229.

[61] J. Serrano, F. J. Jiménez-Espadafor, and A. López. “Analysis of the effect of different hydrogen/diesel ratios on the performance and emissions of a modified compression ignition engine under dual-fuel mode with water injection. Hydrogen-diesel dual-fuel mode”. In: *Energy* 172 (Apr. 2019), pp. 702–711. ISSN: 03605442. DOI: 10.1016/j.energy.2019.02.027.

[62] Midhat Talibi et al. “Hydrogen-diesel fuel co-combustion strategies in light duty and heavy duty CI engines”. In: *International Journal of Hydrogen Energy* 43 (18 May 2018), pp. 9046–9058. ISSN: 03603199. DOI: 10.1016/j.ijhydene.2018.03.176.

[63] H S Homan et al. “HYDROGEN-FUELED DIESEL ENGINE WITHOUT TIMED IGNITION”. In: *International Journal of Hydrogen Energy* 4 (1979), pp. 315–325.

[64] Carlos Eduardo Castilla Alvarez et al. *A review of prechamber ignition systems as lean combustion technology for SI engines*. 2018. DOI: 10.1016/j.applthermaleng.2017.08.118.

[65] Sipeng Zhu et al. *A review of the pre-chamber ignition system applied on future low-carbon spark ignition engines*. Feb. 2022. DOI: 10.1016/j.rser.2021.111872.

[66] S. Molina et al. “Impact of medium-pressure direct injection in a spark-ignition engine fueled by hydrogen”. In: *Fuel* 360 (Mar. 2024). ISSN: 00162361. DOI: 10.1016/j.fuel.2023.130618.

[67] Ali Mohammadi et al. “Performance and combustion characteristics of a direct injection SI hydrogen engine”. In: *International Journal of Hydrogen Energy* 32 (2 Feb. 2007), pp. 296–304. ISSN: 03603199. DOI: 10.1016/j.ijhydene.2006.06.005.

[68] Marcel Ott, Roland Alder, and Ingemar Nylund. “Low Pressure Dual-fuel Technology for Low Speed Marine Engines”. In: *ATZextra worldwide* 20 (S10 Nov. 2015), pp. 34–39. ISSN: 2195-1470. DOI: 10.1007/s40111-015-0506-3. URL: http://link.springer.com/10.1007/s40111-015-0506-3.

[69] Francesco Baldi, Gerasimos Theotokatos, and Karin Andersson. “Development of a combined mean value-zero dimensional model and application for a large marine four-stroke Diesel engine simulation”. In: *Applied Energy* 154 (Sept. 2015), pp. 402–415. ISSN: 03062619. DOI: 10.1016/j.apenergy.2015.05.024.

[70] Gerasimos Theotokatos et al. “Development of an extended mean value engine model for predicting the marine two-stroke engine operation at varying settings”. In: *Energy* 143 (Jan. 2018), pp. 533–545. ISSN: 03605442. DOI: 10.1016/j.energy.2017.10.138.

[71] Suneel Kumar, Manish Kumar Chauhan, and Varun. *Numerical modeling of compression ignition engine: A review*. 2013. DOI: 10.1016/j.rser.2012.11.043.

[72] Frank Schenkel. *Adapting an in-cylinder process model to a 2-stroke Bolnes engine and preparations for ammonia-diesel operation*. Dec. 2023.

[73] Yu Ding and Vereniging voor Studie- en Studentenbelangen (Delft). *Characterising combustion in diesel engines using parameterised finite stage cylinder process models*. VSSD, 2011. ISBN: 9789065622891.

[74] Congbiao Sui et al. “Mean value modelling of diesel engine combustion based on parameterized finite stage cylinder process”. In: *Ocean Engineering* 136 (2017), pp. 218–232. ISSN: 00298018. DOI: 10.1016/j.oceaneng.2017.03.029.

[75] : M Godjevac et al. *Two-part modelling approach for ship engine simulations Author names*. Tech. rep. 2015. URL: http://onepetro.org/snamewmtc/proceedings-pdf/WMTC15/1-WMTC15/D011S003R001/2509684/sname-wmtc-2015-016.pdf/1.

[76] Mike Loonstijn. *Diesel A-M (A-Modular) Model Proposed Expanding the Diesel A model for advanced turbocharging capabilitiesModular) Model Proposed: Expanding the Diesel A model for advanced turbocharging capabilities. (Report-Ship Design Production and Operations (SDPO)*. Tech. rep. 2017.

[77] M. Seiliger. *Graphische Thermodynamik und Berechnen der Verbrennungs-Maschinen und Turbinen*. Springer Berlin Heidelberg, 1922. ISBN: 978-3-662-42706-4. DOI: 10.1007/978-3-662-42983-9.

[78] A A Koekkoek. *An Ammonia-Fuelled Solid Oxide Fuel Cell-Internal Combustion Engine Hybrid System for Ships*. Tech. rep. TU Delft, Dec. 2021. URL: http://repository.tudelft.nl/..

[79] Aart-Jan Van Der Hoeven. *Crankshaft Modeling Identication for Cylinder Pressure Estimation-condential*. Tech. rep. 2012.

[80] Gordon P.. Blair. *The basic design of two-stroke engines*. Volunteer Services for the Visually Handicapped, Inc., 1990. ISBN: 1560910089.

[81] Malcolm W. Jr. Chase. "NIST-JANAF Thermochemical Tables". In: *Journal of Physical and Chemical Reference Data* (1998).

[82] *NIST Chemistry WebBook*. URL: https://webbook.nist.gov/.

[83] Stefan Eicheldinger et al. "Optical screening investigations of backfire in a large bore medium speed hydrogen engine". In: *International Journal of Engine Research* 23 (5 May 2022), pp. 893–906. ISSN: 20413149. DOI: 10.1177/14680874211053171.

[84] Yuki Mogi et al. "Effect of high compression ratio on improving thermal efficiency and NOx formation in jet plume controlled direct-injection near-zero emission hydrogen engines". In: *International Journal of Hydrogen Energy* 47 (73 Aug. 2022), pp. 31459–31467. ISSN: 03603199. DOI: 10.1016/j.ijhydene.2022.07.047.

[85] J. I. Ghojel. "Review of the development and applications of the Wiebe function: A tribute to the contribution of Ivan Wiebe to engine research". In: *International Journal of Engine Research* 11 (4 Aug. 2010), pp. 297–312. ISSN: 14680874. DOI: 10.1243/14680874JER06510.

[86] J. Serrano, F. J. Jiménez-Espadafor, and A. López. "Analysis of the effect of the hydrogen as main fuel on the performance of a modified compression ignition engine with water injection". In: *Energy* 173 (Apr. 2019), pp. 911–925. ISSN: 03605442. DOI: 10.1016/j.energy.2019.02.116.

[87] Colin R. Ferguson. *Internal Combustion Engines : Applied Thermosciences*. John Wiley Sons, Incorporated, 2015.